Thin film microelectrodes for electrochemical detection of neurotransmitters

Larsen, Simon Tylsgaard

Publication date:
2012

Document Version
Publisher's PDF, also known as Version of record

Thin film microelectrodes for electrochemical detection of neurotransmitters

PhD Thesis

By Simon Tylsgaard Larsen

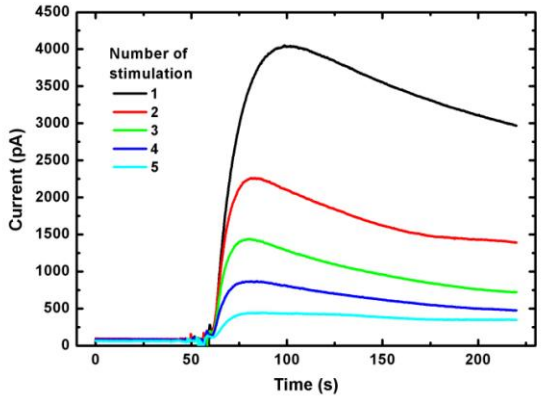

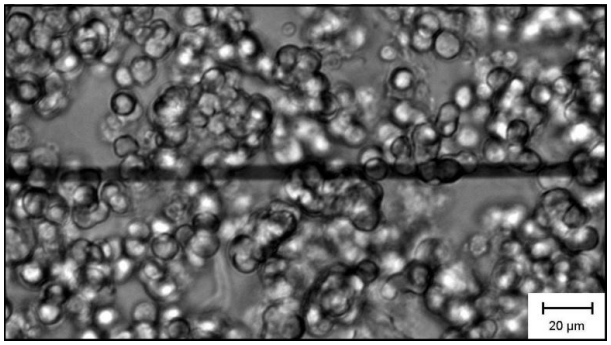

10. august 2012

DTU Nanotech
Department of Micro- and Nanotechnology

Abstract

An important signaling process in the nervous system is the release of chemical messengers called neurotransmitters from neurons. In this thesis alternative thin film electrode materials for applications targeting electrochemical detection of neurotransmitters in chip devices were evaluated. Microelectrodes made of the conductive polymer Pedot:tosylate were characterized with respect to their physical and electrochemical properties and transmitter release from large groups of neuronal PC 12 cells was measured at Pedot:tosylate microelectrodes. Carbon microelectrodes made of pyrolyzed photoresist and conductive polymer microelectrodes made of Pedot:Pss were also fabricated and used successfully to measure transmitter release from cells.

The use of different thin film electrodes for low-noise amperometric measurements of single events of transmitter release from neuronal cells was studied. For this application a very low current noise is needed together with a large temporal resolution. It was shown, that resistive and capacitive properties of thin film electrode materials are determining their usefulness in low-noise amperometric measurements. An analytical expression for the noise was derived and experimental noise measurements supported the theory.

As an alternative to low noise amperometry at single cells, a chip device was developed to measure transmitter release from large groups of neuronal PC 12 cells. The chip was used to study refueling of transmitter reservoirs and the concentrations of potassium needed in a physiological buffer to trigger transmitter release from PC 12 cells. The potential of the chip for electrochemical drug screening of neuroactive drugs was demonstrated.

Dansk resume

En vigtig signaleringsproces i nervesystemet er udskillelsen af kemiske signalstoffer, kaldet neurotransmittere, fra nerveceller. I denne afhandling undersøges en række alternative tyndfilms-elektrodematerialer til brug i elektrokemisk måling af neurotransmittere i mikrofabrikerede chips. Mikroelektroder fremstillet af den ledende polymer Pedot:tosylat blev karakteriseret med hensyn til deres fysiske og elektrokemiske egenskaber og udskillelse af neurotransmittere fra store grupper af neuronale PC12-celler blev målt på Pedot:tosylat mikroelektroder. Kul-mikroelektroder fremstillet af pyrolyseret fotoresist og ledende polymer-mikroelektroder fremstillet af Pedot:Pss blev også anvendt med held til at måle neurotransmitterudskillelse fra celler.

Anvendeligheden af forskellige tyndfilmselektroder til støjkritiske amperometriske målinger af enkelte begivenheder af transmitterudskillelse fra neuronale celler blev undersøgt. Til disse forsøg er en meget lav strømstøj nødvendig sammen med hurtige målingsfrekvenser. Det blev vist, at resistive og kapacitive egenskaber af tyndfilmselektrodematerialer bestemmer deres anvendelighed indenfor støjkritiske amperometriske målinger. Et analytisk udtryk for støjen blev udarbejdet og eksperimentelle støjmålinger støttede teorien.

Som et alternativ til støjkritiske amperometriske målinger på enkelte celler, udviklede vi en chip til måling af transmitterudskillelse fra store grupper af neuronale PC12-celler. Chippen blev anvendt til at undersøge reetableringen af neurotransmitterreservoirer og koncentrationen af kalium der er nødvendig i en fysiologisk buffer for at udløse udskillelse af neurotransmittere fra PC12 celler. Det blev også vist at chippen kan bruges til elektrokemisk lægemiddelscreening af neuroaktive stoffer.

Table of Contents

Preface

The PhD thesis presented here is the result of a 3 year PhD project carried out at the Department of Micro- and Nanotechnology, Technical University of Denmark at the research group of Rafael Taboryski from 2009 to 2012. A four month external stay at the research group of Andrew Ewing at Pennsylvania State University took place during the spring of 2010.

The project was supported by the Danish Council for Strategic Research through the Strategic Research Center PolyNano (grant no. 10-092322/DSF). This research center is aimed at the development of high-volume low-cost lab-on-a-chip technologies for different bioanalytical applications.

The application targeted in this project is the detection of neurotransmitter release from single neuronal cells by use of constant potential amperometry. The main tool in this field of research is still the use of carbon fiber microelectrodes that are manually manipulated into close vicinity of single cells for monitoring of exocytotic secretion. This method requires highly skilled staff and is not feasible for automation. Within the last decade, microfabricated devices for trapping and measuring release from single cells have been presented, but none of these are low-cost devices aimed at high-volume production.

The goal of this project was to develop a cheap device for cell trapping and transmitter release measurement by moving to a polymer platform. A fabrication process for microfluidic devices relying on the thermal bonding of two injection molded polymer parts had previously been developed at our department and been successfully used for on-chip electroporation of cells. In this process, thin film microelectrodes applied to one of the polymer parts can be integrated with microchannels molded directly into the other part. Except for using this cheap and high-volume fabrication process, the use of conductive polymer as electrode material would further improve the low cost of the final chip. Within our department some experience in the fabrication and application of electrodes from the conductive polymer Pedot:tosylate had been collected. The usefulness of this electrode material for electrochemical detection of neurotransmitter release from living cells had not been reported earlier and this question therefore became the first target of our investigation.

A thorough characterization of Pedot:tosylate microelectrodes for transmitter release studies was carried out. This study was published in the peer-reviewed journal Analyst in January 2012 and is reproduced in **chapter 2** of this thesis.

Although Pedot:tosylate microelectrodes exhibited good electrochemical properties for oxidation of transmitter molecules in aqueous buffer solutions and the transmitter release from large groups of neuronal cells could be detected at the electrodes, low noise amperometric measurements of single vesicle release events failed at Pedot:tosylate microelectrodes. The main problem was the current noise, which was at the same level as the expected signals for the high sample frequencies needed. We suspected the large capacitance of the conductive polymer films to be the source of the noise. This led to an investigation of the nature of amperometric noise at microelectrodes fabricated from different thin film materials. This study was submitted to Analytical Chemistry in April 2012 and is reproduced in **chapter 3**.

The noise study confirmed the suspicion that high capacitance properties of an electrode material are a main source of current noise in constant potential amperometry at microelectrodes. This meant that Pedot:tosylate was not an ideal candidate for low-noise amperometric studies of transmitter release. For release studies from large groups of neuronal cells though, noise was not a problem due to larger signals and lower sample frequencies. The method of measuring release from large groups of cells was used and further developed into a polymer chip device for transmitter release studies and drug screening. This study was submitted to Analyst in July 2012 and is reproduced in **chapter 4**.

During the project a few other interesting electrode materials have been used for transmitter release studies. Characterization results for two of them, pyrolyzed photoresist and conductive polymer Pedot:Pss, are presented in **chapter 5**. This chapter also includes a qualitative comparison of the different thin film materials.

Before any results are reported, an introduction to the field is provided in **chapter 1**. The importance of neurotransmitters in neuronal signaling processes and the usefulness of electrochemical detection methods in transmitter detection applications is explained. Also, we summarize recent improvements in transmitter release studies, with special emphasis on chip-based devices and thin film electrode materials used by others. Finally, we give an introduction to conductive polymers, particularly Pedot.

In **chapter 6** a conclusion of the project is given.

Chapter 1: Introduction

1. Neurotransmitters – signaling molecules of the nervous system

Neurotransmitters are essential signaling molecules in the function of the nervous system.[1] While nerve signals are transmitted electrically along individual neurons by means of rapid changes in membrane potential termed action potentials, the transmission of nerve signals from one neuron to another is facilitated by the release and binding of chemical messengers. Early pioneering work on chemical neurotransmission was performed by Katz[2] in the 1950's by measuring electrophysiological reactions at the frog neuromuscular junction. These measurements laid the foundation for the discovery that neurotransmission is quantal of nature.[3, 4] Indeed, neurotransmitters are released in bundles resulting from the intracellular storage of neurotransmitters in vesicles and the release of full vesicles to the extracellular space in a process termed exocytosis.

Classical neurotransmitters include acetylcholine, GABA, glutamate, glycine and monoamines like histamine, serotonin, dopamine, norepinephrine and epinephrine. All of these are known to be synthesized intracellularly in the cytosol and packaged via specific transmembrane protein transporters into vesicles. Figure 1 gives an overview of the mechanisms leading to exocytotic release of neurotransmitters. Packaged vesicles are being transported from vesicle reservoirs to the cell surface area. At the cell membrane the vesicle becomes tightly fixed to the cell membrane through a process termed docking. Once docked, the vesicle undergoes a set of molecular rearrangements and ATP-dependent protein and lipid modifications before release of neurotransmitters can happen. This step is called priming and includes the formation of the SNARE complex, an assembly of proteins responsible for the fusion of vesicle membrane and cell membrane. The fusion step is triggered by the influx of calcium ions to the intracellular environment. During fusion, a small opening between the inside of the vesicle and the extracellular space is first constructed. After a short period of time, the vesicle and cell membranes fuse completely and the vesicle content is released into the extracellular space. In the case of neurotransmission, the extracellular space is typically a small cleft between two neighboring neurons, called the synaptic cleft. Released

neurotransmitters transmit signals by binding to receptors on the post-synaptic neuron. This binding may result in the opening of ion channels or the activation of G proteins.

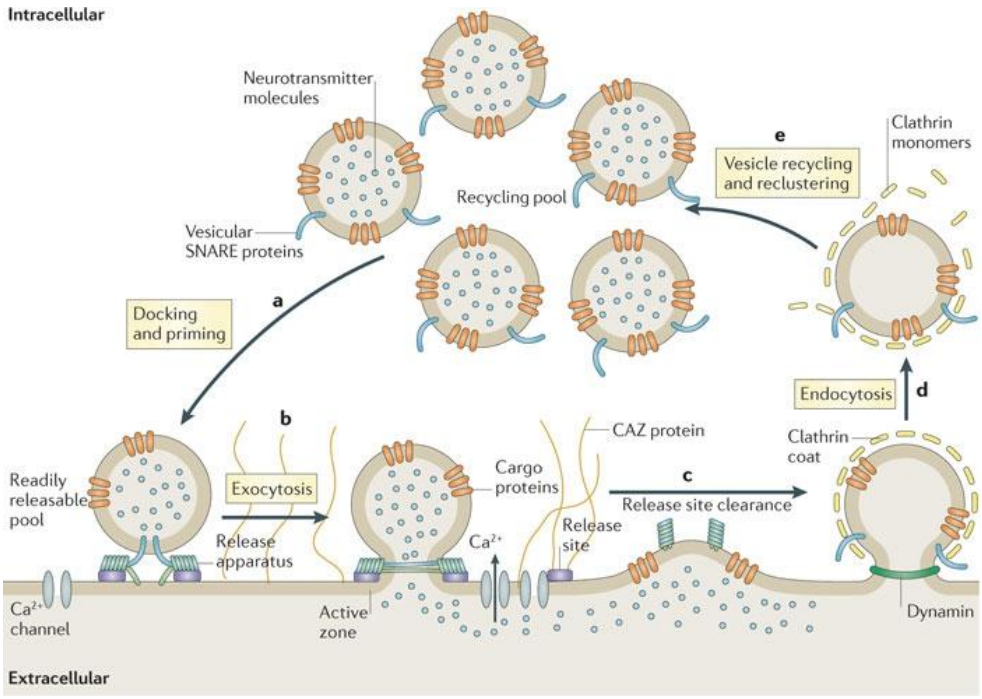

Figure 1 *Overview of exocytotic release of neurotransmitters. Adapted from* [5].

Different theories have been presented concerning the restoration of new vesicles in the pre-synaptic cell.[1] As shown in figure 1, new vesicles may be formed by clathrin-mediated endocytosis. This process is opposite to exocytosis and empty vesicles are formed directly from the cell membrane and later packaged with newly synthesized neurotransmitter molecules. Another theory assumes only partial fusion of the vesicles and the cell membrane followed by release of molecules and loosening of the vesicle[1]. This model has been termed “Kiss and Run”.

A major motivation for research in neurotransmitter release mechanisms is the link between neurotransmitter concentration in different parts of the central nervous system and several diseases and neurological disorders. This can be illustrated by the monoamine neurotransmitter dopamine, which has been shown to play an important role in depression,[6] schizophrenia[7] and Parkinson's disease.[7, 8] Parkinson’s disease is often linked to a decrease in dopamine levels in the substantia nigra of the brain and drugs prescribed to patients with Parkinson’s disease are aimed at increasing dopamine

levels. By contrast, it is argued that one of the causal factors in schizophrenia is a functional excess of dopamine or an oversensitivity of certain dopamine receptors and most antipsychotic drugs block and reduce the effects of dopamine.[7] A good understanding of neurotransmitter release mechanisms has allowed for development of drugs that specifically upregulate or downregulate a certain neurotransmitter by targeting one of the steps involved in exocytosis. Neurotransmitter levels can for example be upregulated by adding precursor molecules or by blocking autoreceptors at the presynaptic neuron, while downregulation could be facilitated by blocking vesicle transporter proteins or by interfering with SNARE-complex proteins.

Several methods have been developed to measure neurotransmitter release and concentration in living systems. The next section gives an introduction to some of these methods. Quantification of neurotransmitter release can be used both to collect new information on the molecular biological mechanisms involved in exocytosis as well as to screen the effect of drug candidates on neurotransmitter release activity.

While concentrations of neurotransmitters can be measured directly inside the brain of living animals (*in vivo*), measurements of single vesicle release have only been performed *in vitro* at isolated and cultured single cells. By using cultured cells, interfering signals from neighboring cells or from biological species in the blood can be avoided. The first electrochemical recordings of single vesicle exocytosis were performed using primary cultures of bovine adrenal medullary chromaffin cells.[9, 10, 11] These cells were prepared from fresh bovine adrenal glands obtained from a local slaughterhouse. The cells could be plated and cultured on dishes and used within 4-8 days. Chromaffin cells, which can also be derived from laboratory animals like rats and mice, have been the most used culture cell for single-vesicle exocytosis studies in the last two decades.[12, 13]

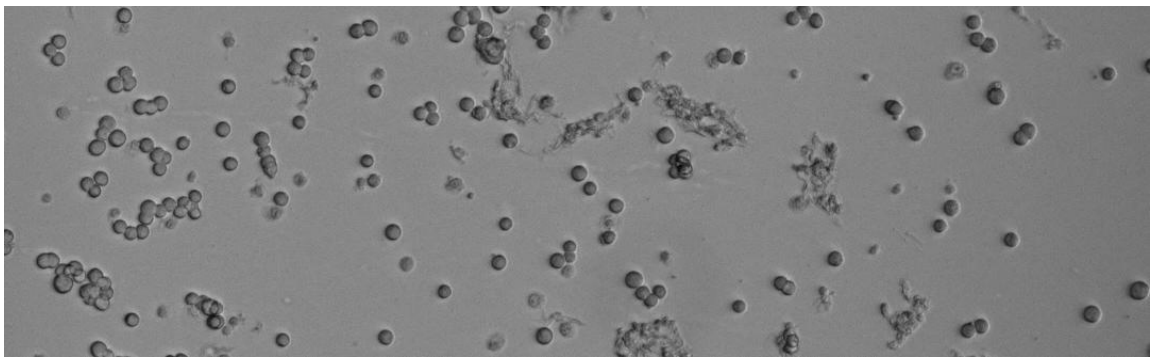

Figure 2 *Microscope image of PC 12 cells.*

The continued need for new laboratory animals in chromaffin cell studies not only gives rise to some ethical matters regarding animal use but also increases the variation in data and requires extensive cell isolation work. Due to these reasons, the use of rat pheochromocytoma (PC 12) cells has developed in parallel as an alternative cell model for exocytosis studies. The PC 12 cell line was originally isolated from a tumor in the adrenal medulla of a rat in 1976.[14] Like chromaffin cells, PC 12 cells release catecholamine neurotransmitters (dopamine, epinephrine and norepinephrine) in a calcium-dependent manner.[15] Some of the advantages of PC 12 cells are their versatility for pharmacological manipulation, ease of culture (they can be subcultured indefinitely) and the large amount of background knowledge on their proliferation and differentiation.[12] PC 12 cells have smaller transmitter vesicle sizes than chromaffin and exocytosis signals can therefore be more difficult to detect. Upon stimulation with nerve growth factor, PC 12 cells can be changed to resemble sympathetic ganglion neurons by cell differentiation and neurite growth.[16] Even though a few studies present exocytotic measurements from MN9D cells[17, 18] which should have a closer resemblance to real neurons than PC 12, PC 12 cells remain the most used cultured cell line for transmitter release studies.

2. Electrochemical methods used to study transmitter release

The study of neurotransmitter release has benefited heavily from the fact that a select number of neurotransmitters (e.g. dopamine epinephrine, norepinephrine, serotonin and histamine) are electroactive, and can therefore be oxidized at a polarized electrode held at a potential higher than the oxidation potential of the molecule. Electrochemical measurements of neurotransmitters have been the fastest and most quantitative methods of neurotransmitter release to date.[4] Around 1990, Wightman and co-workers revolutionized the analytical investigation of exocytosis by presenting the first electrochemical measurements of individual release events at single cells. They used constant potential amperometry at carbon fiber microelectrodes to measure catecholamine release from single chromaffin cells. This technique is still the golden standard for measuring exocytosis.

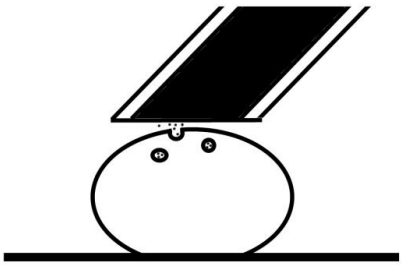

Figure 3: *Illustration of a carbon fiber microelectrode experiment. The carbon fiber is encased in a glass capillary, polished at a 45° angle and positioned directly on top of the target cell. Released neurotransmitter molecules reach the electrode surface by diffusion and oxidize instantly.*

The working principle of a carbon fiber microelectrode experiment is illustrated in figures 3 and 4. The cells are grown on transparent culture dishes and placed in a microscope. The growth buffer is exchanged with a simple salt buffer that resembles the physiological environment without containing interfering biomolecules. Carbon fiber microelectrodes are constructed from carbon fibers (typically 5 µm in diameter) sealed in glass capillaries and polished at an angle of 45°. A carbon fiber microelectrode is attached to a micromanipulator and connected to the working electrode connection of a low-noise potentiostat headstage, while a reference electrode (typically Ag/AgCl) is immersed in the physiological buffer and also connected to the headstage. A cell which is not too close to neighboring cells is chosen and the microelectrode is lowered until it touches the cell membrane of the chosen cell. A micropipette is filled with physiological buffer containing an elevated potassium concentration, attached to another micromanipulator and placed close to the cell. The microelectrode is held at a constant potential (typically 0.7 V) and a current measurement is started. Shortly after release of high potassium buffer from the micropipette, exocytosis signals can be measured as spikes on the current trace. Figure 4 shows some of the first amperometric exocytosis recordings from Wightman et al.[11] The insert shows a detailed image of a single exocytotic spike resulting from the oxidation of neurotransmitters from a single vesicle fusion event. The shape of the spike can reveal valuable information of the dynamics of exocytosis, while an integration of the spike area gives the total charge oxidized at the electrode, which can be converted to the mole amount of transmitter (N) detected per vesicle using Faraday's law (Q=nNF), where n is the number of electrons exchanged in the oxidation reaction, Q is the charge and F is Faraday's constant (96485 C/mol).

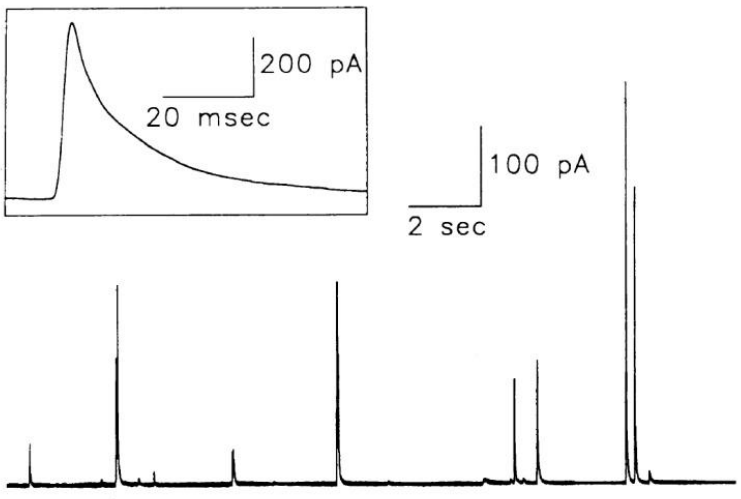

Figure 4: *Early amperometric recordings of exocytotic release from chromaffin cells using constant potential amperometry at carbon fiber microelectrodes. The insert shows a detailed view of a single current spike. Figure adapted from [11].*

20 years after the first experiments on electrochemical detection of exocytosis, constant potential amperometry at carbon fiber microelectrodes is still the golden standard for this field of research. Over the years, carbon fiber microelectrodes have been used on a range of different neuronal cells.[4] The effect of pharmacological manipulations by a range of neuroactive drugs have been investigated,[19, 20, 21, 22] exocytosis has been triggered with different stimulating agents[23] and the effect of manipulations in the expression of exocytosis-controlling proteins have been analyzed.[24, 25, 26] The very high temporal resolution of constant potential amperometry has also been used to unravel some of the biophysical details of transmitter release. One of these is the existence of a small "foot event" preceding the current spike.[27, 28, 29] This feature is thought to be from the oxidation of transmitter molecules escaping through the cell membrane through a small pore shortly before full vesicle fusion.

Carbon fiber microelectrodes have also been used successfully to track specific neurotransmitter changes over time *in vivo*. A popular analytical method for this is fast-scan cyclic voltammetry.[30, 31] In this method, the potential is ramped fast using a triangular waveform spanning a potential range that contains the oxidation potentials of the targeted species. If the oxidation potentials of the targets are not too similar, the

concentration of several transmitters can be recorded simultaneously by following the development of different peaks at the same voltammogram. Even though this method is not as fast as constant potential amperometry, it is the most suitable method currently available to measure transient changes of some neurotransmitters *in vivo*, due to the chemical selectivity.[31] Carbon fiber microelectrodes used for fast-scan cyclic voltammetry are typically cylindrical (5-30 µm in diameter, 25-400 µm in length).

While manual laboratory techniques like carbon fiber microelectrode amperometry have yielded stable and successful tools for years, strong efforts have been undertaken in the last decade to develop chip-based devices for exocytosis studies. Chip-based devices offer advantages such as high throughput, automation, and the ability to integrate different analytical features into one device. Attempts to measure single cell exocytosis on chip devices are typically based on a cell trapping mechanism to isolate a cell from a suspension and bring the cell in contact with a microelectrode. Some examples are shown in figure 5. Stimulation of exocytosis can be integrated in microfluidic devices by addition of microfluidic channels delivering a buffer solution with a high concentration of potassium[32] or by triggering release by electrically depolarizing the cells.[33]

Electrochemical detection of neurotransmitters in chip-based devices has also been used in other bioanalytical fields. In separation techniques, like capillary electrophoresis[36] and high performance liquid chromatography,[36, 37, 38, 39] electrochemical detection is a serious alternative to laser-induced-fluorescence detection due to the fact that many compounds can be detected without derivatization with a fluorophore.[40, 41] High Performance Liquid Chromatography is a form of column chromatography that pumps a sample mixture or analyte in a solvent (known as the mobile phase) at high pressure through a column with chromatographic packing material (stationary phase).[37] In capillary electrophoresis, ionic species can be separated based on their electrophoretic mobility by applying a voltage over the length of a thin capillary. The electrophoretic mobility is dependent upon the charge of the molecule, the viscosity, and the atom's radius. Capillary electrophoresis can be coupled with electrochemical detection by integration of a microelectrode at the end of a long microfuidic channel.[36]

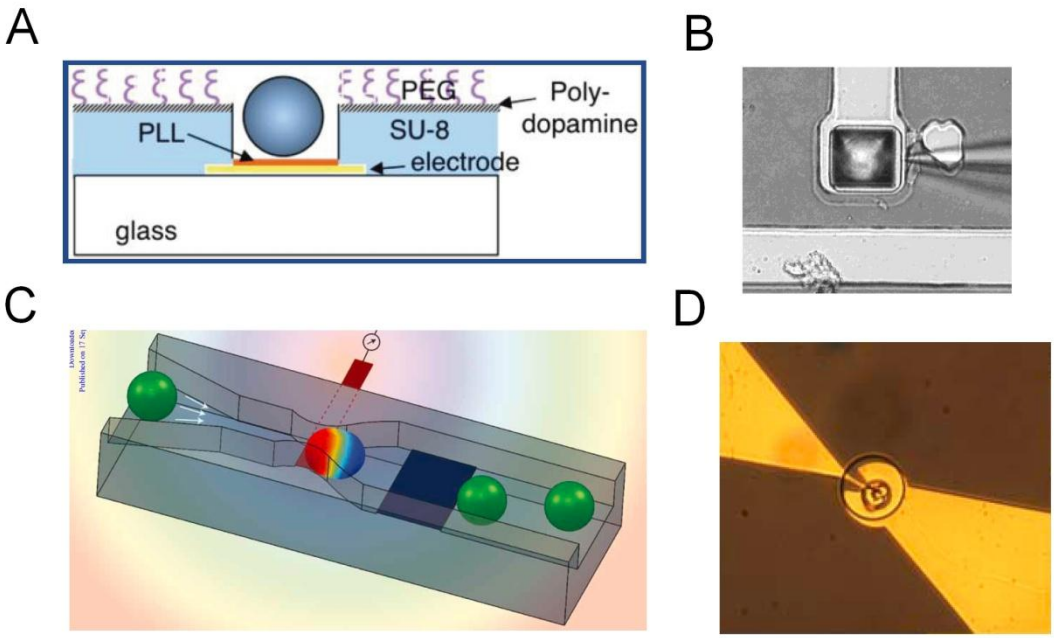

Figure 5: *Chip-based devices for measuring transmitter release from living cells. A) Adapted from Liu et al.[34] Chromaffin cells were trapped on active electrodes by chemical attachment of the cell to a thin layer of poly-l-lysine. Surrounding areas were coated with polyethylene glycol which prevented cell attachment. B) Adapted from Chen et al.[35] A simple microwell device for physical trapping of chromaffin cells on microfabricated gold electrodes. C) Adapted from Dittami and Rabbitt.[33] A microfluidic device for trapping PC 12 cells close to gold microelectrodes by use of a narrowing channel. D) Adapted from Spegel et al.[32] suction applied through a through-hole in silicon is used to trap single PC 12 cells close to mercaptopropionic acid-modified gold microelectrodes.*

One of the main challenges in developing microfabricated devices using electrochemical detection of neurotransmitters has been the choice of electrode material. In traditional microfabrication techniques electrodes are constructed by applying a thin layer of conducting material to a substrate and then patterning the layer to determine the electrodes geometry. Electrodes fabricated in this way are called thin-film electrodes and can be integrated in closed chip devices by bonding the electrode substrate to counterparts containing microfluidic channel structures. One of the main problems in finding an electrode material suitable for on-chip neurotransmitter detection is that it is required to have both good electrochemical properties, low resistivity and the possibility of applying it in thin layers and patterning it.

It is difficult to develop suitable and stable microelectrode structures in carbon, which is the most suitable electrode material for catecholamine detection.[42, 43] As a consequence several chip attempts have used the difficult task of incorporating traditional glass-encased carbon fiber microelectrodes in microfabricated chips for transmitter detection.[44, 45, 46, 47] This is not an elegant method from a microfabrication point of view, since it does not avoid the time-consuming step of manual carbon fiber electrode fabrication and the fabrication method is not suitable for mass production. Others have used carbon electrodes made of carbon ink for microchip-based analysis systems. One method involves bonding of a PDMS microchannel structure to a surface and filling of the channel system with carbon ink, which is then allowed to dry before removal of the PDMS.[48] The resultant patterned electrodes can be integrated in closed chip systems by bonding a new channel system to the electrodes. Carbon electrodes made of screen-printed thick film carbon have also been presented.[49, 50]

If small electrode dimensions are needed, a better method is the fabrication of carbon microelectrodes by pyrolysis of photoresist films. Since photoresist is an organic material it can be carbonized by elevating it to very high temperatures (500 – 1100 °C) in an oxygen-free atmosphere. Pyrolyzed photoresist microelectrodes have been made by pyrolysis of fully developed photoresist structures and used for various bioanalytical methods involving electrochemical detection of neurotransmitters.[51, 52, 53] A serious drawback of pyrolyzed photoresist electrodes is the fact that very heat-resistive substrates are needed. Typically silicon or quartz wafers are used for the process. This is a limitation for the development of cheap and mass-producible chips.

The most popular electrode materials for neurotransmitter detection are noble metals due to the easy deposition methods available like sputtering and evaporation combined with patterning through lift-off of photoresist. Metal microelectrodes made of gold[35, 54] and platinum[55, 56, 57] have been used for detection of exocytosis in chip systems. Metal electrodes suffer from less favorable electrochemistry though, since they are prone to fouling, fx via polymerization of aminochrome, a product from dopamine oxidation.[42, 43, 53, 58, 59] Spegel et al.[42] found that treatment of bare gold electrodes with mercaptopropionic acid decreased the rate of dopamine polymerization and increased the reversibility and sensitivity of the electrodes.

Alternative electrode materials have been tried in order to avoid some of the deficits from carbon and metal electrodes. Several studies use indium tin oxide microelectrodes, the main advantage being the transparency of indium tin oxide opposed to the opaqueness of metal and carbon thin film electrodes.[60, 61] The electrode transparency

has been utilized to combine amperometric recording of release events with fluorescence microscopic observation of vesicle movement in single chromaffin cells.[62] Recently in a similar study, amperometric measurements were combined with total internal reflection fluorescence microscopy (TIRFM) at indium tin oxide microelectrodes[63] (figure 6). Transparent electrodes for transmitter detection can also be made of boron-doped nanocrystalline diamond.[64, 65, 66] These electrodes have been reported to exhibit biocompatibility and an exceptionally large potential window of around 3 V. Sen et al. found that microelectrodes made of nitrogen-doped diamond-like carbon enhanced the attachment of chromaffin cells to microelectrodes.[67]

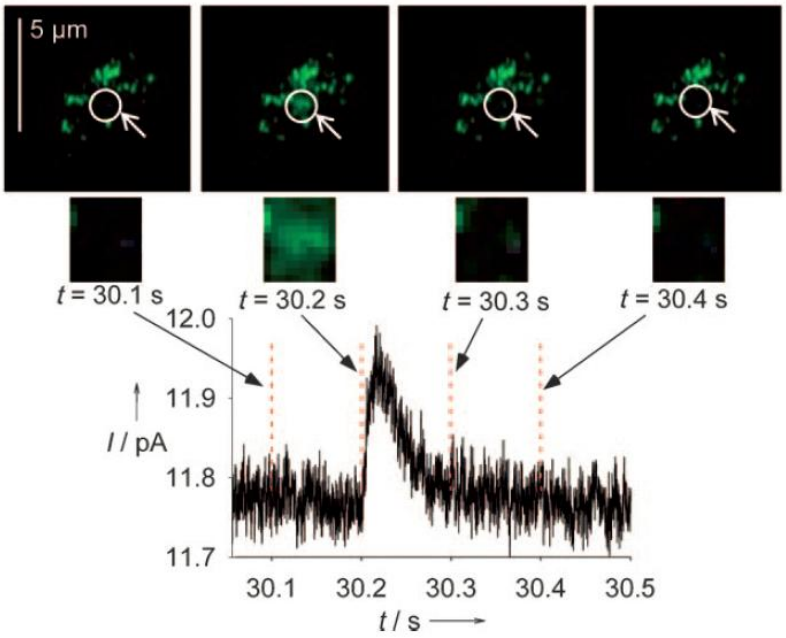

***Figure 6**: Constant potential amperometry was combined with total internal reflection fluorescence microscopy (TIRFM) at transparent indium tin oxide microelectrodes for simultaneous observation of vesicle movement and quantitative recording of released transmitter molecules. Adapted from [63].*

3. Conductive polymers and Pedot

An interesting new class of electrode materials is conductive polymers. Conductive polymers are organic polymers that conduct electrical current. The major break-through in the field of conductive polymers was the development of highly conductive Poly-

acetylene in 1977,[68, 69] which was honored with the Nobel Prize to Shirakawa, MacDiarmid and Heeger in 2000. The high conductivity was achieved by oxidizing the neutral polymer in a process termed doping, where some of the delocalized electrons, belonging to the carbon centers of the polymer backbone were removed. For Poly-acetylene, doping resulted in a polymer with conductivities up to 10^5 S/cm. Due to degradability in air and low processability, Poly-acetylene is not an ideal material for practical applications.[70] Therefore many attempts have been made to develop conductive polymers that combine the high conductivity of Poly-acetylene with good fabrication properties. Some of the most important conductive polymers are polyaniline, polypyrrole and polythiophene.

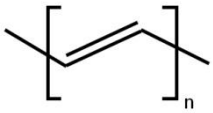

Scheme 1 *The chemical structure of Polyacetylene.*

During the 1980s, scientists at the Bayer AG research laboratories in Germany developed a new polythiophene derivative, poly(3,4-ethylenedioxythiophene), having the backbone structure shown in scheme 2. This conductive polymer, which has been given the short name Pedot, exhibited some very interesting properties. In addition to a relatively high conductivity (up to 600 S/cm), Pedot was found to be almost transparent in thin, oxidized films and showed a very high stability in the oxidized state.[70, 71, 72] Pedot can be polymerized chemically and electrochemically and different counter-ions can be used. The most frequently used counter-ion for Pedot is polystyrene sulfonate (Pss) shown in scheme 2c, which has a high molecular weight, and is to some extent physically trapped by and stably integrated into the Pedot backbone. In this thesis, Pedot:Pss is used in the form of a pre-mixed solution supplied by H. C. Starck. Another choice of counter-ion is tosylate (p-toluene sulfonate) which is shown in scheme 2b. Tosylate can diffuse more easily out of the conductive polymer and can be exchanged with other ions in the surrounding environment.[73] The fabrication of Pedot:tosylate films is a little more complicated. The compound Fe(III) *p*-toluene sulfonate (iron tosylate) was used for the oxidative chemical polymerization of the monomer. The polymerization by iron(III) salts

is kinetically retarded by addition of a base (pyridine). A mixture of monomer, iron tosylate, base and solvent (n-butanol) results in a non-conductive solution that is stable at room temperature, and can be spincoated on substrates. After heating and rinsing in water, Fe(II) salts formed under polymerization are extracted, thus leaving the doped conductive form of Pedot.[72, 74]

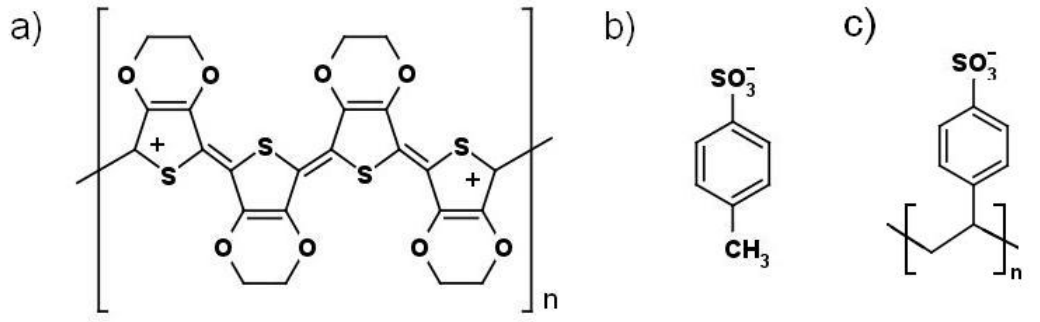

Scheme 2 *The chemical structure of a) positively charged Pedot, b) negatively charged tosylate counter ion and c) negatively charged pss counter ion. Redrawn from [74] and [75].*

Pedot has been used in a wide range of applications, spanning from antistatic and electrically conducting coatings[70] to solar cells,[76, 77] photovoltaics,[78] fuel cells,[79, 80] and actuators.[81, 82] In recent years conductive polymers have also emerged as an alternative to traditional metal electrodes in a wide range of biological and bioanalytical applications.[73, 83, 84] Recent work on conductive polymers include glucose sensors,[85, 86] bioelectronic applications,[87, 88] virus detection[89] and enzyme electrodes.[90, 91] Several studies deal with applications where living cells are grown on Pedot microelectrodes.[92, 93, 94, 95] This implies that Pedot also has excellent biocompatible properties.

In this thesis Pedot conductive polymer microelectrodes are being used for electrochemical detection of neurotransmitters. The motivation for doing so, was to a large extent a series of studies from around 2006 that deal with simultaneous voltammetric detection of dopamine and different interfering electroactive biomolecules.[96, 97, 98, 99, 100] These studies were targeting the problem of detecting dopamine concentrations in biological samples such as blood samples by voltammetric methods like cyclic voltammetry and square-wave voltammetry. A major problem to this method is the presence of other electroactive molecules, such as ascorbic acid, which oxidize at approximately the same potential and are present in the samples in concentrations much higher than dopamine.[96] By using Pedot-modified electrodes the

voltammetric peaks could be separated allowing for very sensitive detection of dopamine in the presence of ascorbic acid. While several studies have shown this effect for different Pedot-modified electrodes using dopamine and ascorbic acid,[100, 101, 102] simultaneous detection of dopamine and uric acid[103, 104, 105, 106] or even a combination of dopamine, uric acid and ascorbic acid[107, 108] have also been demonstrated. In general, the superior performance of Pedot-modified electrodes is due to a negative shift in the voltammetric peaks of ascorbic acid and uric acid on Pedot electrodes. The reason for this is not understood in detail. Kumar et al.[96] explain the effect with different electrostatic and hydrophobic interactions of dopamine and ascorbic acid to “reduced” and “oxidized” regions of the Pedot film. Atta et al. showed that not only dopamine but also epinephrine, norepinephrine and serotonin can be detected in samples containing sodium dodecyl sulfate.[109] Interestingly, a recent study demonstrates that Pedot can be used to study neurotransmitter release from living cells by use of constant potential amperometry. Transmitter release from single chromaffin cells was detected at Pedot:Pss-modified metal microelectrodes by Yang et al.[110]

Chapter 2: Characterization of Poly(3,4-ethylenedioxythiophene):tosylate conductive polymer microelectrodes for transmitter detection

*Simon T. Larsen[1], Richard F. Vreeland[2], Michael L. Heien[2], and Rafael Taboryski[1,]**

** to whom correspondence should be addressed, rata@nanotech.dtu.dk*

1. Department of Micro- and Nanotechnology, Technical University of Denmark, DTU Nanotech, Building 345B, DK-2800 Kongens Lyngby, Denmark

2. Department of Chemistry and Biochemistry, University of Arizona, 1306 E. University Blvd., Tucson, AZ 85721, U.S.A

Abstract

In this paper we investigate the physical and electrochemical properties of micropatterned Poly(3,4-ethylenedioxythiophene):tosylate (Pedot:tosylate) microelectrodes for neurochemical detection. Pedot:tosylate is a promising conductive polymer electrode material for chip-based bioanalytical applications such as capillary electrophoresis, high-performance liquid chromatography, and constant potential amperometry at living cells. Band electrodes with widths down to 3 µm where fabricated on polymer substrates using UV lithographic methods. The electrodes are electrochemically stable in a range between -200 mV and 700 mV vs. Ag/AgCl and show a relatively low resistance. A wide range of transmitters are shown to oxidize readily on the electrodes. Kinetic rate constants and half wave potentials are reported. The capacitance pr area was found to be high 1670 ± 130 µF/cm^2 compared to other thin film microelectrode materials. Finally, we use constant potential amperometry to

measure the release of transmitters from a group of PC 12 cells. The results show how the current response decreases for a series of stimulations with high K^+ buffer.

Introduction

Neurotransmitters are an important class of molecules, enabling neurons to communicate with target cells using chemical signals. These signals are responsible for controlling and integrating sensory inputs into behavioral outputs. Direct measurement of these neurotransmitters and other signaling molecules provides insight into their role in biological systems. Indeed, many studies target a group of biogenic amines including dopamine, epinephrine, norepinephrine, histamine, and serotonin; all of these are electroactive and can be easily oxidized at an electrode. Due to the electroactive nature of these biogenic amines, electrochemical methods have been developed to measure them. Electrochemical methods are sensitive, quantitative, dynamic, and therefore widely used in bioanalytical approaches targeting transmitter detection.[4, 34, 111] Electrochemical methods can be used *in situ* or they can be coupled to an off-line separation technique. An attractive detection scheme for mass-limited samples is capillary electrophoresis (CE) coupled to electrochemical detection. Electrochemical detection is an alternative to laser-induced-fluorescence detection due to the fact that many compounds can be detected without derivatization with a fluorophore. In addition, both the detector and instrumentation can be miniaturized.[36] CE can be used to study transmitter distributions in small biological samples such as cells or even single vesicles.[112] Coupling electrochemical detection to high-performance liquid chromatography (HPLC) delivers comparable benefits (see above).[37] HPLC coupled with electrochemical detection can be used to rapidly measure transmitter concentrations in biological fluids.[39] In other applications, the transmitter is measured as it released *in vivo* or *in vitro*. The release of transmitters from individual vesicles (a process called exocytosis) can be detected using constant potential amperometry performed at single cells.[11] In this technique, a microelectrode is held close to the cell membrane and the released transmitter is oxidized at the electrode surface giving rise to peaks on the resultant current versus time trace.

Chip-based devices offer advantages such as high throughput, automation, and the ability to integrate different analytical features into one device.[113] In contrast, manual laboratory techniques, while they have yielded stable and successful tools for researchers, they require serial measurements and are difficult to automate. In the last

decade a strong effort has been undertaken to develop chip-based devices to overcome these limitations. Micropatterned thin-film electrodes made of platinum, gold, carbon fibers,[114] palladium[115] and pyrolyzed photoresist[51] have been used in microfabricated devices for microchip CE applications. Chip-based devices for measuring exocytosis have also been developed using platinum,[55, 116] gold,[33, 35] mercapto-propionic acid modified gold,[32] indium tin oxide[60, 62] and nitrogen-doped diamond-like-carbon as electrode materials.[34] These electrodes are typically fabricated on a glass or silicon substrate which can be further modified by bonding a PDMS counterpart.

More recently, conductive polymers have emerged as an alternative to traditional electrode materials. Polymer electrodes combine the electrical properties of metals and semiconductors with the light weight and processing properties of common polymers. Among conductive polymers Pedot is a promising material for biosensor devices focusing on neurotransmitter detection.[73] It is biocompatible with a variety of different cells,[87, 94] conductive, transparent, and stable over long time periods.[117] Dopamine and other transmitters can be selectively detected on Pedot-modified metal and glassy carbon electrodes in the presence of ascorbic acid and uric acid.[96, 109] Recently, Yang et al. demonstrated that neurotransmitter release from single chromaffin cells can be detected at Pedot:PSS microelectrodes.[110]

The synthesis of Pedot can be carried out by chemical or electrochemical polymerization of the monomer 3,4-ethylenedioxythiophene (EDOT).[72] An easy and robust chemical polymerization method uses the monomer EDOT and iron tosylate (iron(III) p-toluenesulfonate) catalyst (commercially available from Clevios™) as dopant. By adding a small amount of base (pyridine) to the monomer and dopant, polymerization can be retarded, which allows the solution to be spincoated onto substrates.[118] After baking and rinsing, a film with a positively charged polymer backbone balanced by negatively charged tosylate ions is formed.

Pedot:tosylate electrodes can be fabricated by spin-coating a solution directly onto a variety of substrates. Electrodes can then be easily patterned and integrated in chips by bonding the substrates to counterparts containing a microfluidic channel system.[119] Due to the relatively low resistivity of Pedot:tosylate compared to other conductive polymers, no metal layer is needed for supporting the electrode. This allows for inexpensive and mass-producible all-polymer devices.[119, 120] In this work we characterize the physical and electrochemical properties of Pedot:tosylate microelectrodes to examine their capacity for sensing transmitters. A variety of transmitters are shown to

oxidize at the electrode surface, and heterogeneous rate constants and half wave potentials are reported. In addition, transmitter release from cells is measured. This opens the way for cheap and easy-to-fabricate all polymer devices for electrochemical detection of transmitters in various systems.

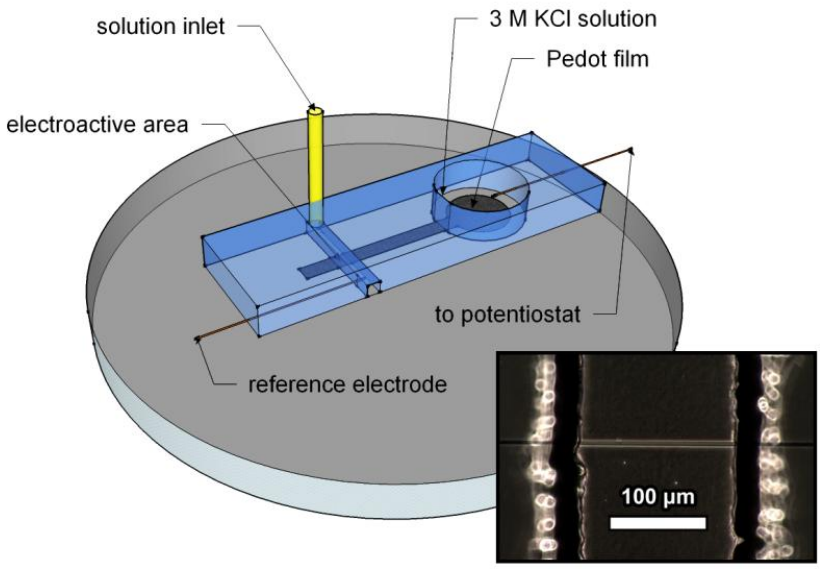

Figure 1 *Diagram of a microfluidic device for electrochemical measurements at Pedot:tosylate electrodes. Electrical contact to the Pedot:tosylate electrode is made through a Ag wire in a KCl solution. The electroactive area is defined by the geometry of the PDMS mold (not to scale). An optical image (inset) is the PDMS mold defining the electroactive area.*

Materials and Methods

Electrode fabrication and characterization. Ø 50 mm polymer substrates were prepared by injection molding of TOPAS® 5013 Cyclic Olefin Copolymer (Topas Advanced Polymers GmbH). Pedot:tosylate films were fabricated by spin-coating a solution of 6.5 mL Clevios™ CB 40 V2 (H.C.Starck), 2 mL butanol, 150 µL pyridine (Fluka) and 220 µL Clevios™ M V2 (H.C.Starck) onto the TOPAS substrates at 1000 rpm for 30 seconds. The substrates were baked on a hot plate at 70 °C to remove the remaining solvent and then washed in deionized water. Conductivity was measured with a four-point probe (Jandel Engineering Ltd) connected to a Keithley 2400 SourceMeter (Keithley Instruments Inc)

using currents in the range 1 – 10 µA. The height of the Pedot:tosylate layer was measured using a Dektak 8 profilometer (Veeco Instruments).

Electrodes were patterned by photolithography. AZ5214E photoresist was spin-coated on the Pedot:tosylate-coated substrates at 4500 rpm for 30 s. The samples were soft baked on a hot plate at 95 °C for 5 minutes before being exposed in a Karl Suss MA6/BA6 Mask Aligner for 3 seconds (intensity 7.0 mW/cm²) and developed with AZ351B Developer. The photomask was ordered at Delta Mask B.V. After photolithographic patterning, the exposed Pedot:tosylate was removed by reactive ion etching. The remaining resist was flood exposed in the Mask Aligner for 35 seconds and stripped off in an acetone bath for 5 minutes. The electrodes were rinsed thoroughly with deionized water and dried using compressed nitrogen. Band electrodes between 3 µm and 50 µm wide were fabricated.

Electrochemical measurements. Electrochemical measurements were made on a device constructed by placing a PDMS mold on a substrate (figure 1). The potentiostat (Dagan Chem Clamp, Dagan Corporation) was connected to the electrode either by a Ag wire immersed in KCl or by using conductive epoxy glue (Conductive Epoxy, Chemtronics). The electroactive area of the Pedot:tosylate film was defined by one of two methods: 1. The electrode protruded into a channel (125 µm x 110 µm, width x height) to create a band electrode (figure 1) whose electroactive area was defined by the width of the channel or 2. the band electrode protruded into a second well which was filled with solution. The electrode length depended on the penetration depth into the well and it was measured using a microscope (Nikon TE2000U, Nikon Inc.). The two geometries enabled different boundary conditions to be probed; semi-infinite or finite conditions. Data was collected using custom programs written in LabVIEW (National Instruments, Austin, Texas). These were used to apply voltages and measure the resultant current. A Ag/AgCl reference electrode (RE-5B, BASi) was placed with the tip in the PDMS well and buffer solution was added. A pneumatically actuated six port HPLC valve (Vici, Austin, TX) was connected to the solution inlet (figure 1). The valve controlled the injection of a bolus onto the electroactive area. A Harvard Ph.D. 2000 pump (Harvard Apparatus, Holliston, MA) controlled the flow rate of solutions (20 – 70 µL per minute). For rate constant determination, the background collected prior to the bolus reaching the electrode was subtracted from the cyclic voltammogram.

Chemicals. Electrochemical measurements were performed in phosphate-buffered saline (Lonza). Ferrocene methanol, carboxy-ferrocene, dopamine, epinephrine, norepinephrine, homovanilic acid, L-3,4-dihydroxyphenylalanine, 5-hydroxyindole acetic

acid, serotonin, histamine and 3,4-dihydroxyphenylacetic acid were purchased from Sigma-Aldrich and dissolved in PBS buffer.

Cell experiments. Passage 12 rat pheochromocytoma (PC 12) cells were cultured on Collagen (type 1, SigmaAldrich) coated Nunclon T25 flasks (Nunc A/S). All cell medium was carefully removed by flushing the cells with a physiological buffer (150 mM NaCl, 5 mM KCl, 1.2 mM $MgCl_2$, 5 mM glucose, 10 mM HEPES and 2 mM $Cacl_2$, from SigmaAldrich). Electrodes were coated with Poly-L-Lysine (incubation in room temperature for 1 hour, 0.01 mg/mL) before being used for cell experiments. Fresh physiological buffer was added to the flask and the cells were loosened by gently agitating the flask. The cell suspension was added to the PDMS well containing the Pedot:tosylate electrode and cells were allowed to sediment on the surface for 10 minutes. Release of transmitters was triggered by exchanging the physiological buffer with an isotonic K^+-rich buffer (KCl increased to 105 mM).

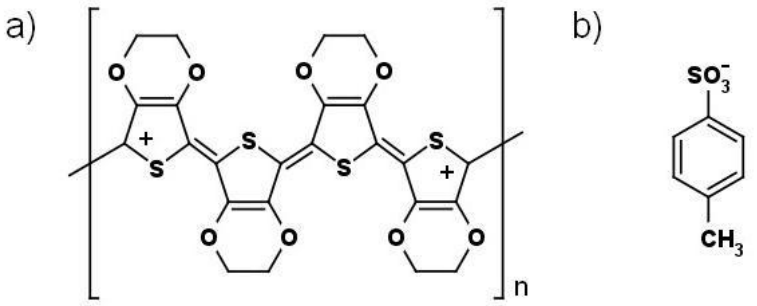

Scheme 1 *The chemical structure of a) positively charged Pedot and b) negatively charged tosylate counter ion. Redrawn from*[74].

Results and Discussion

Physical properties. Pedot:tosylate electrodes were fabricated on Topas substrates. The oxidized structure of the film can be seen in Scheme 1. Then, the physical and electrical properties of the Pedot:tosylate electrodes were characterized (Table 1). The Pedot:tosylate layer was measured to be 190 ± 10 nm high after the deposition of one layer. The height can be increased by adding multiple Pedot:tosylate layers. Four point probe measurements revealed a sheet resistance of 113 ± 7 Ω (n =10) for newly prepared Pedot:tosylate films. The measured sheet resistance corresponds to a bulk

resistivity of 470 ± 30 S/cm which is in concordance with resistivities reported in the literature for Pedot:tosylate films.[117, 120] In addition, the resistance was observed to increase over time. After 3 weeks of exposure to atmospheric conditions at room temperature, the sheet resistance of the films was 151 ± 11 Ω.

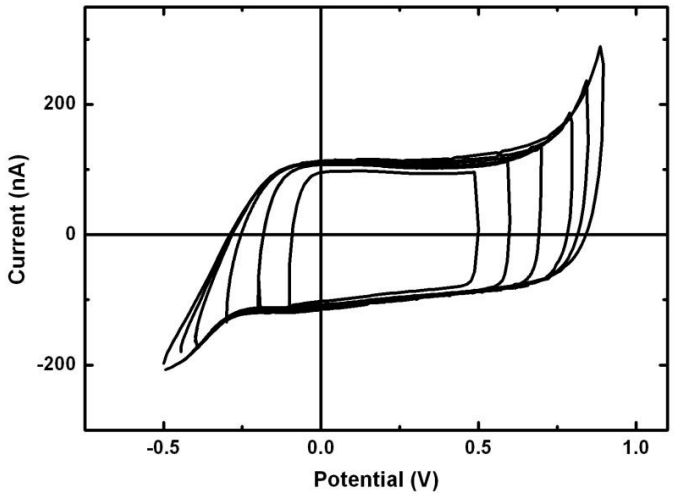

Figure 2 *Cyclic voltammograms showing the background current towards an Ag/AgCl reference electrode for a Pedot:tosylate electrode in PBS buffer. Electrode area 12 µm X 6000 µm. Scan rate 100 mV/s.*

Table 1 *Physical properties of Pedot:tosylate film electrodes (thickness = 190 nm). Error is the standard deviation (n = 10).*

Sheet resistance	113 ± 7 Ω
Capacitance per unit area	1700 ± 100 µF/cm^2
Potential-limits (vs. Ag/AgCl)	-200 mV, 700 mV

The apparent capacitance of the electrodes was measured by collecting background cyclic voltammograms at the electrodes immersed in PBS buffer. A Ag/AgCl reference electrode was used. Figure 2 shows background scans of a Pedot:tosylate band

electrode with dimensions of 12 µm X 6000 µm. Between the potential limits -200 mV and 700 mV the charging current is approximately constant. The apparent capacitance was calculated by dividing the charging current by the scan rate. The capacitance was measured to be 1670 ± 120 µF/cm^2 (n =10). In contrast to the resistance, the capacitance was stable over time and did not change significantly over a period of 8 months. These capacitance values are quite high when compared to traditional electrode materials used for transmitter detection (20 – 100 µF/cm^2 typical).[121] This high capacitance may limit the performance of Pedot:tosylate films. The root mean square noise has been reported to scale with the electrode capacitance in low-noise amperometric experiments performed at carbon-fiber microelectrodes.[122] This means that Pedot:tosylate electrodes have to be patterned on a few micrometer scale for low-noise amperometric experiments. The noise properties of Pedot:tosylate electrodes is a follow up for future studies. The increased capacitance will also affect the RC time constant of the electrode, ultimately limiting the scan rates attainable at Pedot:tosylate electrodes. These measurements indicate that stable films can be mass produced and easily stored for use.

Electrochemical properties. The performance of the Pedot:tosylate films was evaluated. Ferrocene methanol, a well-characterized molecule was oxidized at the electrode and the electrochemical properties of the Pedot:tosylate films were evaluated. Figure 3a shows the oxidation of ferrocene methanol at different concentrations at a Pedot:tosylate electrode. A band electrode was placed in bulk solution and as expected, the current approached a quasi-steady state value at voltages above the oxidation potential (measured to be 210 mV vs. Ag/AgCl). The quasi-steady state current at a band electrode is given by the following equation:

$$i_{qss} = \frac{2\pi nFlDC}{\ln\left(\frac{64Dt}{w^2}\right)} \qquad 1$$

where C is the bulk concentration, n is the number of electrons in the reaction, F is Faraday's constant, D is the diffusion coefficient, and the dimensions of the band electrode are given by the width w and length l.[123] Quasi-steady state current values were measured on each voltammogram by calculating the difference between the current before the peak and the current 100 mV past the half wave potential E½. These data were compared to calculated theoretical values (equation 1), using t = 20 s, F =

96485 C/mol and D = 6 x 10^{-6} cm^2/s. As seen in figure 3b, the measured values are in good agreement with the theoretical values. This suggests that the Pedot:tosylate film is uniform and that the measured eletroactive area is in congruence with the geometric area. This allows for estimation of concentration or geometric area if one of the two is known.

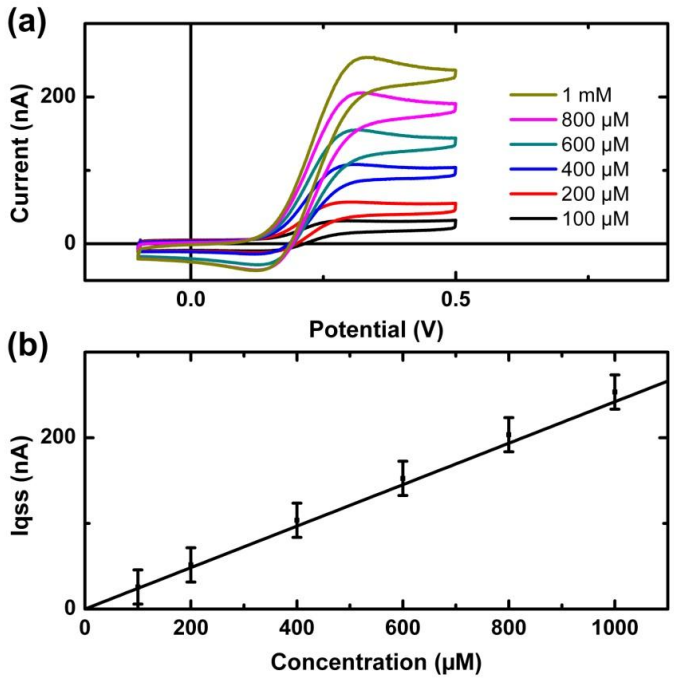

Figure 3 *a) Slow scan cyclic voltammograms showing the oxidation of Ferrocene Methanol at different concentrations at a 13 µm X 5600 µm Pedot:tosylate electrode. Scan rate 5 mV/s. A Ag/AgCl reference electrode was used. b) Quasi steady state oxidation currents for different concentrations of ferrocene methanol compared to Equation 1.*

Next, we investigated the oxidation of biogenic amines at the Pedot:tosylate electrode. The oxidation of dopamine, epinephrine, and norepinephrine at a 12 µm X 6000 µm Pedot:tosylate microelectrode is shown in figure 4. The transmitters were diluted to 20 µM in PBS buffer and a Ag/AgCl reference electrode was used. The same electrode was used for all three scans. Between experiments the electrode was cleaned by rinsing in ethanol and water and flat background scans were measured in PBS buffer in order to assure that all oxidized material was removed before addition of a new solution. The voltammograms show comparable characteristics, reflecting the similar chemical

structure and oxidation potentials of catecholamines. The current reaches an approximate steady state value. By using Equation 1, the theoretical quasi-steady state current at 50 mV above E½ can be calculated to be i_{qss}= 9.2 nA (C = 20 µM, D = 6 x 10^{-6} cm^2/s and t = 50 s, w = 12 µm, l = 6000 µm), which is comparable to the data in figure 4.

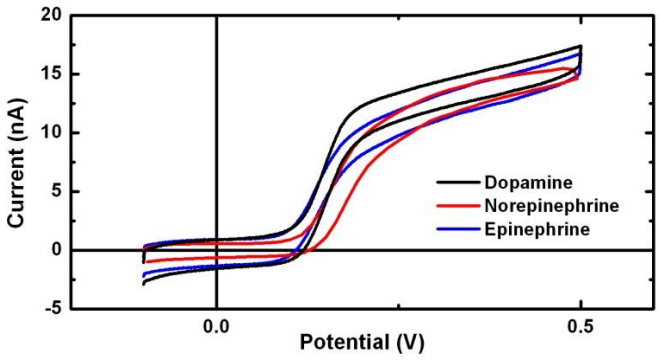

Figure 4 *a) Cyclic voltammograms showing the oxidation of dopamine (DA), norepinephrine (NE) and epinephrine (EPI) at a 12 µm X 6000 µm Pedot:tosylate electrode. Scan rate 1 mV/s. Concentration 20 µM.*

The electrochemical and heterogeneous electron transfer kinetics for different transmitters and their metabolites were evaluated at Pedot:tosylate electrodes. Results are listed in Table 2. PBS buffer (100 mM, pH = 7.4) was flowed over the electrode. A six-port HPLC valve was used to introduce a bolus solution containing the analyte to the electrode. The method of Nicholson[124] was then used to determine the heterogeneous electron transfer rate constants. These electrodes show typical rate constants for the selected neurotransmitters. This suggests that they could be used to measure these neurotransmitters in a variety of applications. However, the anodic potential limit of 0.7 V vs. Ag/AgCl limits their use. For example, histamine could not be oxidized at this potential, and thus could not be detected.

Table 2 *Heterogeneous electron transfer rate constants and half wave potentials for selected molecules.**

	DOPAC	HVA	DA	NE	E
k_{avg}	3.1	1.3	3.1	2.3	1.5
±	0.8	0.2	0.6	0.4	0.7
E ½	141	403	149	164	144
±	4	18	7	4	4
	L-DOPA	5-HIAA	5-HT	Hist	Fc-COOH
k_{avg}	3.3	1.3	2.3	n/a	4.9
±	0.4	0.7	0.9	-	0.6
E ½	163	291	327	-	213
±	2	7	4		3

*** Rate constants (cm/s x 10^{-3}) were determined by the method of Nicholson.[124] Error is the standard deviation (n = 2 -3). Half wave potentials (mV) referenced to Ag/AgCl (n = 3-4). DOPAC: 3,4-dihydroxyphenylacetic acid, HVA: homovanilic acid, DA: dopamine, NE: norepinephrine, E: epinephrine, L-DOPA: L-3,4-dihydroxyphenylalanine, 5-HIAA: 5-hydroxyindoleacetic acid, 5-HT: serotonin, Hist: histamine, Fc-COOH: Ferrocene methanol.*

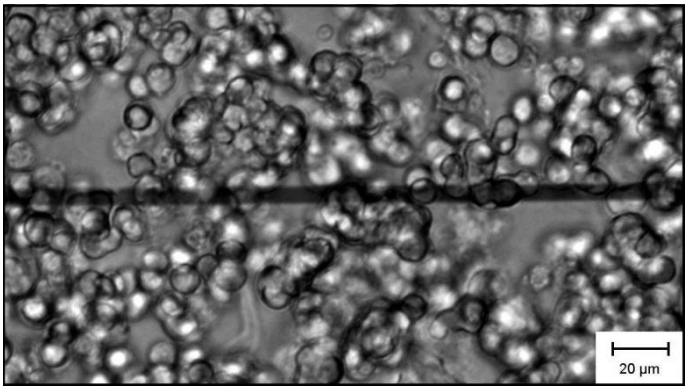

Figure 5 *PC 12 cells sedimented on a 7 µm wide Pedot:tosylate electrode.*

Release from cells. To test the materials ability to measure release from cells, we used a Pedot:tosylate electrode to measure the release of transmitters from a population of PC

12 cells using constant potential amperometry. Prior to measurement, the electrode was coated with Poly-L-Lysine to promote cell adhesion. PC 12 cells are known to release catecholamines upon stimulation with a K^+-rich buffer. In this experiment, the cells were rinsed thoroughly with a physiological buffer prior to harvesting, to ensure that any oxidizing species in the growth buffer was removed. The same buffer was used to transport the suspended cells to the electrodes where they were plated on the substrate. A microscope image of a large group of PC 12 cells on a Pedot:tosylate electrode is shown in figure 5. A 350 mV potential was applied and the recording was started once the current had decayed to a value below 100 pA. Without removing the cells from the surface, the physiological buffer was exchanged with an isotonic buffer containing elevated K^+ (105 mM). The current was recorded for 3 minutes before the buffer was exchanged to physiological buffer. A rest time of 4 minutes was used between subsequent stimulations. The electrode was visually inspected to ensure that the same group of cells was present between each stimulation. Figure 6 shows the current traces obtained by stimulating a group of PC 12 cells five times. The current response clearly decreases after each successive stimulation. This could be due to depletion of vesicles by the long-lasting stimulation used to evoke exocytosis.

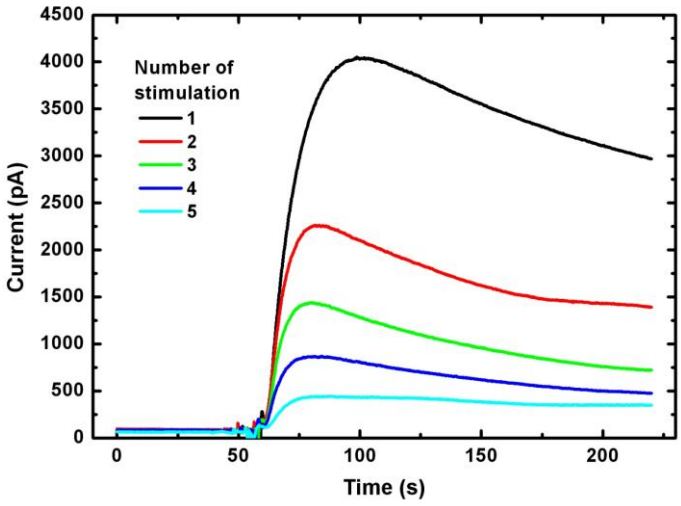

Figure 6 *Amperometric responses resulting from neurotransmitter release from a group of PC 12 cells at a Pedot:tosylate electrode. The cells were alternately exposed to a K^+-rich buffer for 3 minutes and a low K^+ buffer for 4 minutes. The highest response resulted from the first stimulation by a K^+-rich buffer. Subsequent stimulations resulted in decreasing current responses.*

Conclusion

In this paper we demonstrated the use of conductive polymer Pedot:tosylate microelectrodes for electrochemical transmitter detection. A wide range of transmitters were shown to oxidize readily on the electrodes and kinetic rate constants and half wave potentials were reported. Out of 10 tested transmitters, only histamine had its oxidation potential outside the potential-limits of Pedot:tosylate, and could not be detected. The capacitance per area was found to be high compared to other thin film microelectrode materials, which could be a limitation for use in low-noise amperometric measurements. However, this limitation can be overcome by making the electrodes sufficiently small. Further, we used constant potential amperometry to measure the transmitter release from a group of PC 12 cells following a series of stimulations with high K^+ buffer. Since the cells stay fixed during the exchange of buffers, current responses from the same group of cells can be compared and used for pharmacological screening applications. The study shows that Pedot:tosylate is a promising electrode material in chip-based devices for transmitter detection. This opens the way for cheap and easy-to-fabricate all polymer devices for several bioanalytical applications such as HPLC, capillary electrophoresis, and drug screening.

Chapter 3: Amperometric noise at thin film band electrodes

*Simon T. Larsen[1], Michael L. Heien[2], and Rafael Taboryski[1]**

** to whom correspondence should be addressed, rata@nanotech.dtu.dk*

1. Department of Micro- and Nanotechnology, Technical University of Denmark, DTU Nanotech, Building 345B, DK-2800 Kongens Lyngby, Denmark

2. Department of Chemistry and Biochemistry, University of Arizona, 1306 E. University Blvd., Tucson, AZ 85721, U.S.A

Abstract

Background current noise is often a significant limitation when using constant-potential amperometry for biosensor application such as amperometric recordings of transmitter release from single cells through exocytosis. In this paper, we fabricated thin-film electrodes of gold and conductive polymers and measured the current noise in physiological buffer solution for a wide range of different electrode areas. The noise measurements could be modeled by an analytical expression, representing the electrochemical cell as a resistor and capacitor in series. The studies revealed three domains; for electrodes with low capacitance the amplifier noise dominated, for electrodes with large capacitances the noise from the resistance of the electrochemical cell was dominant, while in the intermediate region the current noise scaled with electrode capacitance. The experimental results and the model presented here can be used for choosing an electrode material and dimensions, and when designing chip-based devices for low-noise current measurements.

Introduction

Electrochemical detection using constant-potential amperometry is a widely used technique in biosensor applications. Many biologically interesting molecules are

electroactive and can thus be oxidized at an electrode held at a sufficient positive potential. Amperometric detection is used in applications such as capillary electrophoresis,[112][36] high performance liquid chromatography,[37] and measurements of neurotransmitter release from living cells.[4] Electrical background noise is one of the major limitations of amperometric detection defining the limit for smallest possible detectable signals. The signal-to-noise ratio is often used to quantify the precision of amperometric data.

Microelectrodes coupled with low-noise amplifiers have been used to measure currents with noise levels down to the femtoampere region.[11] Traditionally carbon-fiber microelectrodes have received the most attention due to their excellent low-noise properties, but in the last decade much research has focused on developing thin-film microelectrodes from different electrode materials for amperometric detection using chip-based devices. These materials include gold,[32, 33] platinum,[55] indium tin oxide,[62] pyrolyzed photoresist,[51] diamond-like carbon[125] and conductive polymers like Pedot:Pss[110] and Pedot:tosylate.[126]

Current noise is generally measured in terms of the root mean square of the current. General theories on current noise in electrochemical detectors covering also faradaic currents have been presented.[127, 128] In constant potential amperometric recordings of exocytosis, the faradaic signal only gives rise to small current transients and the major noise concern is typically associated with the background noise of the electrode resulting from non-faradaic interactions between the electrode and the physiological salt buffer.[35, 60, 63, 129] This amperometric background noise is often thought of as being proportional to electrode capacitance and hence electrode area.[122, 130, 131] For carbon fiber-microelectrodes this was shown to be the case except for very small electrodes where the amplifier noise became predominant.[129] The proportionality between the root mean square noise and the electrode area was also demonstrated for thin-film electrodes made of gold[35] and indium tin oxide.[60, 63] For Pedot:Pss conductive polymer microelectrodes larger electrodes were shown to be more noisy,[110] while for micrometer-sized platinum electrodes the current noise was indistinguishable from amplifier noise in the open loop configuration.[55]

In this paper we present extensive amperometric noise data for thin-film microelectrodes held at a constant potential in a physiological buffer. The experimental set-up and the measurement parameters correspond to those used in typical low-noise amperometric measurements of exocytosis from single cells. Electrodes were made of gold and conductive polymers Pedot:Pss and Pedot:tosylate. These materials differ

widely in capacitive properties, allowing for the analysis of noise behavior for a wide range of electrode capacitances. In addition, we present a simple and adequate noise expression, depending only on the electrode capacitance, the resistance of the cell, the filter frequency, and the open loop amplifier noise. Experimental data strongly supports the analytical solution. We find that the noise scales with the electrode capacitance except for very small capacitances where the potentiostat noise dominates and for sufficiently large capacitances where the noise is equal to the Johnson-Nyquist noise of the circuit resistance. The dependence of the noise on circuit resistance is also modeled. Limits for the different noise regimes are reported and some practical suggestions are provided for designing thin-film microelectrodes for low-noise amperometry applications.

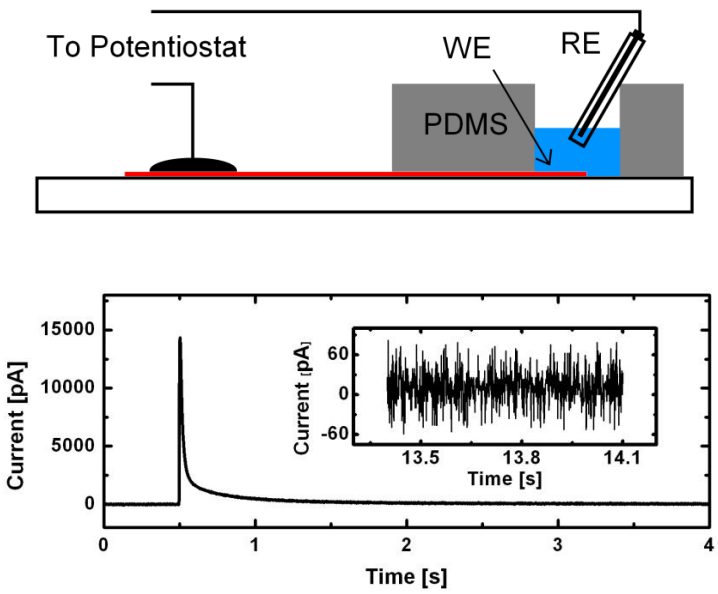

Figure 1. *a) Electrochemical set-up. The active working electrode (WE) is defined by the area of a thin film band electrode (red) protruding into a well made of PDMS. The reference electrode (RE) is placed in the buffer solution (PBS). b) Current response following a voltage step (0 mV to 100 mV) at a Pedot:tosylate microelectrode. The inserted graph is showing the noisy current trace at a later time where the current has reached a constant value.*

Materials and Methods

Pedot:tosylate band microelectrodes were fabricated on polymer (TOPAS) substrates as described earlier.[126] Pedot:Pss band electrodes were prepared by spin-coating Pedot:Pss aqueous solution (483095, Sigma-Aldrich) at 1000 rpm for 30 s onto polymer (TOPAS) substrates. Pedot:Pss samples were subsequently covered with 70% DMSO(>99% purity, Merck, Germany) in water, heated at 70°C for 5 minutes and washed in deionized water. Patterning of the Pedot:Pss layer was done as described earlier for Pedot:tosylate microelectrodes.[126]

Gold microelectrodes were fabricated on 4'' Boron glass wafers. The glass wafers were placed over night in a 250 °C oven and then silylated with hexamethyldisilazane (HMDS). A 1.5 µm layer of AZ5214E photoresist was spin-coated on the glass wafers. The samples were baked at 90 °C for 60 seconds before being exposed in a Karl Suss MA6/BA6 Mask Aligner for 6 seconds (intensity 7.0 mW/cm²) and developed with AZ351B Developer. The photomask was ordered at Delta Mask B.V. Residual resist was removed with a Plasma Asher (TePla). A Wordentec QCL800 Metal evaporator was used to first evaporate a 5 nm adhesion layer of chrome (1 n/s, 5 s) and then 150 nm of gold (1 n/s, 150s). Finally, resist was lifted off in acetone, and the electrode substrates were rinsed with isopropanol and water and dried. For all electrode materials, electrodes between 3 µm and 50 µm wide and 6 mm long were fabricated.

Electrochemical noise measurements were made using an Axopatch 200B (Molecular Devices) amplifier. The resistive feedback configuration was used. In order not to limit the measurement bandwidth we worked in the $\beta = 0.1$ configuration with feedback resistance $R_f = 50$ MΩ, while low-pass filtering at 1 kHz using the 4 pole Bessel filter of the amplifier. The gain used was 20 mV/pA for noise measurements, but in general the noise did not depend on the gain unless a very low gain was used. A PDMS well was fabricated and bonded to an electrode surface. The band electrode protruded into the bonded PDMS well which was filled with PBS buffer (phosphate-buffered saline, Sigma Aldrich). The electrode length depended on the penetration depth into the well and it was measured using a microscope. A Ag/AgCl reference electrode (RE-5B, BASi) was placed with the tip in the PDMS well and connected to the amplifier headstage. Connections to the working electrode were made using conductive epoxy glue (Conductive Epoxy, Chemtronics).

Current data was collected using an amperometry program written in LabVIEW (National Instruments, Austin, Texas). The voltage was applied at the Axopatch 200b amplifier. For each noise measurement, five short noise traces were measured and the average of the offset corrected root mean square of the current was used to describe the magnitude of

the noise. Conductivity was measured with a four-point probe (Jandel Engineering Ltd) connected to a Keithley 2400 SourceMeter (Keithley Instruments Inc).

The uncertainty of experimental noise data was estimated by using the uncertainties of capacitance, resistance and open loop current noise values and calculating the propagated error of the theoretical value for the same parameters. For discrete resistors and capacitors, the uncertainty was provided by the manufacturer to be 5 % for resistors and 20 % for capacitors. For electrodes, the capacitance uncertainty was dominated by the uncertainty in area estimation using optical microscopy.

Results and Discussion

All noise measurements were carried out using an Axopatch 200B amplifier connected to an electrochemical cell corresponding to the one depicted in figure 1a. Thin-film band electrodes were fabricated on either glass or polymer substrates and active areas were defined by bonding the substrates to PDMS wells. After bonding, the exact electrode area could be determined by microscopic observation. Noise traces were recorded after applying a constant voltage (100 mV) to the electrochemical cell and waiting until the current had decayed to approximately zero (figure 1b). Interference noise from 50 Hz noise sources was avoided by shielding with two separate faraday cages, an outer cage held at earth ground and an inner cage connected to signal ground from the amplifier. The noise was low pass filtered at 1 kHz using the 4 pole Bessel filter of the Axopatch 200B amplifier. This frequency is within the range of filter frequencies typically used for amperometric exocytosis measurements at single cells.[34, 132]

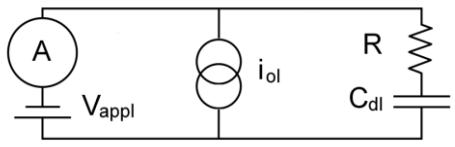

Figure 2: *Simple equivalent circuit for electrochemical cell. V_{appl} is the applied potential, C_{dl} the double-layer capacitance of the electrode, R the sum of resistances in series with the electrode and i_{ol} the open-loop current noise represented as a current source in parallel with the cell.*

The noise model used in this work is based on the simplified equivalent circuit shown in figure 2. Here the electrode is represented as a perfect capacitor while the solution resistance of the buffer and the resistance of wires and isolated electrode connections is represented by a resistor with resistance R. The current noise measured at an open loop configuration is represented as a current source in parallel with the cell. This noise is a measurable quantity and may, except for operational amplifier noise of the headstage, also include microphonic noise in cables or possibly interference noise from non-efficient shielding. Other noise sources of practical nature like noise in liquid junctions are assumed to play a minor role compared to intrinsic voltage noise of the circuit and therefore neglected.

We describe the total current power spectral density S_i as the sum of power spectral densities from uncorrelated random noise sources. Shot noise has been disregarded as a noise source since the background current in our experiment is close to zero. This leaves the open loop current noise $I_{RMS,ol}$ with power spectral density $S_{i,ol}$ as well as current noise from ohmic behavior of voltage noise sources. Since, in this work we are interested in microfabricated thin film electrodes where isolated electrode segments and the buffer solution typically give rise to series resistances above 10^4 Ω, the Johnson-Nyquist noise from R is the main contribution of voltage noise. Since the current noise is given by the voltage noise divided by the impedance, we write the total power spectral density of the current noise as

$$S_i(f) = \frac{4kTR}{R^2 + \frac{1}{(2\pi f C)^2}} + S_{i,ol}(f) \qquad 1$$

where k is Boltzmann's constant (1.38 x 10^{-23} J/K), T the absolute temperature and f the frequency in Hz. The interesting experimental noise parameter is the root mean square of the current trace. The current trace is typically filtered with a low-pass active analog filter with cut-off frequency f_c. Assuming the low-pass filter is ideal, i.e. all signals below f_c pass and all signals above f_c are stopped, the root mean square current noise can be found by integrating the power spectral density from f=0 to f=f_c.

$$I_{RMS}{}^2 = \int_0^{f_c} S_i(f) df \qquad 2$$

Integrating equation 1, we obtain:

$$I_{RMS}{}^2 = \frac{4kT}{R}\left(f_c - \frac{1}{2\pi RC} Arctan(2\pi RC f_c)\right) + I_{RMS,ol}{}^2 \qquad 3$$

Here, $I_{RMS,ol}$ is the root mean square current noise of the headstage in an open loop configuration.

For real low-pass filters, the cut-off is not sharp but extends over a range of frequencies. Therefore a more accurate estimate for the root mean square current noise is found by multiplying the power spectral density of the unfiltered input by the square of the filter transfer function's magnitude response $|H(j\omega)|$ before integration.

$$I_{RMS}{}^2 = \int_0^\infty |H(j\omega)|^2 S_i(f) df \qquad 4$$

where j is the imaginary unit and ω=2πf the angular frequency. Transfer functions can be rather complicated mathematical functions, which makes equation 4 better suited for numerical integration than analytical evaluation.

In this paper, we used the analog 4 pole Bessel filter of the Axopatch 200B amplifier for noise measurements. The filter cut-off frequency was held at 1 kHz for all measurements. The open loop root mean square current noise was measured before each experiment. It was typically around 0.7 pA in the measurement bandwidth[1]. This leaves only two unknown quantities in equations 1 and 3, the electrode capacitance and the resistance in series.

[1] The relatively high open loop noise is due to choice of feedback element on the Axopatch amplifier. The lower (and noisier) feedback resistor (50 MΩ) was chosen in order to get a larger output bandwidth of the probe.

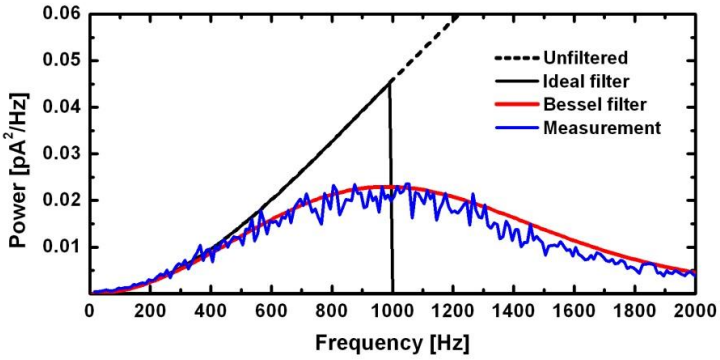

Figure 3: *Measured power spectral density of the current noise for a 1 nF capacitor and a 100 kΩ resistor in series held at 100 mV and low-pass filtered at 1 kHz through an analog 4 pole Bessel filter at an Axopatch 200B amplifier (blue) plotted along with theoretical plots for ideally filtered and 4 pole Bessel filtered power spectral densities.*

First we test our model by replacing the electrochemical cell by discrete resistors and capacitors. The blue line in figure 3 shows the measured power spectral density of the current noise, when using a 1 nF capacitor and a 100 kΩ resistor in series. The dashed black line shows the calculated power spectral density using equation 1. The noise power is plotted as pA^2/Hz and the open loop noise is neglected in this example since it is much lower than the Johnson-Nyquist noise from the resistor. Assuming an ideal filter with cut-off at 1 kHz, the filtered power spectral density would correspond to the solid black line and the root mean square noise would be equal to the integral of this. Taking into account the 4 pole Bessel filter and multiplying the power spectral density with the square of the filter transfer function's magnitude response $|H(j\omega)|$,[133] a better estimate of the power spectral density can be found (red line, figure 3). It should be noted that the choice of resistor and capacitor in this example was made to illustrate the difference between using equation 2 and 4. In most cases, the difference in root mean square currents calculated by taking the Bessel filter transfer function into account or using the simpler analytical solution for an ideal filter is less pronounced than in figure 3.

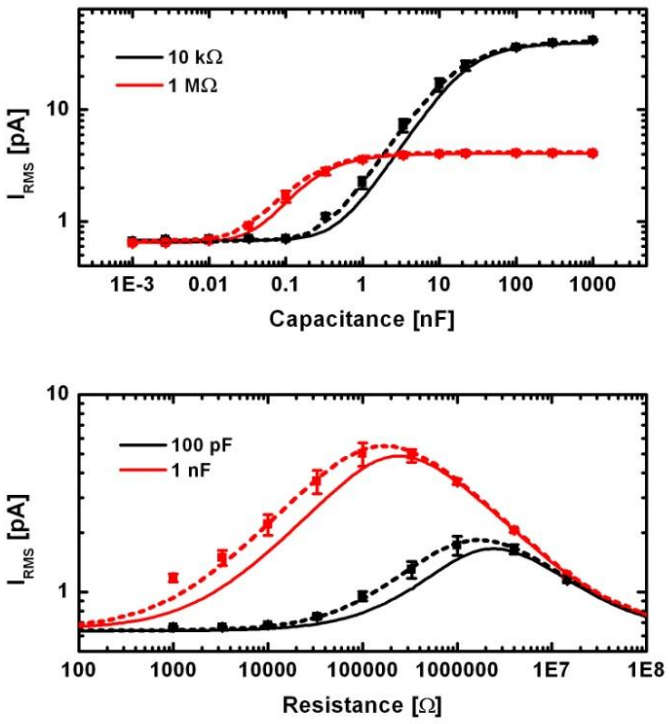

Figure 4: *The root mean square current noise values for sets of discrete resistors and capacitors in series. Capacitance is varied in the upper graph while resistance is varied in the lower graph. Solid lines show calculated noise values corresponding to equation 3. Dashed lines show noise values calculated by numerical integration of equation 4. (Filter frequency: 1 kHz,* $I_{RMS,ol}$*=0.65 pA.)*

In figure 4, we show measured root mean square current noise values for a wide range of different resistors and capacitors. Five short noise traces were measured for each configuration and the average of the offset corrected root mean square current noise was plotted. Along with experimental values, theoretical curves are plotted corresponding to root mean square current noise values calculated using equations 3 and 4. Clearly, the theoretically calculated values fit the measured values nicely. This indicates that equation 3 and 4 can describe current noise at electrodes if the equivalent circuit of the electrochemical cell can be described as a resistor and capacitor in series. As expected, taking the Bessel filter behavior into account, the best match with experiments is obtained, but also the simpler analytical solution of equation 3 describes the noise very well.

Observing the noise behavior in figure 4, we notice three domains; the noise is constant for 1. very low or 2. very large capacitances. At lower capacitances, the open loop current noise dominates completely, while at the large capacitances, the noise is equal to the Johnson-Nyquist noise from the resistor meaning the capacitance has no effect on the noise. 3. In the intermediate region, the root mean square scales with capacitance. Indeed, for small capacitances, using the two first terms of the Arctan Taylor expansion, equation 3 becomes

$$I_{RMS}{}^2 = \frac{4}{3} kTR(2\pi C)^2 f_c{}^3 + I_{RMS,ol}{}^2 \qquad 5$$

Equation 5 fits the measured noise values shown in figure 4 corresponding to low and intermediate capacitances. As long as the open loop noise has no effect, the root mean square current noise is directly proportional to the capacitance. Since the capacitance of an electrode is generally proportional to the electrode area, the root mean square noise is proportional to area. This result is in agreement with literature on the subject of microelectrode noise (*vide supra*). The criterion for being in the large capacitance region is that resistance dominates the total cell impedance, i.e. $R^2 \gg 1/(2\pi fC)^2$. Oppositely, if capacitance dominates the impedance, noise scales with capacitance until amplifier noise becomes dominant.

Varying the resistance results in peak-shaped noise curves (figure 4). For very large resistances, the current noise decreases, but for these values the time constant of the electrochemical cell τ = RC also increases. This is an unwanted side effect for fast sampling experiments. Reducing the resistance is often the best approach although this can be difficult in chip-based devices, where solution resistance in microfluidic channels is often significant.

In the experimental work presented here we limit our noise investigation to variations in cell resistance and capacitance. This is due to the fact that the two other variables in equation 3, the open loop amplifier noise and the low pass cut-off filter frequency, have a much simpler effect on the noise. As mentioned above, the open loop amplifier noise just determines the noise level for very low capacitances. For the filter cut-off frequency, noise increases with increasing frequency except for very low capacitances.

Next, we turn our attention to real electrodes. If the electrochemical cell can be described by a capacitor and resistor in series, the model presented here should apply to

the current noise. As mentioned above, the capacitance of an electrode is generally proportional to the electrode area. It can be described by the expression

$$C = \left(\frac{C}{A}\right)_i A\,, \qquad 6$$

where the capacitance per area $(C/A)_i$ is a constant depending on the electrode material. In this work, we find $(C/A)_i$ for each electrode material by measuring the capacitance of a large electrode and dividing it by the area. The apparent capacitance is found by dividing the charging current measured at a cyclic voltammogram by the scan rate. Although this method is based on a simplification since capacitance can also be a function of voltage and scan rate, it is an appropriate estimate of the electrode capacitance for many electrodes. Substituting C in equation 3 by the above expression (eq. 6) gives us a noise theory depending on electrode area and series resistance of the electrode.

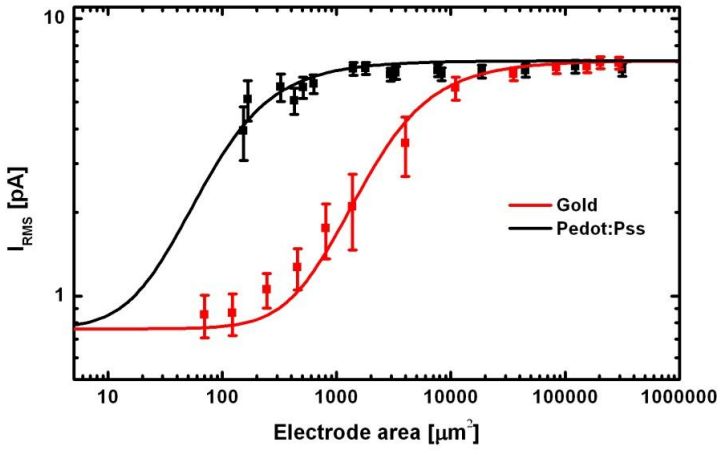

Figure 5: *Measured current noise values as a function of electrode area at gold and Pedot:Pss electrodes. A large external resistor (330 kΩ) was connected in series with the electrodes to give a dominate resistance. Solid lines show expected theoretical noise values given by equation 3.*

Estimating the series resistance of an electrode system is more difficult, since it depends on both electrode connections and the resistance of the solution. In chip-based devices, the working electrode is typically connected to the potentiostat by an electrode segment isolated by the substrate and the bonded counterpart as shown in figure 1a. For a band electrode of length l and width w, the resistance of this wire is given by

$$R = R_s \frac{l}{w}, \qquad 7$$

where R_s is the sheet resistance of the film. For metal electrodes the resistance of isolated electrode connections is typically negligible compared to other resistance sources, but for electrodes made of materials with higher resistivity like conductive polymers or pyrolyzed photoresist, this resistance can be significant.

The solution resistance which makes up another significant part of the total resistance is generally thought to be inversely proportional to electrode radius for disk microelectrodes.[123, 134] Assuming spherical symmetry around the microelectrode, this resistance could be described by the equation

$$R_u = \frac{1}{4\pi\kappa r_0} \qquad 8$$

Here κ is the conductivity of the solution and r_0 the radius of the disk microelectrode. For the band electrodes used in this work equation 6 does not apply directly since we have neither spherical symmetry nor disk shaped electrodes. It is reasonable though to assume the solution resistance to be inversely proportional to a critical electrode dimension. If we assume this dimension to be the length of the band electrode, the total resistance of the electrochemical cell can be expressed as

$$R = R_{el} + \frac{k_s}{l} \qquad 9$$

Here the first tem R_{el} is the resistance of isolated parts of the electrode (and wires), k_s is a constant depending on the buffer solution and placement of the reference electrode and l is the electrode length.

In order to test the applicability of our theory on real electrodes, we first connected a large discrete resistor (330 kΩ) in series with different band electrodes, while keeping electrode connections short and the reference electrode close to the band electrodes. The discrete resistor dominates the total resistance making the measurements easier to compare to theory. Figure 5 shows noise results for Pedot:Pss and gold electrodes varying in area between 100 μm^2 and 10000 μm^2. The noise at gold electrodes is clearly smaller than the noise at Pedot:Pss electrodes. Using cyclic voltammetry, we measured the apparent capacitance per area of the electrodes (table 1). Using these values and equations 3 and 6, we now plot the theoretical electrode noise as a function of area (solid lines, figure 5). Clearly, the theory fits the experimental data well. The large difference in capacitance properties between Pedot:Pss and gold is reflected in the displacement of the two graphs along the x-axis. Much smaller capacitance Pedot:Pss electrodes are needed to achieve the same low noise as at gold electrodes.

Table 1 *Capacitance per area and sheet resistance for electrodes used for noise measurements.*

Gold	18.6 ± 2.0 $\mu F/cm^2$	0.185 Ω ± 0.005 Ω
Pedot:Pss	460 ± 60 $\mu F/cm^2$	3200 Ω ± 200 Ω
Pedot:tosylate	1700 ± 100 $\mu F/cm^2$	580 Ω ± 70 Ω

Finally, we present noise measurements from electrodes with no external resistor connected. The set-up is as shown in figure 1a. The electrode capacitance is still given by equation 6, while the resistance is now coming only from the isolated electrode segments and the solution. In figure 6, we show noise results for Pedot:tosylate and gold electrodes. The area of the electrode is varied by shortening the length of the electrode protruding into the PDMS well. Equation 3 is used to fit the experimental noise data. The expressions for resistance and capacitance given by equations 6 and 9 are used and least squares fitting is done using R_{el} and k_s as fitting parameters. Resulting fits are in good

agreement with experimental values and are shown as solid lines in figure 6. The least squares fitting resulted in the following parameters: R_{el} = 439 Ω,k_s = 41.8 Ω x m for Gold and R_{el} = 152000 Ω,k_s = 35.6 Ω x m for Pedot:tosylate. Since the same reference electrode and buffer solution is used for both electrodes, it is expected that the fitted k_s-values do not differ much. Further, the R_{el} values are also realistic, and reflect the large difference in sheet resistance for thin films of gold and Pedot:tosylate (table 1). Indeed, if the dimensions of the electrode connections used in this experiment (3.75 µm x 2900 µm for Gold and 4.6 µm x 900 µm for Pedot:tosylate) are used together with equation 7 and the sheet resistance values of table 1, calculated electrode connection resistances are 143 Ω for Gold and 114000 Ω for Pedot:tosylate. These values are in the same order of magnitude as the fit R_{el}-values.

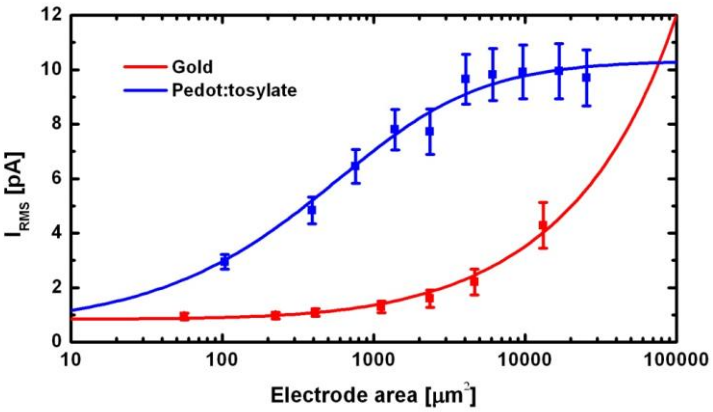

Figure 6: *Current noise measurements at gold and Pedot:tosylate band electrodes. Solid lines show theoretical noise obtained by least squares fitting of equation 3.*

A few practical points can be made in relation to the electrode noise measurements presented here. First, for low noise current amperometry, the choice of electrode material is important. As seen in figure 6, Pedot:tosylate electrodes had to be made almost two orders of magnitude smaller than gold electrodes to reach the same noise level. Second, the resistance of electrode wires and the solution resistance in microfluidic channels also affect the noise. If this resistance dominates the impedance of the electrochemical cell, the noise is equal to the Johnson-Nyquist noise of the resistance as seen for the large Pedot:tosylate electrodes in figure 6. In this regime, the

noise decreases for increasing resistance but simultaneously the time constant increases, making the system more sluggish.

Conclusion

In this work we presented an analytical solution for the current noise at microelectrodes during constant potential amperometry experiments such as amperometric recordings of transmitter release events from single cells. Thin-film band microelectrodes were fabricated in three different electrode materials with different capacitive properties, and current noise was measured for a wide range of different electrode areas. The results agreed very well with the analytical noise expression. Our results emphasize the importance of choosing low capacitive electrode materials and small electrodes if low current noise is crucial. We observed three different noise regimes. 1. For very low capacitances, the noise was equal to the open loop noise of the potentiostat 2. For very large capacitances, the noise was equal to the Johnson-Nyquist noise of the resistance of the electrochemical cell. 3. In the intermediate region, noise scaled with capacitance. The noise expression presented here could be used for designing chip-based devices with integrated microelectrodes for low-noise amperometric sensing

Acknowledgments

This work is supported by the Danish Council for Strategic Research through the Strategic Research Center PolyNano (grant no. 10-092322/DSF)

Chapter 4: All polymer chip for amperometric studies of transmitter release from large groups of neuronal cells

*Simon T. Larsen, and Rafael Taboryski**

** to whom correspondence should be addressed, rata@nanotech.dtu.dk*

Department of Micro- and Nanotechnology, Technical University of Denmark, DTU Nanotech, Building 345B, DK-2800 Kongens Lyngby, Denmark

Abstract

We present an all polymer electrochemical chip for simple detection of transmitter release from large groups of cultured PC 12 cells. Conductive polymer Pedot:tosylate microelectrodes were used together with constant potential amperometry to obtain easy-to-analyze oxidation signals from potassium-induced release of transmitter molecules. The nature of the resulting current peaks is discussed, and the time for restoring transmitter reservoirs is studied. The relationship between released transmitters and potassium concentration was found to fit to a sigmoidal dose-response curve. Finally, we demonstrate how the presented device can be used for simple drug screening purposes, by measuring the increase of transmitter release due to short-term treatment of L-DOPA.

Introduction

Neurotransmitters play an important role in signaling mechanisms of the central nervous system.[1] In response to stimulation, neurons release neurotransmitters stored in membrane-bound vesicles to the extracellular space by a process termed exocytosis. During exocytosis vesicles fuse with the plasma membrane of the cell. The released molecules are recognized by specific receptors at the target cell membrane. A range of transmitter molecules are electroactive and oxidize easily at microelectrodes held at a

sufficiently high potential. In the last two decades, constant potential amperometry has therefore been used heavily to measure the activity of neuronal cells and the dynamics of exocytosis.[4, 11] Traditionally, carbon fiber microelectrodes have been the golden standard for these studies, but in the last decade much research has focused on developing thin-film microelectrodes of other materials like gold,[135] platinum,[55] indium tin oxide[62] and diamond-like carbon[125] for amperometric detection of exocytosis in chip-based devices.[111]

Amperometric studies of exocytosis have been used to investigate the effect of different drugs on the activity of neuronal cells. Rat pheochromocytoma (PC 12) cells are a widely used neuronal model cell for in vitro amperometric exocytosis studies, due to their versatility for pharmacological manipulation, ease of culture and the large amount of background knowledge on their proliferation and differentiation.[12, 136] At PC 12 cells, the dopamine precursor L-DOPA has been shown to up-regulate transmitter release,[22] while other drugs like reserpine,[22, 137] amphetamine[138, 139] and quinpirole[140] seem to reduce transmitter release. Most of these studies were done by measuring vesicle content and release frequency on a large number of single vesicle events. Using carbon fiber microelectrodes, the mean vesicle content was shown to increase with increasing time of exposure of PC 12 cells to L-DOPA.[136] Only a few studies measure the release of transmitters from large groups of PC 12 cells. The increase in overall transmitter release due to L-Dopa and the decrease in release due to reserpine was measured using a silicon based chip with PC 12 cells attached to collagen coated gold electrodes.[54, 141]

In recent years conductive polymers have emerged as an alternative to traditional metal electrodes in a wide range of biological and bioanalytical applications.[73, 83, 84] Recent work on conductive polymers include glucose sensors,[85, 86] bioelectronic applications,[87, 88] virus detection[89] and enzyme electrodes.[90, 91] Conductive polymer electrodes combine the electrical properties of metals and semiconductors with the light weight, biocompatibility and processing properties of common polymers. Among conductive polymers Poly(3,4-ethylenedioxythiophene) (Pedot) has been shown to be a promising material for electrochemical detection of neurotransmitters.[96, 109, 126] Transmitter release from single chromaffin cells was detected at Pedot:PSS microelectrodes.[110] The authors of this paper showed recently, that a wide range of transmitter molecules oxidize readily on free standing Pedot:tosylate microelectrodes.[126]

In this work, we present a simple, cost-efficient and disposable polymer biochip for measuring transmitter release from large groups of PC 12 cells. Pedot:tosylate microelectrodes were fabricated on polymer substrates and bonded with PDMS to

create a flow cell across the microelectrode for buffer exchange. PC 12 cells were trapped on the electrodes using Poly-L-Lysine coating and easily analyzable current responses due to transmitter release were measured. The polymer chips were used to measure the time needed to restore the releasable pool of transmitters in PC 12 cells. The dose response relationship for potassium stimulation was studied and L-DOPA was used to show the potential of the device for drug screening applications.

Materials and Methods

Pedot:tosylate microelectrodes were fabricated on flat, Ø 50 mm injection molded Cyclic Olefin Copolymer (Topas Advanced Polymers GmbH) wafers using UV lithography as described earlier.[126] The electrode width was between 10 and 20 µm and the length 6 mm. A 2-3 mm wide and 3 cm long rectangular well was constructed in PDMS and bonded to the TOPAS substrate perpendicular to the microelectrode. The active area of the electrode was defined by the width of the electrode and the width of the PDMS channel. The Pedot:tosylate microelectrode was connected to a copper wire in one end using conductive epoxy glue (Conductive Epoxy, Chemtronics). Before cell experiments the bottom surface of the wells were incubated in Poly-L-Lysine solution (40 µL per chip, 0.01% solution, P4707, Sigma Aldrich) for one hour, washed with deionized water and dried.

Passage 12 rat pheochromocytoma (PC 12) cells were cultured on Collagen (type 1, SigmaAldrich) coated Nuncleon T25 flasks (Nunc A/S). When close to 100% confluency was reached, the cells were harvested, triturated thoroughly and resuspended in fresh growth medium. The cell solution was then distributed on the chips and the chips were placed in an incubator (37°C, 5% CO2 in air) for 3 – 5 hours. After incubation, the chips were mounted on an optical microscope. Buffer was introduced through a needle at one end of the channel at a uniform flow rate (80 µL/s).Electrochemical measurements were made using an Axopatch 200B (Molecular Devices) amplifier held at 400 mV constant potential. Data was collected using custom programs written in LabVIEW (National Instruments, Austin, Texas). A Ag/AgCl reference electrode (RE-5B, BASi) was placed with the tip in the PDMS well and connected to the back of the amplifier headstage. Two different buffers were used during experiments: a low potassium buffer (150 mM NaCl, 5 mM KCl, 1.2 mM $MgCl_2$, 5 mM glucose, 10 mM HEPES and 2 mM $Cacl_2$, from SigmaAldrich) and a K^+-rich buffer (KCl increased to 100 mM, NaCl decreased to 55 mM). For experiments were potassium concentration is varied, the NaCl concentration was

regulated to maintain a constant total concentration of KCl and NaCl. For drug experiments, L-DOPA (L-3,4-dihydroxyphenylalanine) was acquired at Sigma Aldrich and dissolved to 100 µM in low potassium buffer.

Results and Discussion

Chips were constructed by bonding a piece of PDMS containing a long, rectangular channel to a flat polymer substrate with a Pedot:tosylate conductive polymer band microelectrode placed perpendicular to the PDMS channel (figure 1a). Buffer exchange was provided by a flow cell with uniform flow rate (80 µL/s). The chips were mounted on an optical microscope and the cells could be observed during experiments(figure 1b).

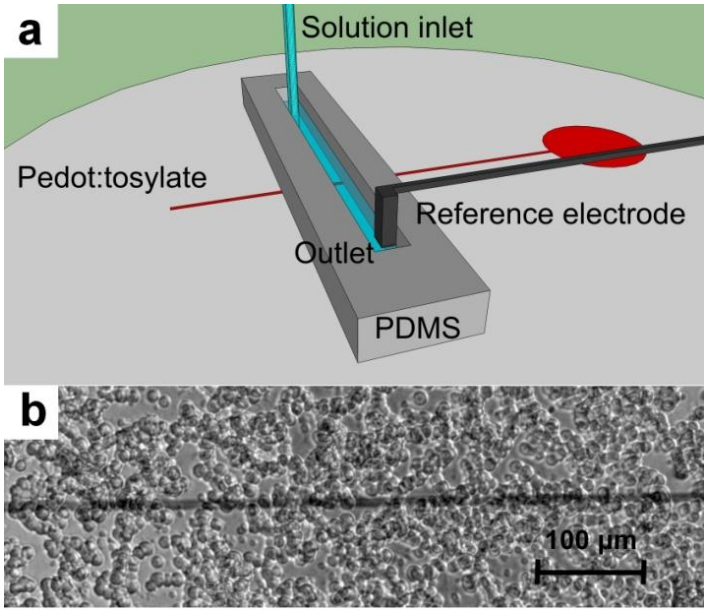

Figure 1: *a) Model of chip design. A 10 – 20 µm wide Pedot:tosylate band microelectrode (red) is fabricated on a polymer substrate. A 2-3 mm wide and 3 cm long rectangular well is constructed in PDMS and placed perpendicular to the microelectrode. b) Microscope image of PC 12 cells sedimented on a Poly-L-Lysine covered Pedot:tosylate microelectrode.*

The protocol for a cell experiment is shown in figure 2. PC 12 cells were cultured in culture flasks, harvested, plated in the PDMS wells and left in an incubator for 3 – 5 hours. The cell culture medium was then exchanged with a physiological buffer. After

flushing the cells a 3 – 4 times, only cells with strong attachment to the surface were left. A potentiostat was connected to the Pedot electrode and to a Ag/AgCl electrode immersed in the buffer and a constant potential at 400 mV was applied. Once the charging current had decreased to a reasonable level, the cells were exposed to a buffer containing a high concentration of potassium (100 mM). After potassium stimulation a rise in current is immediately observed. After 20 – 40 seconds, the current begins to decrease. Two representative current peaks can be seen in figure 2. After the first potassium stimulation, the cells are again flushed with low potassium buffer and left for a fixed time period before another stimulation is triggered by introduction of high potassium buffer. The peak height was estimated as shown in figure 2.

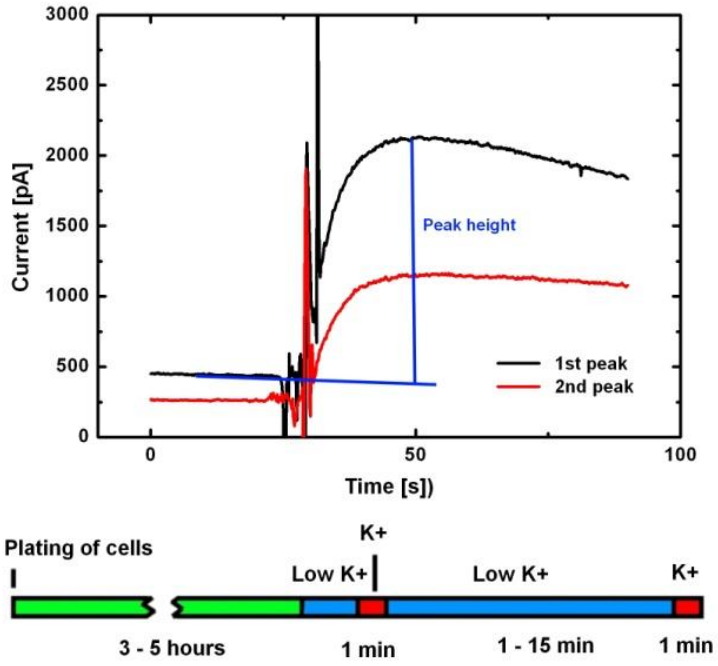

Figure 2: *Two current responses measured at the same chip. The responses were triggered by stimulating PC 12 cells with a buffer containing 100 mM potassium concentration. The protocol of the experiment is shown under the graph. The time between stimulations was varied in this experiment. During this period the cells were exposed to a low concentration of potassium (5 mM).*

The peak shape of the current response can be interpreted as a combination of several effects. Potassium triggers exocytotic release of transmitter molecules from PC 12 cells.

The rapidly increased concentration of transmitters at the cell covered surface is sensed by the Pedot:tosylate electrodes. After some time, the release of new transmitters is balanced by the diffusion of the molecules away from the surface. Also, the depletion of oxidizing molecules in close vicinity to the electrode could contribute to the decrease in current. Indeed, band microelectrodes do not provide true steady-state currents over time for constant concentration of oxidizing species.[123]

The height of the second peak compared to the height of the first peak was relatively constant over a range of chip experiments and was found to be independent on the absolute height of the peaks. For a 15 minute rest period between stimulations, the ratio was measured on four different chips to be 63 ± 9 %. This quantity was therefore chosen as a measure of transmitter release. By keeping the protocol unchanged through the first stimulation, the effect of varying experiment parameters or exposing the cells to different drugs can be investigated by comparing the ratio of peaks.

First, we investigate the effect of the "rest" time between potassium stimulations. Figure 3 shows the ratio of current peaks as a function of the time period between stimulations. Clearly, the response of the second peak increases with increasing rest time with a 5 minute rest time giving approximately half the current response. This could be interpreted as the cells needing to refuel their transmitter reservoirs or to transport transmitter vesicles to release sites at the cell membrane.[1]

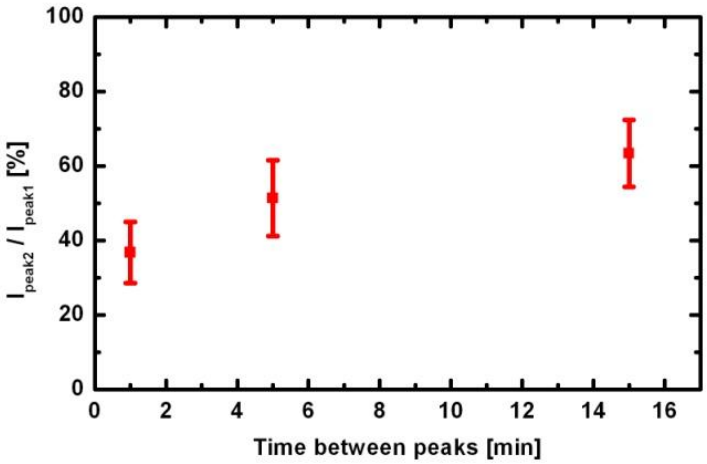

Figure 3: *The ratio of the second peak compared to the first peak as a function of the time between stimulations. The protocol for this experiment is shown in figure 2.*

Next, we vary the concentration of potassium used to stimulate the cells. The first potassium stimulation was carried out with a 100 mM potassium buffer, while the concentration was varied during the second stimulation. The time between the peaks was 5 minutes. As can be seen in figure 4, we observe a clear relationship between response and potassium concentration. At 20 mM, no response was measured, while the full response was observed for concentrations higher than 80 – 100 mM. In figure 4, the data is treated as a sigmoidal dose-response relationship and fitted to the Hill equation.[142] Setting the bottom level to 0, a least squares regression results in the following parameters: Maximum response: 50 %, half maximal effective concentration (EC50): 57 mM, Hill coefficient: 6.1.

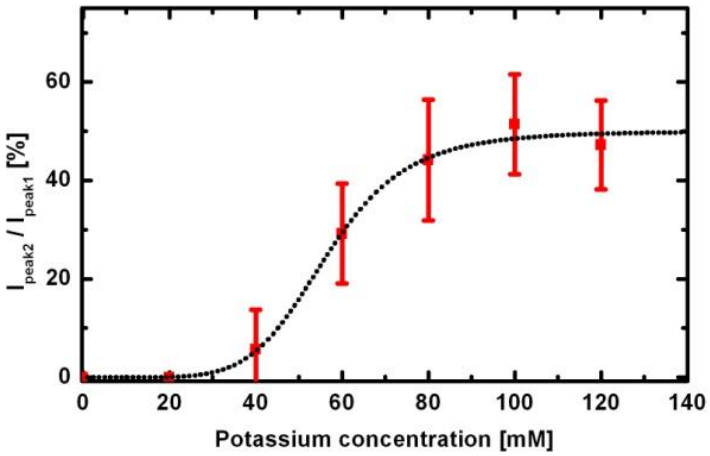

Figure 4: *The ratio of current peaks as a function of potassium concentration during second stimulation. The time period between stimulations was 5 minutes. The concentration during the first stimulation was 100 mM. The experimental data was least squares fitted to the Hill Equation with fitting parameters: Maximum response: 50 %, EC50: 57 mM, Hill coefficient: 6.1. The baseline response was set to 0.*

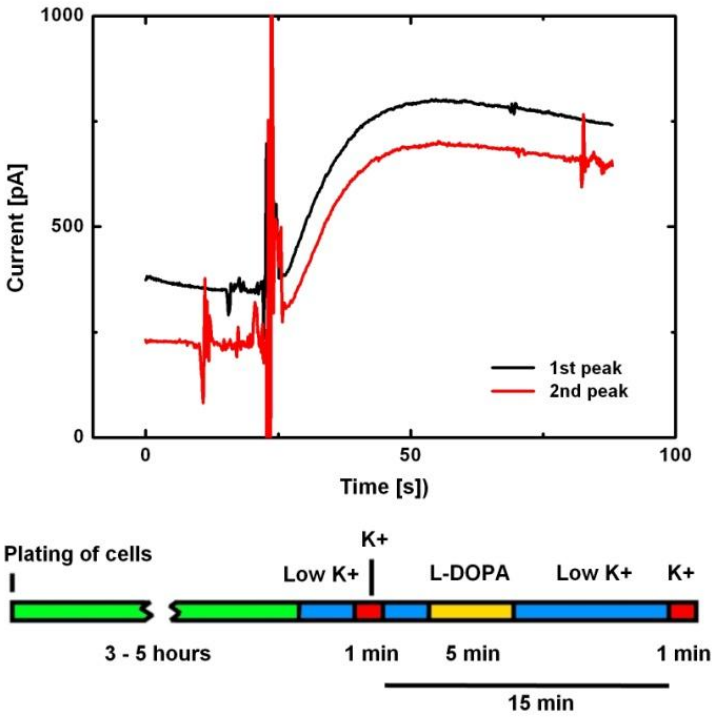

Figure 5: *Two representative current responses and protocol for drug exposure experiment. During the 15 minute rest period between stimulations, a buffer containing 100 µM L-Dopa was introduced to the chip for 5 minutes.*

Finally, we demonstrate the potential of using the presented device as a simple tool for drug screening. We demonstrate this by using the compound L-DOPA (L-3,4-dihydroxyphenylalanine), which is known to increase the size of transmitter vesicles in PC 12 cells.[12] L-Dopa is a precursor of the neurotransmitter dopamine and can be converted into dopamine inside neuronal cells. The experiment protocol is shown in figure 5 together with two representative current peaks. The time between potassium stimulations was set to 15 minutes. During this period the cells were exposed to a buffer containing 100 µM L-Dopa for 5 minutes. The ratio of peak currents was measured to be 97 ± 12 % for L-Dopa treated cells. In figure 6, the response of L-Dopa-treated cells is compared to that of untreated cells. The increase in peak current is statistically significant. This result supports earlier carbon fiber microelectrode experiments where treatment with L-Dopa even for very short time periods increased the mean vesicle content at PC 12 cells.[136] The results plotted in figure 6 show that the method presented in this paper can be used as a simple screening method for drugs affecting transmitter release in neuronal cells.

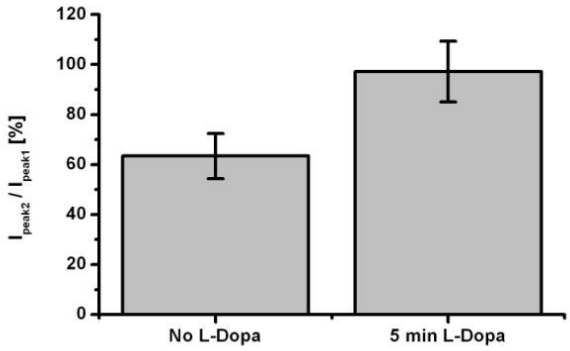

Figure 6: *Ratio of current peaks for cells exposed to L-Dopa and for cells only exposed to low potassium buffer. The time between stimulations was 15 minutes for both experiments.*

Conclusion

In this paper, we presented a simple chip for studying the overall release of transmitter from a large group of PC 12 cells. The chip was constructed of only polymer materials with electrodes made of micropatterned Pedot:tosylate conductive polymer. Potassium-induced stimulation of surface-trapped PC 12 cells gave rise easy-to-analyze current peaks due to oxidation of the released transmitters on the Pedot:tosylate electrodes. Subsequent stimulations of the same group of cells resulted in signals that increased in size with increasing time between stimulations. This result indicates that PC 12 cells need a certain time to refuel their transmitter reservoirs or to transport transmitter vesicles to release sites at the cell membrane. The release of transmitters depended heavily on the concentration of potassium. Experimental data of release versus potassium concentration was fitted to a sigmoidal dose-response curve with half maximal effective concentration (EC50) at 56.6 mM potassium. The presented chip could be used for simple pharmacological screening of neurochemical drugs. This was demonstrated by measuring the increase in released transmitter of PC 12 cells being exposed to 100 µM L-DOPA for 5 minutes. The method used in this paper has both advantages and disadvantages compared to conventional single cell amperometric analysis. Information on single vesicle size is lost, but on the other hand time-consuming statistical analysis of single vesicle release events can be avoided in applications

targeting overall release activity of neuronal cells. Using only polymer materials makes the presented chip an easy-to-fabricate, cost efficient and disposable device.

Acknowledgments

This work is supported by the Danish Council for Strategic Research through the Strategic Research Center PolyNano (grant no. 10-092322/DSF)

Chapter 5: Other thin film electrodes and integration of electrodes into closed chips

This chapter will cover work done on other thin film electrode materials and integration of electrodes into chips. The first part deals with carbon microelectrodes fabricated by pyrolysis of photoresist. Most of the experimental work on pyrolyzed photoresist was done during the Master thesis project of Aikaterini Argyraki,[143] where the author of this thesis was co-supervisor. The main idea of the project was to make pyrolyzed photoresist microelectrodes in the local Danchip cleanroom and to test if these electrodes would have satisfying physical and electrochemical properties. The second section contains a short evaluation of Pedot:Pss microelectrodes for transmitter detection studies. The third section of this chapter summarizes some of the physical properties of the thin film electrodes fabricated during this PhD project; Pedot:tosylate, Pedot:Pss, pyrolyzed photoresist and gold. The advantages of the different materials in terms of physical, electrochemical and optical properties are discussed. A discussion of the large variations in capacitance is a major part of this section. Finally, a short section deals with the integration of conductive polymer microelectrodes into closed chip systems. A closed chip approach to improve transmitter release measurements on large groups of cells is presented and preliminary results are shown.

1. Pyrolyzed photoresist microelectrodes

Photoresists are organic materials and can therefore be carbonized by elevation to very high temperatures (500 – 1100 °C) in an oxygen-free atmosphere. Pyrolyzed photoresist microelectrodes have been made by pyrolysis of fully developed photoresist structures and used for various neurotransmitter detection applications[52] including Fast Scan Cyclic Voltammetry[53] and Microchip Electrophoresis.[144] Also, it was shown that neuronal cells can be grown directly on pyrolyzed photoresist.[145] Detection of transmitter release from neuronal cells has not been reported so far on pyrolyzed photoresist electrodes. From an electrochemical point of view this should be possible due to the success of traditional carbon fiber microelectrodes in this area. The possibility of detecting single cell exocytosis events depends on the resistive and capacitive

performance of the material, as we showed in chapter 3. In this project, we produced pyrolyzed photoresist structures and characterized them with focus on the conductivity, capacitance and electrochemical properties. Further, we compared two different precursor positive photoresist materials (AZ 4562 and AZ 5214).

Several precursor photoresists have been used for the fabrication of pyrolyzed photoresist electrodes, including OIR-897,[146] SPR 220-7.0,[145] OCG 825,[147] Shipley 1813,[148] SU8[149, 150] and various AZ resists.[151, 152, 153, 154] A few studies make direct comparisons of different photoresists. The bulk conductivity was shown to depend on the photoresist precursor.[152, 155] According to two studies on negative photoresists SU-8 and Polyamide[150] and positive photoresists AZ 4330 and OCG-825[155] processed at the same conditions, positive photoresists were found to exhibit higher conductivities than negative photoresists while the variation between the two positive photoresists was small.

Pyrolyzed films from positive AZ resists have been shown to exhibit near-atomic flatness[156] (rms roughness from AFM measurements: 0.5 nm), shrinkages of around 80%,[157] resistivities in the range of 2-10 (mΩ cm)[157] and capacitances in the range of 7-100 µF/cm^2.[157] In this section we characterize the physical and electrochemical properties of pyrolyzed microelectrodes made from positive resists AZ 4562 and AZ 5214 with emphasis on the use of the electrodes for neurotransmitter studies.

Pyrolyzed photoresist electrodes were fabricated as described in detail in [143]. Shortly, band microelectrode structures were first defined in photoresist (AZ 4562 and AZ 5214) on silicon and quartz wafers by spin-coating, soft baking (90 °C for 15 minutes), exposure (Karl Suss MA6/BA6 Mask Aligner, 3 seconds, intensity 7.0 mW/cm²) and development with AZ351B Developer. Height measurements were performed using a Dektak 8 profilometer (Veeco Instruments). Resist structures were pyrolyzed using a pyrolysis furnace (ATV Technologies GMBH). Various temperature profiles were implemented including two or more stabilization steps at 500℃ (1 hour) and 700℃ (1 hour) and a final temperature of up to 900℃. The waiting time at the maximum temperature was 1 hour, while the cooling of the chamber took place slowly (approximately 9 hours to reach room temperature). Conductivity was measured with a four-point probe (Jandel Engineering Ltd) connected to a Keithley 2400 SourceMeter (Keithley Instruments Inc). AFM images were recorded with a DME-SPM (Dualscope II, Denmark). Conductive AFM measurements were done with and ElectriCont-G probe (BudgetSensors) with

electrically conductive coating of 5 nm Chromium and 25 nm Platinum on both sides of the cantilever. A protective resistance of 43.7 kΩ was used. XEI software (Park Systems Corp.) was used for data analysis. Cyclic voltammograms were performed with an Axopatch 200B (Molecular Devices) amplifier combined with homemade Labview programs. Electrochemical measurements were performed in phosphate-buffered saline (Lonza). Epinephrine was acquired at Sigma Aldrich. SEM imaging and XPS characterization was performed as described in [143]. Cell experiments were performed as described for Pedot:tosylate microelectrodes in chapter 4.

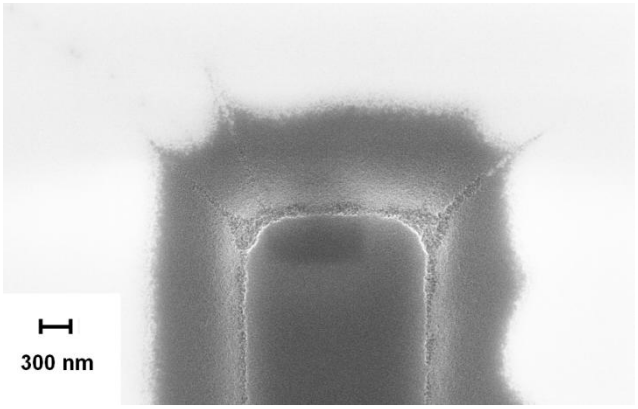

Figure 1: *SEM image of pyrolyzed photoresist band microelectrode resulting from the pyrolysis of AZ 5214 photoresist.*

A SEM image of a 3 µm wide band electrode made of pyrolyzed AZ 5214 photoresist is shown in figure 1. It is quite clear how the shrinkage caused by the pyrolysis process results in slightly sloped sidewalls. In figure 2, we show profilometer profiles of 200 µm wide band electrodes measured before and after pyrolysis at 900°C. Interestingly, quite different shapes of the electrodes are measured depending on the photoresist precursor. This phenomenon was not reported in earlier studies and we think it might be related to the chemical composition of the photoresists. The elevated edge structures observed at the thinner photoresist (AZ 5214) might be due to reflow of the photoresist during the first stages of pyrolysis. The thicker resist (AZ 4562) is able to resist this reflow and instead retracts during shrinkage to form peak-shaped structures. The addition of an early soft-baking step in the pyrolysis of AZ 5214 structures seems to affect significantly the elevation at the edges. We think that this soft baking step reduces the solvent content and strengthens the structures to better resist reflow effects. The shrinkage of the photoresist structures increased approximately linearly with maximum

process temperature for both resists (results not shown here) while the shrinkage seemed to be slightly larger for AZ 5214 structures.

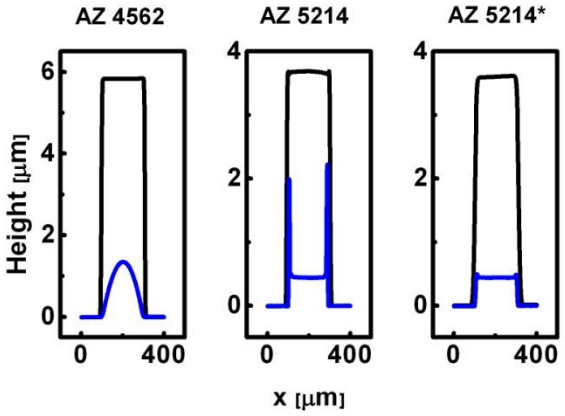

Figure 2: *Contact profilometer cross-sections of 200 µm wide band electrodes measured before and after pyrolysis. The maximum process temperature was 900° C for all electrodes. *A soft-baking step is performed before exposure and development of the photoresist for this sample.*

Bulk conductivities of pyrolyzed photoresist films seem to depend almost exponentially on the maximum process temperature used during pyrolysis (figure 3). This observation and the conductivities achieved for high process temperatures (~180 S/cm) are in agreement with earlier findings.[147, 156, 157] The conductivity of AZ 5214 films seems to be higher for all maximum process temperatures compared to AZ 4562 films. This phenomenon is not fully understood, but it could be related the following two things: 1) The shrinkage of AZ 5214 films was observed to be larger than that for AZ 4562 films. This could be due to more evaporation of solvent from AZ 5214 which might also result in higher conductivities. 2) XPS studies at pyrolyzed film surfaces show that the binding energy of the carbon peak decreases faster with higher temperatures for AZ 5214 films than for AZ 4562 films (figure 4). The decrease in binding energy is expected due to graphitization of the carbon structures. The results in figure 4 indicate that AZ 5214 films pyrolyzed at high temperatures might be more graphite-like in structure. This could be an explanation for the higher conductivities.

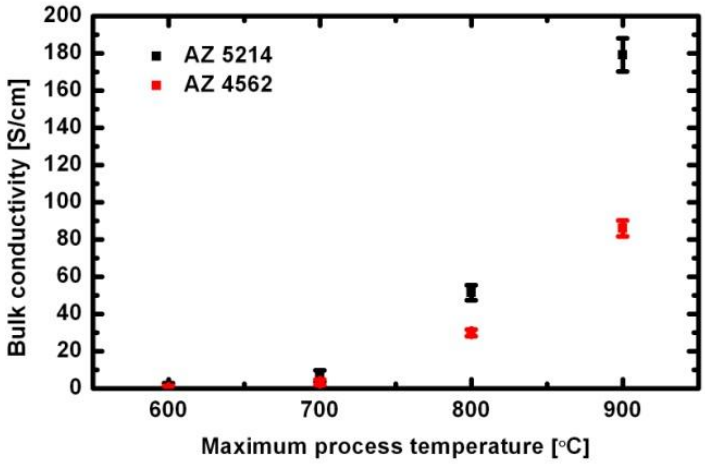

Figure 3: *Bulk conductivity as a function of maximum process temperature for pyrolyzed photoresist electrodes.*

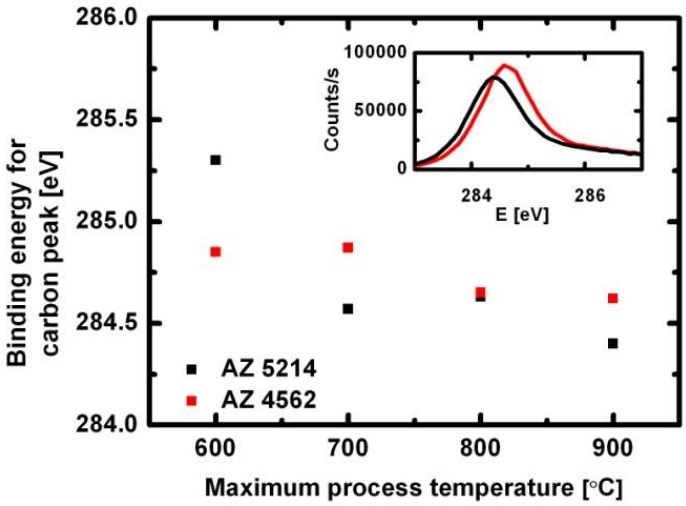

Figure 4: *Binding energy of carbon peak as a function of maximum process temperature for different pyrolyzed photoresist electrodes. The insert shows the XPS spectrum at the carbon peaks for electrodes pyrolyzed from AZ 5214 and AZ 4562 photoresist respectively and processed at 900° C maximum process temperature.*

To test the capacitive and electrochemical properties of the pyrolyzed electrodes, cyclic voltammograms were measured in phosphate buffered saline. Flat background scans could be obtained (figure 5 a), with electrochemical limits due to water dissociation of

around – 400 mV and 1300 mV (table 1). This is a good potential window, comparable to that for metal electrodes (1.5 V[158]) and considerably larger than that for Pedot:tosylate (chapter 2). The apparent capacitance of the film was calculated based on background scans from 7 different pyrolyzed photoresist electrodes (table 1). The calculated value, 61 ± 14 µF/cm^2, lies within the range of capacitances reported in most other studies,[157] although two studies reported unusually low capacitances below 10 µF/cm^2.

Table 1 *Physical properties of pyrolyzed photoresist electrodes. Error is the standard deviation (n = 7).*

Capacitance per unit area	61 ± 14 µF/cm^2
Potential-limits (vs. Ag/AgCl)	-400 mV, 1300 mV

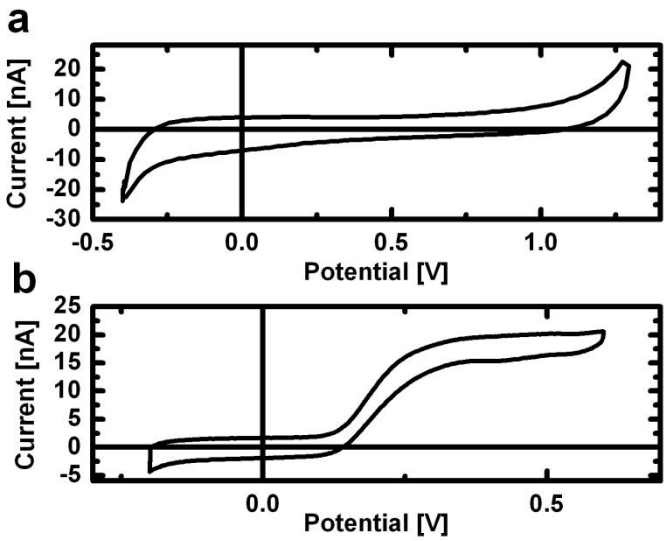

Figure 5*: Electrochemical measurements at pyrolyzed photoresist electrodes processed at 900° C maximum process temperature. A) Cyclic voltammograms showing the background current towards an Ag/AgCl reference electrode for a Pedot:tosylate electrode in PBS buffer. Scan rate 200 mV/s. b) Cyclic voltammogram showing the oxidation of epinephrine. Scan rate 2 mV/s. Concentration 20 µM.*

Several factors can affect the capacitance of electrode surfaces. Roughness increases the capacitance by increasing the microscopic surface where the double layer can be formed. On the other hand, the existence of islands of non-conducting film would decrease the capacitance by decreasing the actual electrode area. To test if these effects were present at the pyrolyzed photoresist, we performed atomic force microscopy (AFM) and conducting atomic force microscopy (cAFM) at representative electrode films. As shown in table 2, topographic AFM results show a near-atomic flatness of the films for wafers pyrolyzed at 900°C (both photoresists). The rms roughness measured, 0.58 ± 0.15 nm, agrees with earlier findings (0.5 nm[156]). A much larger roughness was measured at films pyrolyzed only at 700°C (table 2). The development in surface roughness with increasing temperature has to our knowledge not been reported earlier and would be an interesting target for future studies.

Table 2 *Topographic AFM results. Error is the standard deviation (n = 5).*

	900°C max T	700°C max T
Surface area ratio	0.35 ± 0.19 %	33.6 ± 4.6 %
R_{rms}	0.58 ± 0.15 nm	5.8 ± 0.3 nm
$IR_{sk}I$	0.19 ± 0.11	0.36 ± 0.19

Conducting AFM studies were also performed on pyrolyzed photoresist films. In this method an AFM tip with conductive coating is used. A constant potential of 0.1 V is applied between the tip and the film, a protective resistance of 43.7 Ω is placed in the circuit and the current is measured with a current-to-voltage converter. Figure 6 shows a representative cAFM image and a profile measured along the line shown in green. As can be seen, only very small fluctuations in conductivity can be observed. This suggests that non-conductive islands are not present at the fabricated pyrolyzed photoresist films. The AFM and cAFM measurements presented here imply that the films are homogeneously conducting with negligible surface roughness. The electroactive

microscopic surface area of the electrodes can therefore be assumed to be equal to the geometric surface area.

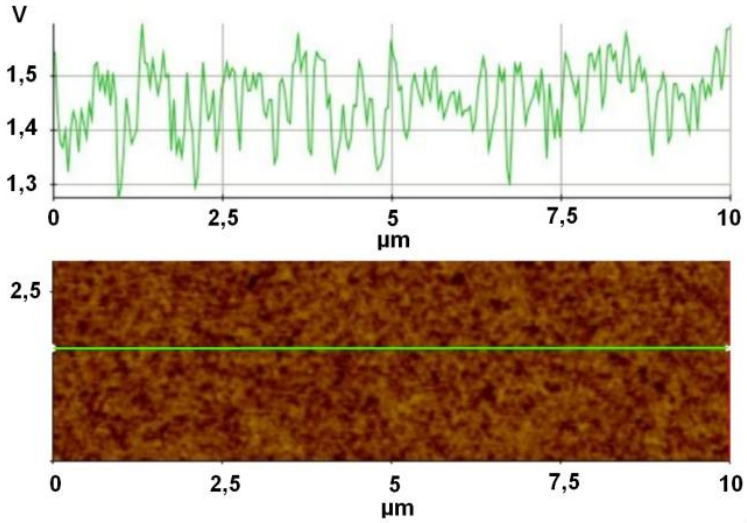

Figure 6: *Conductive atomic force microscopy image and cross-sectional profile for a pyrolyzed photoresist electrode. Resist: AZ 5214. Maximum process temperature: 900° C. The y scale is the measured current by the current-to-voltage converter with feedback resistance 100 kΩ. Voltage bias is -0.1 V.*

Pyrolyzed photoresist microelectrodes could be used to measure transmitter release from large groups of PC 12 cells as described for Pedot:tosylate microelectrodes in chapter 4. A typical amperometric current peak resulting from potassium stimulated transmitter release at a pyrolyzed photoresist microelectrode is shown in figure 7, upper panel.

2. Pedot:Pss microelectrodes

As an alternative to Pedot:tosylate microelectrodes, another commercially available Pedot variant, Pedot:Pss, was also used for fabrication of microelectrodes for neurotransmitter detection. The chemical structure of the counter-ion Pss (Polystyrene sulfonate) is shown in Scheme 2 in chapter 1. The fabrication details are described in Chapter 3 where Pedot:Pss microelectrodes were used for amperometric noise measurements. In this short section, results of resistance and capacitance

measurements at Pedot:Pss are presented and the use of the electrodes for amperometric measurements of transmitter release is demonstrated.

The fabrication of Pedot:Pss microelectrodes is described in chapter 3. Measurements of resistance, capacitance and transmitter oxidation were performed as described for Pedot:tosylate electrodes in chapter 2. Cell measurements were performed as described in chapter 4.

4-point measurements revealed a sheet resistance of 1100 ± 300 Ω. The result of apparent capacitance measurements was 630 ± 60 µF/cm^2. These results are quite different from Pedot:tosylate and will be discussed in the next section. Rigorous tests of electrochemical oxidation of neurotransmitter molecules were not performed on Pedot:Pss, but cyclic voltammograms of catecholamine (dopamine, epinephrine, and norepinephrine) oxidation showed that the oxidation potentials for these molecules at Pedot:Pss are indistinguishable from those observed at Pedot:tosylate. Finally, potassium stimulated transmitter release from large groups of PC 12 cells was measured at Pedot:Pss microelectrodes. The results can be seen in figure 7, lower panel. The large amplitude of this peak is not a property related to the electrode material, but to the number of cells present at the electrode.

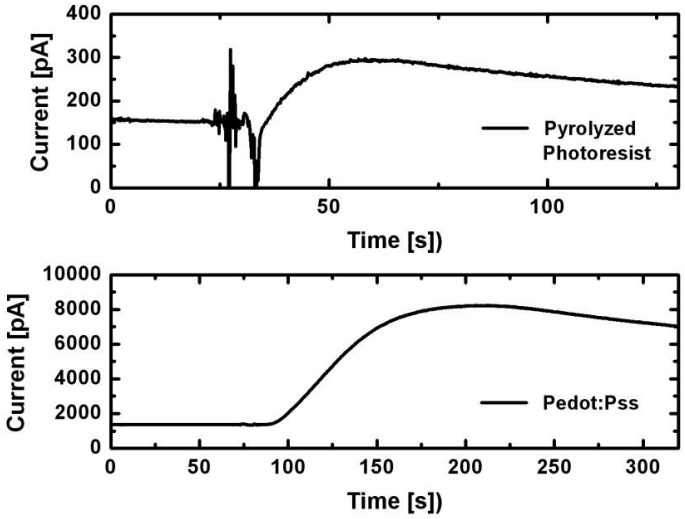

Figure 7: *Amperometric measurements of potassium triggered transmitter release from large groups of PC 12 cells at pyrolyzed photoresist microelectrodes and Pedot:Pss microelectrodes.*

3. Comparison of thin film electrode materials for use in amperometric detection of transmitters

In this PhD project one of the goals was to find suitable electrode materials for integration in polymer chips targeting electrochemical neurotransmitter detection. For this purpose traditional noble metal electrodes of gold and platinum, conductive polymer electrodes of Pedot:tosylate and Pedot:Pss and carbon electrodes of pyrolyzed photoresist were fabricated. Table 3 shows some of the important physical, electrochemical and fabrication properties of these materials for neurotransmitter detection applications. Unless references to other studies are given, the observations were made in this project.

When it comes to conductivity, traditional metal electrodes are difficult to compete with. Alternative electrodes showed much higher sheet resistances, the highest measured at the 200 nm thick Pedot:Pss films (1100 ± 300 Ω). It should be mentioned that the sheet resistances of conductive polymer electrodes increased with time and deviated between batches and sometimes even larger resistances were measured for a full batch.

The measured apparent capacitance per area values varied within a range of two orders of magnitude with gold having the lowest capacitance (18.6 ± 2.0 $\mu F/cm^2$) and Pedot:tosylate films being the most capacitive (1700 ± 100 $\mu F/cm^2$). The large difference in capacitance can be explained by the different charge storage mechanisms involved. An electrode can be charged by ions from the solution filling a double-layer at the electrode surface (double-layer capacitance) or by a pseudocapacitive behavior, where charge is being stored indirectly through chemical processes but the electrical behavior of the electrode is like that of a capacitor (pseudocapacitance).

Table 3 *Summary of physical and electrochemical properties and fabrication issues of 4 thin film electrode materials.*

	Gold (~150 nm)	Pedot:tosylate (~190 nm)	Pedot:Pss (~200 nm)	Pyrolyzed photoresist, (AZ5214,~1 µm)
Fabrication method	Evaporation and lift-off	Spin-coating and etch-down	Spin-coating and etch-down	Lithography and pyrolysis
R_s [Ω]	0.185 ± 0.005	113 ± 7	1100 ± 300	56 ± 5
C/A [µF/cm^2]	18.6 ± 2.0	1700 ± 100	630 ± 60	61 ± 14
Electrochemical limits (vs Ag/AgCl)	1.5 V window[158]	-200 mV, 700 mV	-200 mV, 700 mV	-400 mV, 1300 mV
Optical properties	Opaque	Transparent	Transparent	Opaque
Electrochemical properties	Fouling of neurotransmitters reported[42, 43, 53, 58, 59]	Good (chapter 2)	Similar to Pedot:tosylate	Good[42, 43]
Issues related to integration in polymer chips		Reactive Ion Etching complicates thermal bonding of polymer parts	Reactive Ion Etching complicates thermal bonding of polymer parts	Substrates must resist pyrolysis temperatures (only quartz and Si possible)

At carbon and noble metal electrodes only double-layer capacitance plays a role. This capacitance arises at all electrodes and for flat electrodes it typically has values of between 15 and 80 µF/cm^2 in aqueous buffers and less in non-aqueous solvents.[159, 160, 161] The double-layer capacitance depends on the physicochemical nature of the electrode surface. For carbon electrodes, factors like provenance, conditioning treatment and extent of graphitization have been reported to play a role.[162] At noble metal electrodes like gold and platinum, the double-layer capacitance depends on whether the metal has a thin oxide film and at which surface plane of single-crystal electrodes the capacitance is measured.[162] For all electrodes, the capacitance depends heavily on surface roughness, since roughness increases the actual area of the electrode. The apparent capacitance values measured for gold and pyrolyzed photoresist agree well with the typically reported values.

We used phosphate buffered saline as buffer for apparent capacitance measurements. For this buffer, the capacitance at a perfectly flat polarized electrode can be calculated theoretically.[143] In this calculation, the apparent capacitance was found to be 54 µF/cm^2 using the Debye length 0.7 nm, relative permittivity 78 and assuming the existence of a Stern layer.[143] This is within one standard deviation of the measured capacitance of pyrolyzed photoresist, while it is somewhat larger than the measured capacitance of gold. The presence of a thin oxide film on the gold electrodes could explain this deviation.

In contrast to carbon and noble metal electrodes, the main contribution to the capacitance of conductive polymers comes from pseudocapacitive effects.[163, 164, 165, 166] Conductive polymers can be switched between oxidized (doped) and reduced (dedoped) states by changing the applied potential.[167] During this process counter-ions diffuse into and out of the conductive polymer to keep the electroneutrality.[167] The large capacitance of Pedot coupled with its high stability has been utilized in supercapacitor applications.[165, 168] The apparent capacitances measured for Pedot:tosylate and Pedot:Pss in this project are both within the reported range of capacitances for typical pseudocapacitive films.[162] The larger capacitance of Pedot:tosylate compared to Pedot:Pss may be related to the different chemical structure of the counter-ions (Scheme 2, chapter 1), where tosylate, being smaller than Pss, can diffuse easier out of and into the polymer matrix.

For many electroanalytical applications, relatively large values of resistance and capacitance are not major problems. As described in chapter 4, Pedot:tosylate microelectrodes were used to successfully record transmitter release from large groups

of PC 12 cells. The signal-to-noise ratio was excellent in these experiments due to the relatively large signals (few nA's) and the low temporal resolution (10 Hz) needed. For similar reasons, the use of Pedot electrodes should also be possible for neurotransmitter detection in separation-based applications. Indeed, Pedot:tosylate microelectrodes fabricated in this project were successfully integrated in a microchip for capillary electrophoresis by collaborators at the University of Arizona (unpublished results).

For low-noise amperometric recordings of single exocytosis events, the requirements for low resistance and capacitance are much higher as discussed in chapter 3. A decrease in size of about 2 orders of magnitude was required for obtaining Pedot:tosylate microelectrodes with low-noise properties comparable to gold microelectrodes. The lowest noise levels reached at cell-sized Pedot:tosylate microelectrodes was around 3 pA rms at 1 kHz low pass filtered current traces. This is a problematic noise level since exocytotic signals from PC 12 cells are usually characterized by amplitudes of 10-20 pA,[4, 42] and since low pass filter frequencies of 5-10 kHz are typically needed, which would increase the measured noise substantially. Another problematic feature of conductive polymer microelectrodes for single exocytosis measurements is the time constant $\tau = RC$ of the electrochemical cell. Since conductive polymer electrodes have relatively high resistances as well as capacitances, the time constant may be too large to resolve millisecond current spikes. Exocytosis measurements at conductive polymer microelectrodes have only been reported once.[110] In that study, Pedot:Pss was used which has a lower capacitance than Pedot:tosylate and the resistance of the electrode was decreased by applying a layer of gold under the Pedot:Pss. Also importantly, the cells used were chromaffin cells, which are endocrine cells with much larger signals than PC 12 cells (amplitudes up to 1 nA[110]).

An interesting property of Pedot:tosylate and Pedot:Pss electrodes is their transparency. Transparency can be used to combine amperometric recording of release events with fluorescence microscopic observation of vesicle movement in single cells.[62, 63] In contrast, metal electrodes and pyrolyzed electrodes are usually opaque. It should be mentioned though that recent studies report the fabrication of ultra-thin (5-80 nm) pyrolyzed photoresist structures that are transparent enough to be used for fluorescent imaging.[153, 154]

As described in the next section Pedot microelectrodes can be integrated in thermally bonded polymer chips. The same was done with gold electrodes. The bonding process was better and more stable for gold electrodes, probably due to the fact that the polymer substrates containing Pedot electrodes were chemically modified by a reactive

ion etching step required for patterning of Pedot electrodes. Gold electrodes were fabricated with lift-off techniques, leaving the polymer surface next to the electrodes unchanged. A serious drawback of pyrolyzed photoresist electrodes is the fact that very heat-resistive substrates are needed. If transparent substrates are needed, quartz is the best choice. Since quartz is relatively expensive, this limits the use of pyrolyzed photoresist for cheap and mass-producible chip devices.

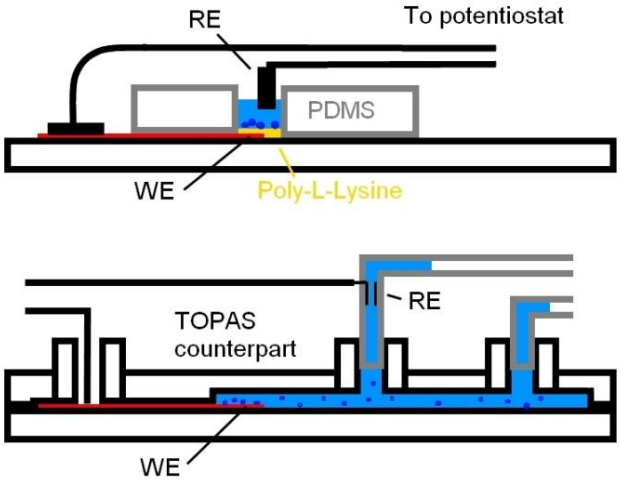

Figure 8: *Upper panel: Open chip system with PDMS structures and Poly-L-Lysine coated electrodes as used for the device presented in chapter 4. Lower panel: Closed chip system resulting from thermal bonding of electrode substrates and injection molded counterparts made of the same thermoplast. The counterparts contain the microchannel system and holes for electrode connections and microfluidic connections. Abbreviations: WE - working electrode, RE - reference electrode.*

4. Integration of electrodes into chip devices

One of the main motivations for testing conductive polymer microelectrodes for neurotransmitter detection was the possibility to produce inexpensive and mass-producible polymer devices for bioanalytical applications. A PDMS-based all-polymer open chip for transmitter release studies was presented in chapter 4. Another chip fabrication method targeted was the fabrication of closed polymer chips by thermal

bonding of two injection molded polymer parts: a flat part containing electrodes and another part containing injection molded microfluidic channels and holes for electrode connection and microfluidic connections. This fabrication procedure has clear advantages as it makes use of mass-production techniques (injection molding) and the rigid, closed chip design is more stable. The fabrication principles are described in detail in references [119, 169] and will not be covered here. A comparison of the two methods for integration of Pedot electrodes in polymer chips can be seen in figure 8.

For the chip device presented in chapter 4, we use the amplitude ratio of two subsequent current peaks to quantify the release of transmitters. The first peak is needed as a reference since the number of cells contributing to the signal is not known and varies from chip to chip. If a fixed number of cells could be captured close to a microelectrode, the reference peak would not be needed to compare signals and exposure of the cells to drugs could be done for longer time periods than the short time interval between subsequent peaks. This idea is implemented in the closed chip design illustrated in figure 9. The goal is to capture a fixed amount of cells close to a microelectrode in a 30 µm x 30 µm x 100 µm large chamber that is in contact with a larger channel where cells are introduced. The cell trapping mechanism relies on suction from a side channel through a 3 µm high slit that physically retains the cells.

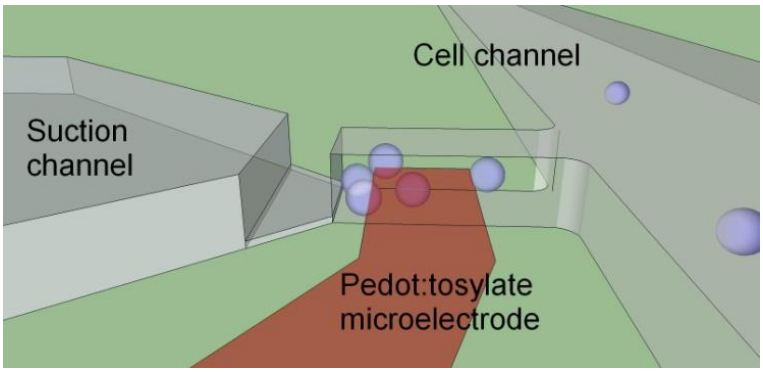

Figure 9: *3-D illustration showing the idea of a closed chip for capture of a group of neuronal cells in a 30 µm x 30 µm x 100 µm "microchamber". Negative pressure applied to the suction channel would attract cells to fill up the chamber. Electrode width is 40 µm.*

In figure 10 a preliminary result of a closed polymer chip with the abovementioned design is shown. The Pedot:tosylate microelectrode is integrated nicely with the

microfluidic channel system. The width of the microelectrode is 40 µm. Since the width of the chamber is 30 µm, the electroactive area of the electrode is 40 µm x 30 µm. It is important for the comparability of signals that this area is constant from chip to chip. As can be seen in figure 10, the capture of a few PC 12 cells into a microchamber has been realized, but the first cells seem to block the slit opening too much to attract additional cells. This problem has to be addressed in future iterations of the device.

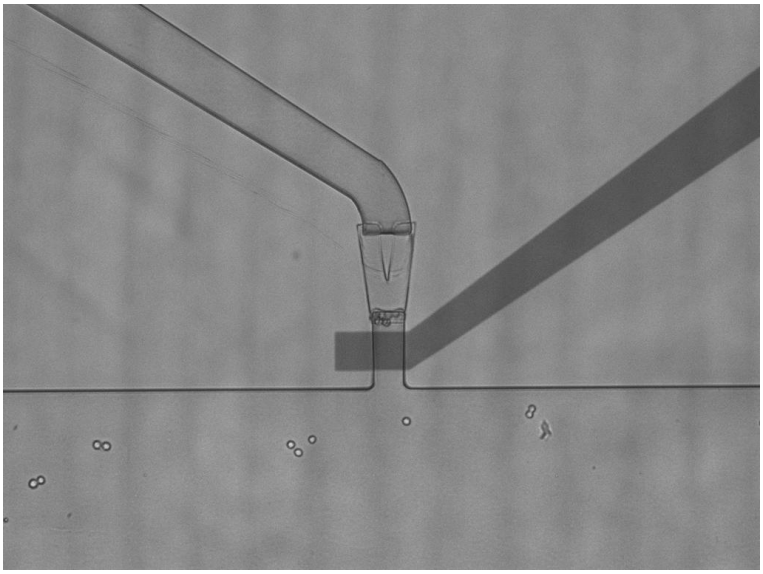

Figure 10: *Microscope image of polymer chip with integrated Pedot:tosylate microelectrodes for physically trapping and electrochemically measuring transmitter release from groups of PC 12 cells.*

Chapter 6: Conclusion

The **main outcome of this thesis** was the evaluation and characterization of alternative thin film electrode materials for applications targeting electrochemical detection of neurotransmitters in chip devices. Special attention was given to the conductive polymer Pedot:tosylate. It was shown, that resistive and capacitive properties of thin film electrode materials are determining their usefulness in low-noise amperometric measurements at single cells. As an alternative to low noise amperometry at single cells, a chip device was developed to measure transmitter release from large groups of neuronal cells.

The original aim of this PhD project was to integrate Pedot:tosylate microelectrodes in all polymer chips to measure single vesicle transmitter release events from trapped neuronal cells by use of low-noise constant potential amperometry. The first step on the road was a thorough **characterization of Pedot:tosylate** as an electrode material for transmitter detection. A wide range of transmitters were shown to oxidize readily on Pedot:tosylate microelectrodes and kinetic rate constants and half wave potentials were reported. A limitation of the electrodes was the relatively low anodic potential limit of 0.7 V vs. Ag/AgCl, which for example meant that the oxidation of histamine could not be detected at the electrodes.

The capacitance pr area was found to be high 1670 ± 130 $\mu F/cm^2$ compared to conventional microelectrode materials like gold and carbon. This capacitance is really a pseudocapacitance related with the diffusion of counter-ions into and out of the conductive polymer during potential changes. Large capacitances may limit an electrodes performance in applications that require fast time-scales and low noise.

Attempts to measure single vesicle exocytosis events from single PC 12 cells at Pedot:tosylate microelectrodes were not successful. The main problem was the current noise at cell-sized Pedot:tosylate microelectrodes, which was at the same level as the expected exocytosis signals for the high sample frequencies needed. We suspected the large capacitance to be a contributing factor of the large noise, but the relation between

current noise and electrode area was not linear as reported by others for gold and indium tin oxide microelectrodes.

This led to a comprehensive **study of the current noise** at microelectrodes during constant potential amperometry experiments with high sampling frequencies in physiological buffers. Thin-film band microelectrodes were fabricated in three different electrode materials (Pedot:tosylate, Pedot:Pss, gold) with different capacitive properties, and current noise was measured for a wide range of different electrode areas. The results agreed very well with an analytical noise expression derived from a simplified equivalent circuit model of the electrochemical cell. The results emphasize the importance of choosing low capacitive electrode materials and/or small electrodes if low current noise is crucial. We observed three different noise regimes. 1. For very low capacitances, the noise was equal to the open loop noise of the potentiostat 2. For very large capacitances, the noise was equal to the Johnson-Nyquist noise of the resistance of the electrochemical cell. 3. In the intermediate region, noise scaled with capacitance.

For Pedot:tosylate microelectrodes, the noise study implied that either very small (1-2 µm-sized) electrodes had to be fabricated or transmitter release had to be measured on systems with larger signals and slower time-scale. We successfully measured the increase in transmitter concentration due to potassium-stimulated release from a large group of PC 12 cells on a Poly-L-Lysine-coated Pedot:tosylate microelectrode.

This experiment was further developed by measuring signals from subsequent stimulations of the same group of cells. The amplitude of the second current peak relative to the first was used as a quantitative and comparable measure for release activity of the cells. A simple **chip for studying transmitter release** was constructed by bonding a PDMS flow cell to the microelectrode substrates. Experiments performed with this chip included an investigation of the relationship between potassium concentration and transmitter release response. The presented chip could also be used for simple pharmacological screening of neurochemical drugs. This was demonstrated by measuring the increase in released transmitter of PC 12 cells being exposed to 100 µM L-DOPA for 5 minutes. The method of measuring release from large groups of neuronal cells has both advantages and disadvantages compared to conventional single cell amperometric analysis. Information on single vesicle size is lost, but on the other hand time-consuming statistical analysis of single vesicle release events can be avoided in applications targeting overall release activity of neuronal cells.

We also fabricated and characterized two other alternative thin film electrode materials, **pyrolyzed photoresist and Pedot:Pss**. Carbon is an electrochemically attractive electrode material. By direct pyrolysis of patterned photoresist, microstructured electrodes of carbon were fabricated. These electrodes exhibit decent conductivity at high pyrolysis temperatures, extraordinary flatness and homogeneous conductance. The capacitance is low and as expected for flat electrodes with double layer capacitance. A drawback of pyrolyzed photoresist is that very heat-resistive substrates are needed. Pedot:Pss differs mainly from Pedot:tosylate in having significantly lower capacitance and higher sheet resistance. The lower capacitance is probably related to the larger size of the counter-ion. Transmitter release from living cells was successfully measured on both pyrolyzed photoresist and Pedot:Pss microelectrodes.

We hope and believe that the results presented in this thesis will have an impact in several research areas. Pedot:tosylate is a promising electrode material in chip-based devices for transmitter detection. This opens the way for cheap and easy-to-fabricate all polymer devices for several bioanalytical applications. These applications could include separation techniques such as high performance liquid chromatography or capillary electrophoresis, coupled with electrochemical detection.

The noise expression presented here is not limited to the electrode materials used in this project, but is a general theory only depending on the capacitance and resistance of the electrode, the filter frequency and the open loop noise of the potentiostat. It explains the linear relationship between measured noise and microelectrode area found by others as well as the non-linearity at more capacitive electrodes observed in this project. Our analytical noise expression could be used for designing chip-based devices with integrated microelectrodes for low-noise amperometric sensing.

The technique of measuring transmitter release from large groups of cells is a serious alternative to single cell studies for fast drug screening. The approach could be further improved by developing a device where a fixed number of cells can be trapped close to an electrode. This would avoid the measurement of a second spike for reference and the additional error associated with it.

REFERENCES

1 Squire, L., Berg, D., Bloom, F., du Lac, S., Ghosh, A. and Spitzer, N. *Fundamental Neuroscience,* ed.; Elsevier Inc.:2008.

2 Fatt, P.; Katz, B. *Journal of Physiology-London.* **1952**, *117*, 109-128.

3 Martin, A. *Physiol.Rev.* **1966**, *46*, 51-&.

4 Omiatek, D. M.; Cans, A.; Heien, M. L.; Ewing, A. G. *Anal.Bioanal.Chem.* **2010**, *397*, 3269-3279.

5 Haucke, V.; Neher, E.; Sigrist, S. J. *Nature Reviews Neuroscience.* **2011**, *12*, 127-138.

6 Nutt, D. J.; Baldwin, D. S.; Clayton, A. H.; Elgie, R.; Lecrubier, Y.; Montejo, A. L.; Papakostas, G. I.; Souery, D.; Trivedi, M. H.; Tylee, A. *J.Clin.Psychiatry.* **2006**, *67*, 46-49.

7 Birtwistle, J.; Baldwin, D. **1998**, *7*, 838-841.

8 Joyce, J. *Eur.Neuropsychopharmacol.* **2003**, *13*, S169-S170.

9 Leszczyszyn, D.; Jankowski, J.; Viveros, O.; Diliberto, E.; Near, J.; Wightman, R. *J.Neurochem.* **1991**, *56*, 1855-1863.

10 Leszczyszyn, D.; Jankowski, J.; Viveros, O.; Diliberto, E.; Near, J.; Wightman, R. *J.Biol.Chem.* **1990**, *265*, 14736-14737.

11 Wightman, R.; Jankowski, J.; Kennedy, R.; Kawaoge, K.; Schroeder, T.; Leszczyszyn, D.; Near, J.; Diliberto, E.; Viveros, O. *Proc.Natl.Acad.Sci.U.S.A.* **1991**, *88*, 10754-10758.

12 Westerink, R. H. S.; Ewing, A. G. *Acta Physiologica.* **2008**, *192*, 273-285.

13 Bader, M.; Holz, R.; Kumakura, K.; Vitale, N. *Chromaffin Cell: Trnsmitter Biosynthesis, Storage, Release, Actions, and Informatics.* **2002**, *971*, 178-183.

14 Greene, L.; Tischler, A. *Proc.Natl.Acad.Sci.U.S.A.* **1976**, *73*, 2424-2428.

15 Greene, L.; Rein, G. *Brain Res.* **1977**, *129*, 247-263.

16 Levi, A.; Biocca, S.; Cattaneo, A.; Calissano, P. *Mol.Neurobiol.* **1988**, *2*, 201-226.

17 Dong, Y.; Heien, M. L.; Maxson, M. M.; Ewing, A. G. *J.Neurochem.* **2008**, *107*, 1589-1595.

18 Cui, H.; Ye, J.; Chen, Y.; Chong, S.; Liu, X.; Lim, T.; Sheu, F. *Sensors and Actuators B-Chemical.* **2006**, *115*, 634-641.

19 Borges, R.; Machado, J.; Betancor, G.; Camacho, M. *Chromaffin Cell: Trnsmitter Biosynthesis, Storage, Release, Actions, and Informatics.* **2002**, *971*, 184-192.

20 Westerink, R. *Neurotoxicology.* **2004**, *25*, 461-470.

21 Sombers, L. A.; Hanchar, H. J.; Colliver, T. L.; Wittenberg, N.; Cans, A.; Arbault, S.; Amatore, C.; Ewing, A. G. *Journal of Neuroscience.* **2004**, *24*, 303-309.

22 Kozminski, K. D.; Gutman, D. A.; Davila, V.; Sulzer, D.; Ewing, A. G. *Anal.Chem.* **1998**, *70*, 3123-3130.

23 Zerby, S. E.; Ewing, A. G. *J.Neurochem.* **1996**, *66*, 651-657.

24 Fisher, R. J.; Pevsner, J.; Burgoyne, R. D. *Science.* **2001**, *291*, 875-878.

25 Voets, T.; Toonen, R. F.; Brian, E. C.; de Wit, H.; Moser, T.; Rettig, J.; Sudhof, T. C.; Neher, E.; Verhage, M. *Neuron.* **2001**, *31*, 581-591.

26 Borisovska, M.; Zhao, Y.; Tsytsyura, Y.; Glyvuk, N.; Takamori, S.; Matti, U.; Rettig, J.; Sudhof, T.; Bruns, D. *EMBO J.* **2005**, *24*, 2114-2126.

27 Detoledo, G. A.; Fernandezchacon, R.; Fernandez, J. M. *Nature.* **1993**, *363*, 554-558.

28 Chow, R. H.; Vonruden, L.; Neher, E. *Nature.* **1992**, *356*, 60-63.

29 Amatore, C.; Arbault, S.; Bonifas, I.; Guille, M.; Lemaitre, F.; Verchier, Y. *Biophys.Chem.* **2007**, *129*, 181-189.

30 Michael, D. J.; Wightman, R. M. *J.Pharm.Biomed.Anal.* **1999**, *19*, 33-46.

31 Robinson, D. L.; Venton, B. J.; Heien, M. L. A. V.; Wightman, R. M. *Clin.Chem.* **2003**, *49*, 1763-1773.

32 Spegel, C.; Heiskanen, A.; Pedersen, S.; Emneus, J.; Ruzgas, T.; Taboryski, R. *Lab Chip.* **2008**, *8*, 323-329.

33 Dittami, G. M.; Rabbitt, R. D. *Lab Chip.* **2010**, *10*, 30-35.

34 Liu, X.; Barizuddin, S.; Shin, W.; Mathai, C. J.; Gangopadhyay, S.; Gillis, K. D. *Anal.Chem.* **2011**, *83*, 2445-2451.

35 Chen, P.; Xu, B.; Tokranova, N.; Feng, X.; Castracane, J.; Gillis, K. *Anal.Chem.* **2003**, *75*, 518-524.

36 Vandaveer, W.; Pasas-Farmer, S.; Fischer, D.; Frankenfeld, C.; Lunte, S. *Electrophoresis.* **2004**, *25*, 3528-3549.

37 Lavrik, N. V.; Taylor, L. T.; Sepaniak, M. J. *Anal.Chim.Acta.* **2011**, *694*, 6-20.

38 Seo, J.; Leow, P. L.; Cho, S.; Lim, H.; Kim, J.; Patel, B. A.; Park, J.; O'Hare, D. *Lab on a Chip.* **2009**, *9*, 2238-2244.

39 Hubbard, K. E.; Wells, A.; Owens, T. S.; Tagen, M.; Fraga, C. H.; Stewart, C. F. *Biomed.Chromatogr.* **2010**, *24*, 626-631.

40 Ohno, K.; Tachikawa, K.; Manz, A. *Electrophoresis.* **2008**, *29*, 4443-4453.

41 Xu, X.; Li, L.; Weber, S. G. *Trac-Trends in Analytical Chemistry.* **2007**, *26*, 68-79.

42 Spegel, C.; Heiskanen, A.; Acklid, J.; Wolff, A.; Taboryski, R.; Emneus, J.; Ruzgas, T. *Electroanalysis.* **2007**, *19*, 263-271.

43 Eliaz, N. *Applications of Electrchemistry and Nanotechnology in Biology and Medizine II,* ed.; Springer:2012.

44 Cheng, H.; Huang, W.; Chen, R.; Wang, Z.; Cheng, J. *Electrophoresis.* **2007**, *28*, 1579-1586.

45 Bao, N.; Xu, J.; Dou, Y.; Cai, Y.; Chen, H.; Xia, X. *Journal of Chromatography a.* **2004**, *1041*, 245-248.

46 Osbourn, D. M.; Lunte, C. E. *Anal.Chem.* **2003**, *75*, 2710-2714.

47 Huang, W. H.; Cheng, W.; Zhang, Z.; Pang, D. W.; Wang, Z. L.; Cheng, J. K.; Cui, D. F. *Anal.Chem.* **2004**, *76*, 483-488.

48 Kovarik, M. L.; Torrence, N. J.; Spence, D. M.; Martin, R. S. *Analyst.* **2004**, *129*, 400-405.

49 Muck, A.; Wang, J.; Jacobs, M.; Chen, G.; Chatrathi, M. P.; Jurka, V.; Vyborny, Z.; Spillman, S. D.; Sridharan, G.; Schoning, M. J. *Anal.Chem.* **2004**, *76*, 2290-2297.

50 Wang, J.; Tian, B. M.; Sahlin, E. *Anal.Chem.* **1999**, *71*, 5436-5440.

51 Hebert, N.; Snyder, B.; McCreery, R.; Kuhr, W.; Brazill, S. *Anal.Chem.* **2003**, *75*, 4265-4271.

52 Takmakov, P.; Zachek, M. K.; Keithley, R. B.; Walsh, P. L.; Donley, C.; McCarty, G. S.; Wightman, R. M. *Anal.Chem.* **2010**, *82*, 2020-2028.

53 Zachek, M. K.; Takmakov, P.; Moody, B.; Wightman, R. M.; McCarty, G. S. *Anal.Chem.* **2009**, *81*, 6258-6265.

54 Cui, H.; Ye, J.; Chen, Y.; Chong, S.; Sheu, F. *Anal.Chem.* **2006**, *78*, 6347-6355.

55 Berberian, K.; Kisler, K.; Fang, Q.; Lindau, M. *Anal.Chem.* **2009**, *81*, 8734-8740.

56 Dias, A.; Dernick, G.; Valero, V.; Yong, M.; James, C.; Craighead, H.; Lindau, M. *Nanotechnology.* **2002**, *13*, 285-289.

57 Dias, A.; Dernick, G.; Yong, M.; Valero, V.; James, C.; Craighead, H.; Lindau, M. *Biophys.J.* **2002**, *82*, 11A-11A.

58 Lane, R.; Hubbard, A. *Anal.Chem.* **1976**, *48*, 1287-1293.

59 Lane, R.; Hubbard, A.; Fukunaga, K.; Blanchard, R. *Brain Res.* **1976**, *114*, 346-352.

60 Sun, X.; Gillis, K. *Anal.Chem.* **2006**, *78*, 2521-2525.

61 Amatore, C.; Arbault, S.; Lemaitre, F.; Verchier, Y. *Biophys.Chem.* **2007**, *127*, 165-171.

62 Amatore, C.; Arbault, S.; Chen, Y.; Crozatier, C.; Lemaitre, F.; Verchier, Y. *Angew.Chem.-Int.Edit.* **2006**, *45*, 4000-4003.

63 Meunier, A.; Fulcrand, R.; Darchen, F.; Collignon, M. G.; Lemaitre, F.; Amatore, C. *Biophys.Chem.* **2012**, *162*, 14-21.

64 Colombo, E.; Men, Y.; Scharpf, J.; Pietzka, C.; Dipalo, M.; Herfurth, P.; Gao, Z.; Schneider, M.; Carabelli, V.; Carbone, E.; Kohn, E.; Pasquarelli, A. *Diamond and Related Materials.* **2011**, *20*, 793-797.

65 Carabelli, V.; Gosso, S.; Marcantoni, A.; Xu, Y.; Colombo, E.; Gao, Z.; Vittone, E.; Kohn, E.; Pasquarelli, A.; Carbone, E. *Biosens.Bioelectron.* **2010**, *26*, 92-98.

66 Pasquarelli, A.; Carabelli, V.; Xu, Y.; Colombo, E.; Gao, Z.; Scharpf, J.; Carbone, E.; Kohn, E. *Int.J.Environ.Anal.Chem.* **2011**, *91*, 150-160.

67 Sen, A.; Barizuddin, S.; Hossain, M.; Polo-Parada, L.; Gillis, K. D.; Gangopadhyay, S. *Biomaterials.* **2009**, *30*, 1604-1612.

68 Chiang, C.; Fincher, C.; Park, Y.; Heeger, A.; Shirakawa, H.; Louis, E.; Gau, S.; Macdiarmid, A. *Phys.Rev.Lett.* **1977**, *39*, 1098-1101.

69 Shirakawa, H.; Louis, E.; Macdiarmid, A.; Chiang, C.; Heeger, A. *Journal of the Chemical Society-Chemical Communications.* **1977**, , 578-580.

70 Kirchmeyer, S.; Reuter, K. *Journal of Materials Chemistry.* **2005**, *15*, 2077-2088.

71 Dietrich, M.; Heinze, J.; Heywang, G.; Jonas, F. *J Electroanal Chem.* **1994**, *369*, 87-92.

72 Groenendaal, B.; Jonas, F.; Freitag, D.; Pielartzik, H.; Reynolds, J. *Adv Mater.* **2000**, *12*, 481-494.

73 Rozlosnik, N. *Anal.Bioanal.Chem.* **2009**, *395*, 637-645.

74 Deleeuw, D.; Kraakman, P.; Bongaerts, P.; Mutsaers, C.; Klaassen, D. *Synth.Met.* **1994**, *66*, 263-273.

75 Irwin, M. D.; Buchholz, B.; Hains, A. W.; Chang, R. P. H.; Marks, T. J. *Proc.Natl.Acad.Sci.U.S.A.* **2008**, *105*, 2783-2787.

76 Krebs, F. C.; Gevorgyan, S. A.; Alstrup, J. *Journal of Materials Chemistry.* **2009**, *19*, 5442-5451.

77 Sakurai, S.; Jiang, H.; Takahashi, M.; Kobayashi, K. *Electrochim.Acta.* **2009**, *54*, 5463-5469.

78 Armstrong, N. R.; Wang, W.; Alloway, D. M.; Placencia, D.; Ratcliff, E.; Brumbach, M. *Macromolecular Rapid Communications.* **2009**, *30*, 717-731.

79 Winther-Jensen, B.; Winther-Jensen, O.; Forsyth, M.; MacFarlane, D. R. *Science.* **2008**, *321*, 671-674.

80 Winther-Jensen, B.; Fraser, K.; Ong, C.; Forsyth, M.; MacFarlane, D. R. *Adv Mater.* **2010**, *22*, 1727-+.

81 Vidal, F.; Plesse, C.; Palaprat, G.; Kheddar, A.; Citerin, J.; Teyssie, D.; Chevrot, C. *Synth.Met.* **2006**, *156*, 1299-1304.

82 Okuzaki, H.; Suzuki, H.; Ito, T. *Synth.Met.* **2009**, *159*, 2233-2236.

83 Forzani, E. S.; Li, X.; Tao, N. *Anal.Chem.* **2007**, *79*, 5217-5224.

84 Nambiar, S.; Yeow, J. T. W. *Biosens.Bioelectron.* **2011**, *26*, 1825-1832.

85 Macaya, D. J.; Nikolou, M.; Takamatsu, S.; Mabeck, J. T.; Owens, R. M.; Malliaras, G. G. *Sensors and Actuators B-Chemical.* **2007**, *123*, 374-378.

86 Liu, J.; Agarwal, M.; Varahramyan, K. *Sensors and Actuators B-Chemical.* **2008**, *135*, 195-199.

87 Berggren, M.; Richter-Dahlfors, A. *Adv Mater.* **2007**, *19*, 3201-3213.

88 Asplund, M.; Nyberg, T.; Inganas, O. *Polymer Chemistry.* **2010**, *1*, 1374-1391.

89 Kiilerich-Pedersen, K.; Poulsen, C. R.; Jain, T.; Rozlosnik, N. *Biosens.Bioelectron.* **2011**, *28*, 386-392.

90 Sarma, A. K.; Vatsyayan, P.; Goswami, P.; Minteer, S. D. *Biosens.Bioelectron.* **2009**, *24*, 2313-2322.

91 Setti, L.; Fraleoni-Morgera, A.; Mencarelli, I.; Filippini, A.; Ballarin, B.; Di Biase, M. *Sensors and Actuators B-Chemical.* **2007**, *126*, 252-257.

92 Green, R. A.; Lovell, N. H.; Poole-Warren, L. A. *Acta Biomaterialia.* **2010**, *6*, 63-71.

93 Green, R. A.; Lovell, N. H.; Poole-Warren, L. A. *Biomaterials.* **2009**, *30*, 3637-3644.

94 Richardson-Burns, S. M.; Hendricks, J. L.; Foster, B.; Povlich, L. K.; Kim, D.; Martin, D. C. *Biomaterials.* **2007**, *28*, 1539-1552.

95 Sekine, S.; Ido, Y.; Miyake, T.; Nagamine, K.; Nishizawa, M. *J.Am.Chem.Soc.* **2010**, *132*, 13174-13175.

96 Kumar, S. S.; Mathiyarasu, J.; Phani, K. L. N.; Yegnaraman, V. *J.Solid State Electrochem.* **2006**, *10*, 905-913.

97 Kumar, S.; Mathiyarasu, J.; Phani, K. *J Electroanal Chem.* **2005**, *578*, 95-103.

98 Vasantha, V. S.; Chen, S. *J Electroanal Chem.* **2006**, *592*, 77-87.

99 Vasantha, V.; Chen, S. *Electrochim.Acta.* **2005**, *51*, 347-355.

100 Lupu, S. *Revue Roumaine De Chimie.* **2005**, *50*, 213-217.

101 Lupu, S.; Javier del Campo, F.; Xavier Munoz, F. *J Electroanal Chem.* **2010**, *639*, 147-153.

102 Stoyanova, A.; Tsakova, V. *Journal of Solid State Electrochemistry.* **2010**, *14*, 1947-1955.

103 Harish, S.; Mathiyarasu, J.; Phani, K. L. N.; Yegnaraman, V. *J.Appl.Electrochem.* **2008**, *38*, 1583-1588.

104 Jeyalakshmi, S. R.; Kumar, S. S.; Mathiyarasu, J.; Phani, K. L. N.; Yegnaraman, V. *Indian Journal of Chemistry Section A-Inorganic Bio-Inorganic Physical Theoretical & Analytical Chemistry.* **2007**, *46*, 957-961.

105 Sekli-Belaidi, F.; Temple-Boyer, P.; Gros, P. *J Electroanal Chem.* **2010**, *647*, 159-168.

106 Seldi-Belaidi, F.; Evrard, D.; Gros, P. *Electrochemistry Communications.* **2011**, *13*, 423-425.

107 Balamurugan, A.; Chen, S. *Anal.Chim.Acta.* **2007**, *596*, 92-98.

108 Lin, K.; Tsai, T.; Chen, S. *Biosens.Bioelectron.* **2010**, *26*, 608-614.

109 Atta, N. F.; Galal, A.; Ahmed, R. A. *J.Electrochem.Soc.* **2011**, *158*, F52-F60.

110 Yang, S. Y.; Kim, B. N.; Zakhidov, A. A.; Taylor, P. G.; Lee, J.; Ober, C. K.; Lindau, M.; Malliaras, G. G. *Adv Mater.* **2011**, *23*, H184-H188.

111 Huang, Y.; Cai, D.; Chen, P. *Anal.Chem.* **2011**, *83*, 4393-4406.

112 Ge, S.; Koseoglu, S.; Haynes, C. L. *Anal.Bioanal.Chem.* **2010**, *397*, 3281-3304.

113 Spegel, C.; Heiskanen, A.; Skjolding, L. H. D.; Emneus, J. *Electroanalysis.* **2008**, *20*, 680-702.

114 Chen, Z.; Gao, Y.; Lin, J.; Su, R.; Xie, Y. *J.Chromatogr.A.* **2004**, *1038*, 239-245.

115 Lacher, N.; Lunte, S.; Martin, R. *Anal.Chem.* **2004**, *76*, 2482-2491.

116 Shi, B.; Wang, Y.; Lam, T.; Huang, W.; Zhang, K.; Leung, Y.; Chan, H. L. W. *Biomicrofluidics.* **2010**, *4*, 043009.

117 Winther-Jensen, B.; West, K. *React Funct Polym.* **2006**, *66*, 479-483.

118 Winther-Jensen, B.; Breiby, D.; West, K. *Synth.Met.* **2005**, *152*, 1-4.

119 Andresen, K. O.; Hansen, M.; Matschuk, M.; Jepsen, S. T.; Sorensen, H. S.; Utko, P.; Selmeczi, D.; Hansen, T. S.; Larsen, N. B.; Rozlosnik, N.; Taboryski, R. *J Micromech Microengineering.* **2010**, *20*, 055010.

120 Hansen, T. S.; West, K.; Hassager, O.; Larsen, N. B. *J Micromech Microengineering.* **2007**, *17*, 860-866.

121 Heien, M.; Phillips, P.; Stuber, G.; Seipel, A.; Wightman, R. *Analyst.* **2003**, *128*, 1413-1419.

122 Hochstetler, S.; Puopolo, M.; Gustincich, S.; Raviola, E.; Wightman, R. *Anal.Chem.* **2000**, *72*, 489-496.

123 Bard, A. J. and Faulkner, L. R. *Electrochemical Methods,* ed.; John Wiley & Sons, Inc.:2001.

124 Nicholson, RS. *Anal.Chem.* **1965**, *37*, 1351-&.

125 Gao, Y.; Chen, X.; Gupta, S.; Gillis, K. D.; Gangopadhyay, S. *Biomed.Microdevices.* **2008**, *10*, 623-629.

126 Larsen, S. T.; Vreeland, R. F.; Heien, M. L.; Taboryski, R. *Analyst.* **2012**, *137*, 1831-1836.

127 Morgan, D.; Weber, S. *Anal.Chem.* **1984**, *56*, 2560-2567.

128 Hassibi, A.; Navid, R.; Dutton, R.; Lee, T. *J.Appl.Phys.* **2005**, *98*, 069903.

129 Schulte, A.; Chow, R. *Anal.Chem.* **1998**, *70*, 985-990.

130 Long, J.; Weber, S. *Anal.Chem.* **1988**, *60*, 2309-2311.

131 Li, Z.; Zhou, W.; Wu, Z.; Zhang, R.; Xu, T. *Biosens.Bioelectron.* **2009**, *24*, 1358-1364.

132 Hafez, I.; Kisler, K.; Berberian, K.; Dernick, G.; Valero, V.; Yong, M.; Craighead, H.; Lindau, M. *Proc.Natl.Acad.Sci.U.S.A.* **2005**, *102*, 13879-13884.

133 Winder, S. *Analog and Digital Filter Design,* 2nd ed.; Newnes:2002.

134 Zoski, C. G. *Handbook of Electrochemistry,* ed.; Elsevier:2007.

135 Dittami, G. M.; Ayliffe, H. E.; King, C. S.; Rabbitt, R. D. *J Microelectromech Syst.* **2008**, *17*, 850-862.

136 Westerink, R.; de Groot, A.; Vijverberg, H. *Biochem.Biophys.Res.Commun.* **2000**, *270*, 625-630.

137 Pothos, E.; Desmond, M.; Sulzer, D. *J.Neurochem.* **1996**, *66*, 629-636.

138 Sulzer, D.; Chen, T. K.; Lau, Y. Y.; Kristensen, H.; Rayport, S.; Ewing, A. *Journal of Neuroscience.* **1995**, *15*, 4102-4108.

139 Hondebrink, L.; Meulenbelt, J.; Timmerman, J. G.; van den Berg, M.; Westerink, R. H. S. *J.Neurochem.* **2009**, *111*, 624-633.

140 Pothos, E. N.; Przedborski, S.; Davila, V.; Schmitz, Y.; Sulzer, D. *Journal of Neuroscience.* **1998**, *18*, 5575-5585.

141 Chen, Y.; Guo, C.; Lim, L.; Cheong, S.; Zhang, Q.; Tang, K.; Reboud, J. *Anal.Chem.* **2008**, *80*, 1133-1140.

142 Motulsky, H. and Christopoulos, A. *Fitting Models to Biological Data using Linear and Nonlinear Regression,* 2nd ed.; GraphPad Software, Inc.:2003.

143 Argyraki, A. **2012**,

144 Fischer, D.; Vandaveer, W.; Grigsby, R.; Lunte, S. *Electroanalysis.* **2005**, *17*, 1153-1159.

145 Zhou, H.; Gupta, A.; Zou, T.; Zhou, J. *International Journal of Molecular Sciences.* **2007**, *8*, 884-893.

146 Kostecki, R.; Schnyder, B.; Alliata, D.; Song, X.; Kinoshita, K.; Kotz, R. *Thin Solid Films.* **2001**, *396*, 36-43.

147 Madou, M., Lal, A., Schmidt, G., Song, X., Kinoshita, K., Fendorf, M., Zettl, A. and White, R. *Carbon Micromachining (C-MEMS),* ed.; 1997.

148 Rehacek, V.; Hotovy, I.; Vojs, M.; Kotlar, M.; Kups, T.; Spiess, L. *Journal of Electrical Engineering-Elektrotechnicky Casopis.* **2011**, *62*, 49-53.

149 Tang, Z.; Shi, T.; Gong, J.; Nie, L.; Liu, S. *Thin Solid Films.* **2010**, *518*, 2701-2706.

150 Singh, A.; Jayaram, J.; Madou, M.; Akbar, S. *J.Electrochem.Soc.* **2002**, *149*, E78-E83.

151 Fairman, C.; Yu, S. S. C.; Liu, G.; Downard, A. J.; Hibbert, D. B.; Gooding, J. J. *Journal of Solid State Electrochemistry.* **2008**, *12*, 1357-1365.

152 Javier del Campo, F.; Godignon, P.; Aldous, L.; Pausas, E.; Sarrion, M.; Zabala, M.; Prehn, R.; Compton, R. G. *J.Electrochem.Soc.* **2011**, *158*, H63-H68.

153 Donner, S.; Li, H.; Yeung, E.; Porter, M. *Anal.Chem.* **2006**, *78*, 2816-2822.

154 Schreiber, M.; Lutz, T.; Keeley, G. P.; Kumar, S.; Boese, M.; Krishnamurthy, S.; Duesberg, G. S. *Appl.Surf.Sci.* **2010**, *256*, 6186-6190.

155 Kim, J.; Song, X.; Kinoshita, K.; Madou, M.; White, B. *J.Electrochem.Soc.* **1998**, *145*, 2314-2319.

156 Ranganathan, S.; McCreery, R. *Anal.Chem.* **2001**, *73*, 893-900.

157 Ranganathan, S.; McCreery, R.; Majji, S.; Madou, M. *J.Electrochem.Soc.* **2000**, *147*, 277-282.

158 Gao, Z.; Carabelli, V.; Carbone, E.; Colombo, E.; Dipalo, M.; Manfredotti, C.; Pasquarelli, A.; Feneberg, M.; Thonke, K.; Vittone, E.; Kohn, E. *J. Micro-Nano Mech.* **2011**, *6*, 33-37.

159 Conway, B. E.; Birss, V.; Wojtowicz, J. *J.Power Sources.* **1997**, *66*

160 Sahlin, E.; ter Halle, A.; Schaefer, K.; Horn, J.; Then, M.; Weber, S. *Anal.Chem.* **2003**, *75*, 1031-1036.

161 Strand, A. M.; Venton, B. J. *Anal.Chem.* **2008**, *80*, 3708-3715.

162 Conway, B.; Pell, W. *Journal of Solid State Electrochemistry.* **2003**, *7*, 637-644.

163 Lota, K.; Khomenko, V.; Frackowiak, E. *Journal of Physics and Chemistry of Solids.* **2004**, *65*

164 Beguin, F.; Raymundo-Pinero, E.; Lota, G.; Frackowiak, E. *Abstracts of Papers of the American Chemical Society.* **2006**, *231*

165 Frackowiak, E. *Journal of the Brazilian Chemical Society.* **2006**, *17*, 1074-1082.

166 Song, H.; Palmore, G. T. R. *Adv Mater.* **2006**, *18*

167 Liu, R.; Il Cho, S.; Lee, S. B. *Nanotechnology.* **2008**, *19*, 215710.

168 Carlberg, J. C.; Inganas, O. *J.Electrochem.Soc.* **1997**, *144*

169 Tanzi, S.; Larsen, S. T.; Matteucci, M.; Taboryski, R. *Nanotech 2012 Proceedings.* **2012**, *2*, 376-379.

Acknowledgments

I would like to thank all the people who have contributed to this thesis. Especially:

My supervisor Rafael Taboryski, for great guidance and helpful discussions throughout the project.

Dr Michael Heien, who was my supervisor during my external research stay, for good discussions and frequent mails and phone calls about electrochemical matters.

All the lab technicians at building 423, DTU Nanotech. Especially Ina Blom and Ole Kristoffersen for help in the cell lab and with ordering of equipment.

My colleagues and fellow students: Simone Tanzi, Aikaterini Argyraki, Emil Søgaard, Marco Matteucci, Kristian Andresen, Jiri Cech, Peter Østergaard, Johan Lind, Katrine Kiilerich-Pedersen, Maria Matschuk, Alicia Johansson, Thor Hobæk, Claus Poulsen, Thomas Christiansen, Jacqueline Trosborg and others for help in everyday lab situations and a lot of fun!

My wife Lea, for great support!

List of publications

Characterization of Poly(3,4-ethylenedioxythiophene):tosylate conductive polymer microelectrodes for transmitter detection

Larsen, S. T.; Vreeland, R. F.; Heien, M. L.; Taboryski, R.

Analyst. **2012**, *137*, 1831-1836

Amperometric noise at thin film band electrodes

Larsen, S. T.; Heien, M. L.; Taboryski, R.

Manuscript submitted to Analytical Chemistry, april 2012

All polymer chip for amperometric studies of transmitter release from large groups of neuronal cells

Larsen, S. T.; Taboryski, R.

Manuscript submitted to Analyst, july 2012

Conductive Polymer Microelectrodes for on-chip measurement of transmitter release from living cells

S. Tylsgaard Larsen, M. Matteucci, R. Taboryski

Nanotech 2012 Proceedings. 2012, 2, 302 - 305.

Conference contributions

(Only presenter contributions are listed)

Poster: Simon Tylsgaard Larsen and Rafael Taboryski, *A polymer chip for the electrochemical detection of neurotransmitters from single cells*, Pittcon conference and expo 2010, Orlando, USA

Poster: Simon Tylsgaard Larsen, Simone Tanzi and Rafael Taboryski, *Polymer Chip for Amperometric Detection of Neurotransmitter Release from Single Cells*, Pittcon conference and expo 2011, Atlanta, USA

Poster: Simon T Larsen, Richard F Vreeland, Michael L Heien, Rafael J Taboryski, *Characterization of Pedot:tosylate Microelectrodes for Transmitter Detection*, Pittcon conference and expo 2012, Orlando, USA

Poster: Simone Tanzi*, Simon Tylsgaard Larsen* and Rafael Taboryski, *Injection molded polymer chip for electrochemical and electrophysiological recordings from single cells*, MNE 2011, Berlin, Germany, *contributed equally

Oral: S. Tylsgaard Larsen, M. Matteucci, R. Taboryski, *Conductive Polymer Microelectrodes for on-chip measurement of transmitter release from living cells*, Nanotech 2012, Santa Clara, USA

Appendix: Publications

In this appendix the original versions of the publications listed on page 91 are reprinted.

Analyst

Dynamic Article Links

Cite this: *Analyst*, 2012, **137**, 1831

www.rsc.org/analyst

PAPER

Characterization of poly(3,4-ethylenedioxythiophene):tosylate conductive polymer microelectrodes for transmitter detection

Simon T. Larsen,[a] Richard F. Vreeland,[b] Michael L. Heien[b] and Rafael Taboryski*[a]

Received 22nd December 2011, Accepted 26th January 2012
DOI: 10.1039/c2an16288a

In this paper we investigate the physical and electrochemical properties of micropatterned poly(3,4-ethylenedioxythiophene):tosylate (PEDOT:tosylate) microelectrodes for neurochemical detection. PEDOT:tosylate is a promising conductive polymer electrode material for chip-based bioanalytical applications such as capillary electrophoresis, high-performance liquid chromatography, and constant potential amperometry at living cells. Band electrodes with widths down to 3 μm were fabricated on polymer substrates using UV lithographic methods. The electrodes are electrochemically stable in a range between −200 mV and 700 mV *vs.* Ag/AgCl and show a relatively low resistance. A wide range of transmitters is shown to oxidize readily on the electrodes. Kinetic rate constants and half wave potentials are reported. The capacitance per area was found to be high (1670 ± 130 μF cm^{-2}) compared to other thin film microelectrode materials. Finally, we use constant potential amperometry to measure the release of transmitters from a group of PC 12 cells. The results show how the current response decreases for a series of stimulations with high K^+ buffer.

Introduction

Neurotransmitters are an important class of molecules, enabling neurons to communicate with target cells using chemical signals. These signals are responsible for controlling and integrating sensory inputs into behavioral outputs. Direct measurement of these neurotransmitters and other signaling molecules provides insight into their role in biological systems. Indeed, many studies target a group of biogenic amines including dopamine, epinephrine, norepinephrine, histamine, and serotonin; all of these are electroactive and can be easily oxidized at an electrode. Due to the electroactive nature of these biogenic amines, electrochemical methods have been developed to measure them. Electrochemical methods are sensitive, quantitative, and dynamic, and therefore widely used in bioanalytical approaches targeting transmitter detection.[1–3] Electrochemical methods can be used *in situ* or they can be coupled to an off-line separation technique. An attractive detection scheme for mass-limited samples is capillary electrophoresis (CE) coupled with electrochemical detection. Electrochemical detection is an alternative to laser-induced-fluorescence detection due to the fact that many compounds can be detected without derivatization with a fluorophore. In addition, both the detector and instrumentation can be miniaturized.[4] CE can be used to study transmitter distributions in small biological samples such as cells or even single vesicles.[5] Coupling electrochemical detection with high-performance liquid chromatography (HPLC) delivers comparable benefits (*see above*).[6] HPLC coupled with electrochemical detection can be used to rapidly measure transmitter concentrations in biological fluids.[7] In other applications, the transmitter is measured as it is released *in vivo* or *in vitro*. The release of transmitters from individual vesicles (a process called exocytosis) can be detected using constant potential amperometry performed at single cells.[8] In this technique, a microelectrode is held close to the cell membrane and the released transmitter is oxidized at the electrode surface giving rise to peaks on the resultant current *versus* time trace.

Chip-based devices offer advantages such as high throughput, automation, and the ability to integrate different analytical features into one device.[9] In contrast, manual laboratory techniques, while they have yielded stable and successful tools for researchers, require serial measurements and are difficult to automate. In the last decade a strong effort has been undertaken to develop chip-based devices to overcome these limitations. Micropatterned thin-film electrodes made of platinum, gold,[4] carbon fibers,[10] palladium[11] and pyrolyzed photoresist[12] have been used in microfabricated devices for microchip CE applications. Chip-based devices for measuring exocytosis have also been developed using platinum,[13,14] gold,[15,16] mercapto-propionic acid modified gold,[17] indium tin oxide[18,19] and nitrogen-doped diamond-like-carbon as electrode materials.[20] These electrodes are typically fabricated on a glass or silicon substrate which can be further modified by bonding a PDMS counterpart.

More recently, conductive polymers have emerged as an alternative to traditional electrode materials.[21–25] Polymer

[a]*Department of Micro- and Nanotechnology, Technical University of Denmark, DTU Nanotech, Building 345B, DK-2800 Kongens Lyngby, Denmark. E-mail: rata@nanotech.dtu.dk*
[b]*Department of Chemistry and Biochemistry, University of Arizona, 1306 E. University Blvd., Tucson, AZ 85721, USA*

electrodes combine the electrical properties of metals and semiconductors with the light weight and processing properties of common polymers. Among conductive polymers PEDOT is a promising material for biosensor devices focusing on neurotransmitter detection.[26] It is biocompatible with a variety of different cells,[27,28] conductive, transparent, and stable over long time periods.[29] Dopamine and other transmitters can be selectively detected on PEDOT-modified metal and glassy carbon electrodes in the presence of ascorbic acid and uric acid.[30,31] Recently, Yang *et al.* demonstrated that transmitter release from single chromaffin cells can be detected at PEDOT:PSS microelectrodes.[32]

The synthesis of PEDOT can be carried out by chemical or electrochemical polymerization of the monomer 3,4-ethylenedioxythiophene (EDOT).[33] An easy and robust chemical polymerization method uses the monomer EDOT and iron tosylate (iron(III) *p*-toluenesulfonate) catalyst (commercially available from Clevios™) as dopant. By adding a small amount of base (pyridine) to the monomer and dopant, polymerization can be retarded, which allows the solution to be spin-coated onto substrates.[34] After baking and rinsing, a film with a positively charged polymer backbone balanced by negatively charged tosylate ions is formed.

PEDOT:tosylate electrodes can be fabricated by spin-coating a solution directly onto a variety of substrates. Electrodes can then be easily patterned and integrated in chips by bonding the substrates to counterparts containing a microfluidic channel system.[35] Due to the relatively low resistivity of PEDOT:tosylate compared to other conductive polymers, no metal layer is needed for supporting the electrode. This allows for inexpensive and mass-producible all-polymer devices.[35,36] In this work we characterize the physical and electrochemical properties of PEDOT:tosylate microelectrodes to examine their capacity for sensing transmitters. A variety of transmitters are shown to oxidize at the electrode surface, and heterogeneous rate constants and half wave potentials are reported. In addition, transmitter release from cells is measured. This opens the way for cheap and easy-to-fabricate all-polymer devices for electrochemical detection of transmitters in various systems.

Materials and methods

Electrode fabrication and characterization

Ø 50 mm polymer substrates were prepared by injection molding of TOPAS® 5013 Cyclic Olefin Copolymer (Topas Advanced Polymers GmbH). PEDOT:tosylate films were fabricated by spin-coating a solution of 6.5 mL Clevios™ CB 40 V2 (H.C. Starck), 2 mL butanol, 150 μL pyridine (Fluka) and 220 μL Clevios™ M V2 (H.C.Starck) onto the TOPAS substrates at 1000 rpm for 30 seconds. The substrates were baked on a hot plate at 70 °C to remove the remaining solvent and then washed in deionized water. Conductivity was measured with a four-point probe (Jandel Engineering Ltd) connected to a Keithley 2400 SourceMeter (Keithley Instruments Inc.) using currents in the range 1–10 μA. The height of the PEDOT:tosylate layer was measured using a Dektak 8 profilometer (Veeco Instruments).

Electrodes were patterned by photolithography. AZ5214E photoresist was spin-coated on the PEDOT:tosylate-coated substrates at 4500 rpm for 30 s. The samples were soft baked on a hot plate at 95 °C for 5 minutes before being exposed in a Karl Suss MA6/BA6 Mask Aligner for 3 seconds (intensity 7.0 mW cm^{-2}) and developed with an AZ351B developer. The photomask was ordered at Delta Mask B.V. After photolithographic patterning, the exposed PEDOT:tosylate was removed by reactive ion etching. The remaining resist was flood exposed in the Mask Aligner for 35 seconds and stripped off in an acetone bath for 5 minutes. The electrodes were rinsed thoroughly with deionized water and dried using compressed nitrogen. Band electrodes between 3 μm and 50 μm wide were fabricated.

Electrochemical measurements

Electrochemical measurements were made on a device constructed by placing a PDMS mold on a substrate (Fig. 1). The potentiostat (Dagan Chem Clamp, Dagan Corporation) was connected to the electrode either by a Ag wire immersed in KCl or by using conductive epoxy glue (Conductive Epoxy, Chemtronics). The electroactive area of the PEDOT:tosylate film was defined by one of two methods: (1) the electrode protruded into a channel (125 μm × 110 μm, width × height) to create a band electrode (Fig. 1) whose electroactive area was defined by the width of the channel or (2) the band electrode protruded into a second well which was filled with solution. The electrode length depended on the penetration depth into the well and it was measured using a microscope (Nikon TE2000U, Nikon Inc.). The two geometries enabled different boundary conditions to be probed, semi-infinite or finite conditions. Data were collected using custom programs written in LabVIEW (National Instruments, Austin, Texas). These were used to apply voltages and measure the resultant current. A Ag/AgCl reference electrode (RE-5B, BASi) was placed with the tip in the PDMS well and buffer solution was added. A pneumatically actuated six port HPLC valve (Vici, Austin, TX) was connected to the solution inlet (Fig. 1). The valve controlled the injection of a bolus onto the electroactive area. A Harvard PhD 2000 pump (Harvard Apparatus, Holliston, MA) controlled the flow rate of solutions (20–70 μL per minute). For rate constant determination, the

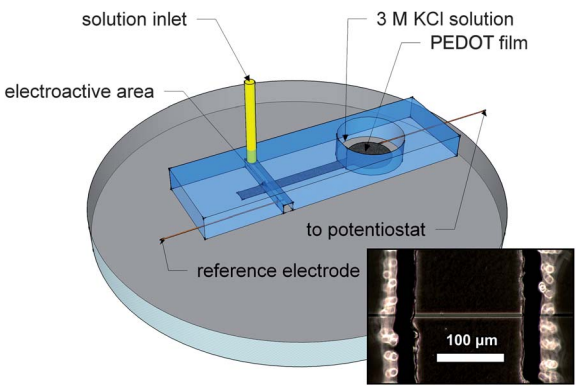

Fig. 1 Diagram of a microfluidic device for electrochemical measurements at PEDOT:tosylate electrodes. Electrical contact to the PEDOT:tosylate electrode is made through a Ag wire in a KCl solution. The electroactive area is defined by the geometry of the PDMS mold (not to scale). An optical image (inset) is the PDMS mold defining the electroactive area.

background collected prior to the bolus reaching the electrode was subtracted from the cyclic voltammogram.

Chemicals

Electrochemical measurements were performed in phosphate-buffered saline (Lonza). Ferrocene methanol, carboxy-ferrocene, dopamine, epinephrine, norepinephrine, homovanilic acid, L-3,4-dihydroxyphenylalanine, 5-hydroxyindole acetic acid, serotonin, histamine and 3,4-dihydroxyphenylacetic acid were purchased from Sigma-Aldrich and dissolved in PBS buffer.

Cell experiments

Passage 12 rat pheochromocytoma (PC 12) cells were cultured on collagen (type 1, Sigma-Aldrich) coated Nunclon T25 flasks (Nunc A/S). All cell medium was carefully removed by flushing the cells with a physiological buffer (150 mM NaCl, 5 mM KCl, 1.2 mM $MgCl_2$, 5 mM glucose, 10 mM HEPES and 2 mM $CaCl_2$, from Sigma-Aldrich). Electrodes were coated with poly-L-lysine (incubation in room temperature for 1 h, 0.01 mg mL^{-1}) before being used for cell experiments. Fresh physiological buffer was added to the flask and the cells were loosened by gently agitating the flask. The cell suspension was added to the PDMS well containing the PEDOT:tosylate electrode and cells were allowed to sediment on the surface for 10 minutes. Release of transmitters was triggered by exchanging the physiological buffer with an isotonic K^+-rich buffer (KCl increased to 105 mM).

Results and discussion

Physical properties

PEDOT:tosylate electrodes were fabricated on Topas substrates. The oxidized structure of the film can be seen in Scheme 1. Then, the physical and electrical properties of the PEDOT:tosylate electrodes were characterized (Table 1). The PEDOT:tosylate layer was measured to be 190 ± 10 nm high after the deposition of one layer. The height can be increased by adding multiple PEDOT:tosylate layers. Four point probe measurements revealed a sheet resistance of 113 ± 7 Ω (n = 10) for newly prepared PEDOT:tosylate films. The measured sheet resistance corresponds to a bulk conductivity of 470 ± 30 S cm^{-1} which is in concordance with conductivities reported in the literature for PEDOT:tosylate films.[29,36] In addition, the resistance was observed to increase over time. After 3 weeks of exposure to atmospheric conditions at room temperature, the sheet resistance of the films was 151 ± 11 Ω.

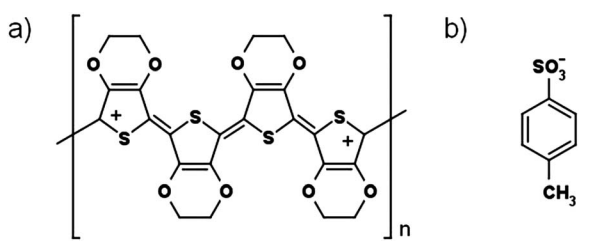

Scheme 1 The chemical structure of (a) positively charged PEDOT and (b) negatively charged tosylate counter ion. Redrawn from ref. 41.

Table 1 Physical properties of PEDOT:tosylate film electrodes (thickness = 190 nm). Error is the standard deviation (n = 10)

Sheet resistance	113 ± 7 Ω
Capacitance per unit area	1700 ± 100 μF cm^{-2}
Potential limits (*vs.* Ag/AgCl)	−200 mV, 700 mV

The apparent capacitance of the electrodes was measured by collecting background cyclic voltammograms at the electrodes immersed in PBS buffer. A Ag/AgCl reference electrode was used. Fig. 2 shows background scans of a PEDOT:tosylate band electrode with dimensions of 12 μm × 6000 μm. Between the potential limits −200 mV and 700 mV the charging current is approximately constant. The apparent capacitance was calculated by dividing the charging current by the scan rate. The capacitance was measured to be 1670 ± 120 μF cm^{-2} (n = 10). In contrast to the resistance, the capacitance was stable over time and did not change significantly over a period of 8 months. These capacitance values are quite high when compared to traditional electrode materials used for transmitter detection (20–100 μF cm^{-2} typical).[37] This high capacitance may limit the performance of PEDOT:tosylate films in some applications. The root mean square noise has been reported to scale with the electrode capacitance in low-noise amperometric experiments performed at carbon-fiber microelectrodes.[38] This means that PEDOT:tosylate electrodes have to be patterned on a few micrometre scale for low-noise amperometric experiments. The noise properties of PEDOT:tosylate electrodes are a follow-up for future studies. The increased capacitance will also affect the RC time constant of the electrode, ultimately limiting the scan rates attainable at PEDOT:tosylate electrodes. These measurements indicate that stable films can be mass produced and easily stored for use.

Electrochemical properties

The performance of the PEDOT:tosylate films was evaluated. Ferrocene methanol, a well-characterized molecule, was oxidized at the electrode and the electrochemical properties of the PEDOT:tosylate films were evaluated. Fig. 3a shows the

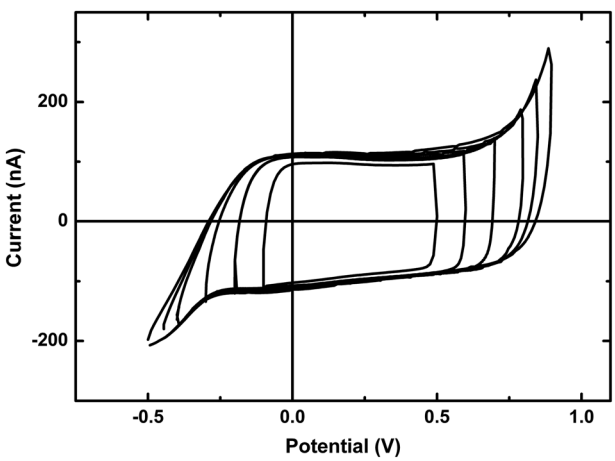

Fig. 2 Cyclic voltammograms showing the background current towards an Ag/AgCl reference electrode for a PEDOT:tosylate electrode in PBS buffer. Electrode area 12 μm × 6000 μm. Scan rate 100 mV s^{-1}.

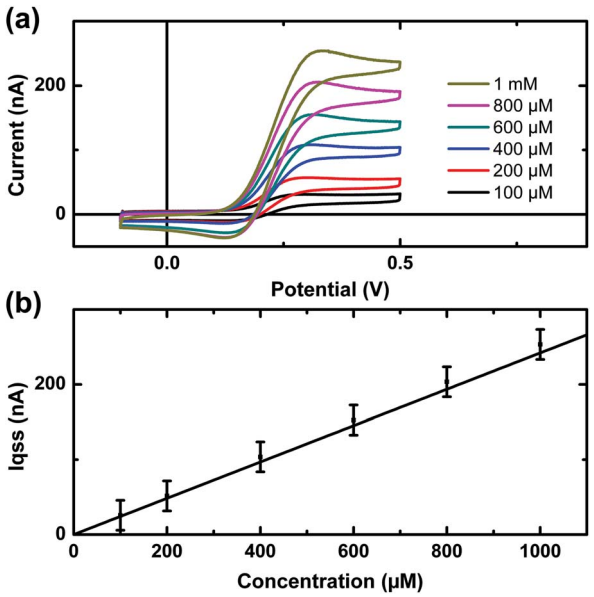

Fig. 3 (a) Slow scan cyclic voltammograms showing the oxidation of ferrocene methanol at different concentrations at a 13 μm × 5600 μm PEDOT:tosylate electrode. Scan rate 5 mV s^{-1}. A Ag/AgCl reference electrode was used. (b) Quasi-steady state oxidation currents for different concentrations of ferrocene methanol compared to eqn (1).

oxidation of ferrocene methanol at different concentrations at a PEDOT:tosylate electrode. A band electrode was placed in bulk solution and, as expected, the current approached a quasi-steady state value at voltages above the oxidation potential (measured to be 210 mV *vs.* Ag/AgCl). The quasi-steady state current at a band electrode is given by the following equation:

$$i_{qss} = \frac{2\pi nFlDC}{\ln(64Dt/w^2)} \quad (1)$$

where C is the bulk concentration, n is the number of electrons in the reaction, F is Faraday's constant, D is the diffusion coefficient, and the dimensions of the band electrode are given by the width w and length l.[39] Quasi-steady state current values were measured on each voltammogram by calculating the difference between the current before the peak and the current 100 mV past the half wave potential $E½$. These data were compared to calculated theoretical values (eqn (1)), using t = 20 s, F = 96 485 C mol^{-1} and $D = 6 \times 10^{-6}$ cm^2 s^{-1}. As seen in Fig. 3b, the measured values are in good agreement with the theoretical values. This suggests that the PEDOT:tosylate film is uniform and that the measured electroactive area is in congruence with the geometric area. This allows for estimation of concentration or geometric area if one of the two is known.

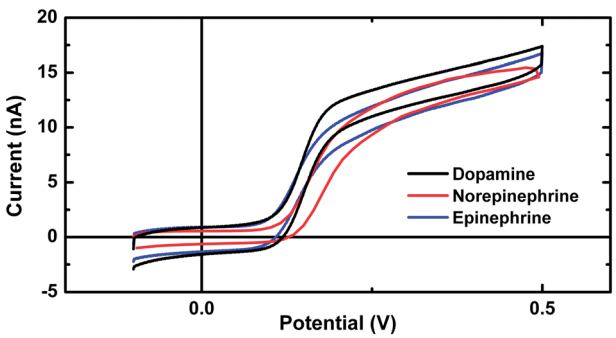

Fig. 4 (a) Cyclic voltammograms showing the oxidation of dopamine (DA), norepinephrine (NE) and epinephrine (EPI) at a 12 μm × 6000 μm PEDOT:tosylate electrode. Scan rate 1 mV s^{-1}. Concentration 20 μM.

Next, we investigated the oxidation of biogenic amines at the PEDOT:tosylate electrode. The oxidation of dopamine, epinephrine, and norepinephrine at a 12 μm × 6000 μm PEDOT:tosylate microelectrode is shown in Fig. 4. The transmitters were diluted to 20 μM in PBS buffer and a Ag/AgCl reference electrode was used. The same electrode was used for all three scans. Between experiments the electrode was cleaned by rinsing in ethanol and water and flat background scans were measured in PBS buffer in order to assure that all oxidized material was removed before addition of a new solution. The voltammograms show comparable characteristics, reflecting the similar chemical structure and oxidation potentials of catecholamines. The current reaches an approximate steady state value. By using eqn (1), the theoretical quasi-steady state current at 50 mV above $E½$ can be calculated to be i_{qss} = 9.2 nA (C = 20 μM, $D = 6 \times 10^{-6}$ cm^2 s^{-1} and t = 50 s, w = 12 μm, l = 6000 μm), which is comparable to the data in Fig. 4.

The electrochemical and heterogeneous electron transfer kinetics for different transmitters and their metabolites were evaluated at PEDOT:tosylate electrodes. Results are listed in Table 2. PBS buffer (100 mM, pH = 7.4) was flowed over the electrode. A six-port HPLC valve was used to introduce a bolus solution containing the analyte to the electrode. The method of Nicholson[40] was then used to determine the heterogeneous electron transfer rate constants. These electrodes show typical rate constants for the selected transmitters. This suggests that they could be used to measure these transmitters in a variety of applications. However, the anodic potential limit of 0.7 V *vs.* Ag/AgCl should be taken into account. For example, histamine could not be oxidized at this potential, and thus could not be detected.

Release from cells

To test the materials ability to measure release from cells, we used a PEDOT:tosylate electrode to measure the release of transmitters from a population of PC 12 cells using constant potential amperometry. Prior to measurement, the electrode was coated with poly-L-lysine to promote cell adhesion. PC 12 cells are known to release catecholamines upon stimulation with a K^+-rich buffer. In this experiment, the cells were rinsed thoroughly with a physiological buffer prior to harvesting, to ensure that any oxidizing species in the growth buffer was removed. The same buffer was used to transport the suspended cells to the electrodes where they were plated on the substrate. A microscope image of a large group of PC 12 cells on a PEDOT:tosylate electrode is shown in Fig. 5. A 350 mV potential was applied and the recording was started once the current had decayed to a value below 100 pA. Without removing the cells from the surface, the physiological buffer was exchanged with an isotonic buffer containing elevated K^+ (105 mM). The current was recorded for 3 minutes before the buffer was exchanged to physiological buffer. A rest time of 4 minutes was used between subsequent stimulations. The electrode was visually inspected to ensure that the

Table 2 Heterogeneous electron transfer rate constants and half wave potentials for selected molecules[a]

	DOPAC	HVA	DA	NE	E	L-DOPA	5-HIAA	5-HT	Hist	Fc-COOH
k_{avg}	3.1	1.3	3.1	2.3	1.5	3.3	1.3	2.3	n/a	4.9
±	0.8	0.2	0.6	0.4	0.7	0.4	0.7	0.9	—	0.6
$E^1/_2$	141	403	149	164	144	163	291	327	—	213
±	4	18	7	4	4	2	7	4	—	3

[a] Rate constants (cm $s^{-1} \times 10^{-3}$) were determined by the method of Nicholson.[40] Error is the standard deviation ($n = 2$–3). Half wave potentials (mV) referenced to Ag/AgCl ($n = 3$–4).

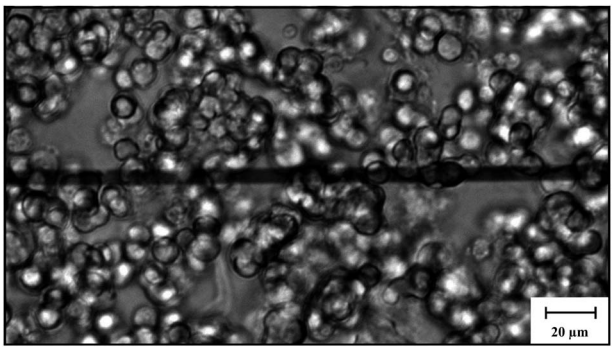

Fig. 5 PC 12 cells sedimented on a 7 µm wide PEDOT:tosylate electrode.

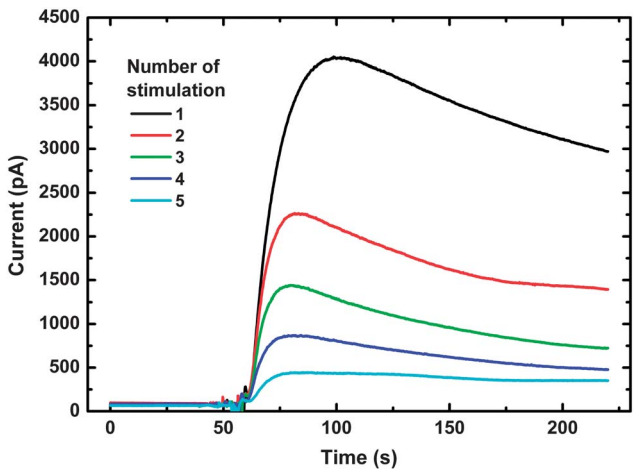

Fig. 6 Amperometric responses resulting from transmitter release from a group of PC 12 cells at a PEDOT:tosylate electrode. The cells were alternately exposed to a K^+-rich buffer for 3 minutes and a low K^+ buffer for 4 minutes. The highest response resulted from the first stimulation by a K^+-rich buffer. Subsequent stimulations resulted in decreasing current responses.

same group of cells was present between each stimulation. Fig. 6 shows the current traces obtained by stimulating a group of PC 12 cells five times. The current response clearly decreases after each successive stimulation. This could be due to depletion of vesicles by the long-lasting stimulation used to evoke exocytosis.

Conclusion

In this paper we demonstrated the use of conductive polymer PEDOT:tosylate microelectrodes for electrochemical transmitter detection. A wide range of transmitters were shown to oxidize readily on the electrodes and kinetic rate constants and half wave potentials were reported. Out of 10 tested transmitters, only histamine had its oxidation potential outside the potential limits of PEDOT:tosylate, and could not be detected. The capacitance per area was found to be high compared to other thin film microelectrode materials, which could be a limitation for use in low-noise amperometric measurements. However, this limitation can be overcome by making the electrodes sufficiently small. Further, we used constant potential amperometry to measure the transmitter release from a group of PC 12 cells following a series of stimulations with high K^+ buffer. Since the cells stay fixed during the exchange of buffers, current responses from the same group of cells can be compared and used for pharmacological screening applications. The study shows that PEDOT:tosylate is a promising electrode material in chip-based devices for transmitter detection. This opens the way for cheap and easy-to-fabricate all-polymer devices for several bioanalytical applications such as HPLC, capillary electrophoresis, and drug screening.

Acknowledgements

This work is supported by the Danish Council for Strategic Research through the Strategic Research Center PolyNano (grant no. 10-092322/DSF), and the University of Arizona start up funds. The authors would also like to acknowledge fruitful discussions with Professor Andrew G. Ewing, Department of Chemistry, University of Gothenburg.

References

1 Y. Huang, D. Cai and P. Chen, *Anal. Chem.*, 2011, **83**, 4393–4406.
2 Y. Lin, R. Trouillon, G. Safina and A. Ewing, *Anal. Chem.*, 2011, **83**, 4369–4392.
3 D. Omiatek, A.-S. Cans, M. Heien and A. Ewing, *Anal. Bioanal. Chem.*, 2010, **397**, 3269–3279.
4 W. R. Vandaveer, IV, S. A. Pasas-Farmer, D. J. Fischer, C. N. Frankenfeld and S. M. Lunte, *Electrophoresis*, 2004, **25**, 3528–3549.
5 S. Ge, S. Koseoglu and C. L. Haynes, *Anal. Bioanal. Chem.*, 2010, **397**, 3281–3304.
6 N. V. Lavrik, L. T. Taylor and M. J. Sepaniak, *Anal. Chim. Acta*, 2011, **694**, 6–20.
7 K. E. Hubbard, A. Wells, T. S. Owens, M. Tagen, C. H. Fraga and C. F. Stewart, *Biomed. Chromatogr.*, 2010, **24**, 626–631.
8 R. M. Wightman, J. A. Jankowski, R. T. Kennedy, K. T. Kawagoe, T. J. Schroeder, D. J. Leszczyszyn, J. A. Near, E. J. Diliberto and O. H. Viveros, *Proc. Natl. Acad. Sci. U. S. A.*, 1991, **88**, 10754–10758.
9 C. Spegel, A. Heiskanen, L. H. D. Skjolding and J. Emneus, *Electroanalysis*, 2008, **20**, 680–702.
10 Z. Chen, Y. Goa, J. Lin, R. Su and Y. Xie, *J. Chromatogr., A*, 2004, **1038**, 239–245.

11 N. A. Lacher, S. M. Lunte and R. S. Martin, *Anal. Chem.*, 2004, **76**, 2482–2491.
12 N. E. Hebert, B. Snyder, R. McCreery, W. G. Kuhr and S. A. Brazill, *Anal. Chem.*, 2003, **75**, 4265–4421.
13 K. Berberian, K. Kisler, Q. Fang and M. Lindau, *Anal. Chem.*, 2009, **81**, 8734–8740.
14 B.-X. Shi, Y. Wang, T.-L. Lam, W.-H. Huang, K. Zhang, Y. C. Leung and H. L. W. Chan, *Biomicrofluidics*, 2010, **4**, 043009.
15 P. Chen, B. Xu, N. Tokranova, X. Feng, J. Castracane and K. D. Gillis, *Anal. Chem.*, 2003, **75**, 518–524.
16 G. M. Dittami and R. D. Rabbitt, *Lab Chip*, 2010, **10**, 30–35.
17 C. Spegel, A. Heiskanen, S. Pedersen, J. Emneus, T. Ruzgas and R. Taboryski, *Lab Chip*, 2008, **8**, 323–329.
18 X. Sun and K. Gillis, *Anal. Chem.*, 2006, **78**, 2521–2525.
19 C. Amatore, S. Arbault, Y. Chen, C. Crozatier, F. Lemaitre and Y. Verchier, *Angew. Chem.*, 2006, **45**, 4000–4003.
20 X. Liu, S. Barizuddin, W. Shin, C. J. Mathai, S. Gangopadhyay and K. Gillis, *Anal. Chem.*, 2011, **83**, 2445–2451.
21 R. D. Henderson, M. C. Breadmore, L. Dennany, R. M. Guijt, P. R. Haddad, E. F. Hilder, P. C. Innis, T. W. Lewis and G. G. Wallace, *Synth. Met.*, 2010, **160**, 1405–1409.
22 Z. Nie and E. Kumacheva, *Nat. Mater.*, 2008, **7**, 277–290.
23 S. Takamatsu, T. Takahata, K. Matsumoto and I. Shimoyama, *J. Micromech. Microeng.*, 2011, **21**, 075021.
24 P. G. Taylor, J.-K. Lee, A. A. Zakhidov, M. Chatzichristidi, H. H. Fong, J. A. DeFranco, G. G. Malliaras and C. K. Ober, *Adv. Mater.*, 2009, **21**, 2314–2317.
25 L. Li, M. Hirtz, W. Wang, C. Du, H. Fuchs and L. Chi, *Adv. Mater.*, 2010, **22**, 1374–1378.
26 N. Rozlosnik, *Anal. Bioanal. Chem.*, 2009, **395**, 637–645.
27 M. Berggren and A. Richter-Dahlfors, *Adv. Mater.*, 2007, **19**, 3201–3213.
28 S. M. Richardson-Burns, J. L. Hendricks, B. Foster, L. K. Povlich, D.-H. Kim and D. C. Martins, *Biomaterials*, 2007, **28**, 1539–1552.
29 B. Winther-Jensen and K. West, *React. Funct. Polym.*, 2006, **66**, 479–483.
30 S. S. Kumar, J. Mathiyarasu and K. L. N. Phani, *J. Solid State Electrochem.*, 2006, **10**, 905–913.
31 N. F. Atta, A. Galal and R. Ahmed, *J. Electrochem. Soc.*, 2011, **158**, F52–F60.
32 S. Y. Yang, B. N. Kim, A. A. Zhakidov, P. G. Taylor, J.-K. Lee, C. K. Ober, M. Lindau and G. G. Malliaras, *Adv. Mater.*, 2011, **23**, H184–H188.
33 L. Groenendaal, F. Jonas, D. Freitag, H. Pielartzik and J. R. Reynolds, *Adv. Mater.*, 2000, **12**, 481–494.
34 B. Winther-Jensen, D. W. Breiby and K. West, *Synth. Met.*, 2005, **152**, 1–4.
35 K. Ø. Andresen, M. Hansen, M. Matschuk, S. T. Jepsen, H. S. Sørensen, P. Utko, D. Selmeczi, T. S. Hansen, N. B. Larsen, N. Rozlosnik and R. Taboryski, *J. Micromech. Microeng.*, 2010, **20**, 055010.
36 T. S. Hansen, K. West, O. Hassager and N. B. Larsen, *J. Micromech. Microeng.*, 2007, **17**, 860–866.
37 M. L. A. V. Heien, P. E. M. Phillips, G. D. Stuber, A. T. Seipel and R. M. Wightman, *Analyst*, 2003, **128**, 1413–1419.
38 S. E. Hochstetler, M. Puopolo, S. Gustincich, E. Raviola and R. M. Wightman, *Anal. Chem.*, 2000, **72**, 489–496.
39 A. J. Bard and L. R. Faulkner, *Electrochemical Methods, Fundamentals and Applications*, John Wiley & Sons Inc, 2001.
40 R. S. Nicholson, *Anal. Chem.*, 1965, **37**(11), 1351–1355.
41 D. M. de Leeuw, P. A. Kraakman, P. F. G. Bongaerts, C. M. J. Mutsaers and D. B. M. Klaassen, *Synth. Met.*, 1994, **66**, 263–273.

Amperometric noise at thin film band electrodes

Journal:	*Analytical Chemistry*
Manuscript ID:	ac-2012-01136x
Manuscript Type:	Article
Date Submitted by the Author:	30-Apr-2012

Complete List of Authors:	Larsen, Simon; Technical University of Denmark, Department of Micro- and Nanotechnology Heien, Michael; University of Arizona, Department of Chemistry and Biochemistry Taboryski, Rafael; Technical University of Denmark, Department of Micro- and Nanotechnology

Amperometric noise at thin film band electrodes

Simon T. Larsen[1], Michael L. Heien[2], and Rafael Taboryski[1]*

* to whom correspondence should be addressed, rata@nanotech.dtu.dk

1. Department of Micro- and Nanotechnology, Technical University of Denmark, DTU Nanotech, Building 345B, DK-2800 Kongens Lyngby, Denmark

2. Department of Chemistry and Biochemistry, University of Arizona, 1306 E. University Blvd., Tucson, AZ 85721, U.S.A

Abstract

Background current noise is often a significant limitation when using constant-potential amperometry for biosensor applications. In this paper, we fabricated thin-film electrodes of gold and conductive polymers and measured the current noise in physiological buffer solution for a wide range of different electrode areas. The noise measurements could be modeled by an analytical expression, representing the electrochemical cell as a resistor and capacitor in series. The studies revealed three domains; for electrodes with low capacitance the amplifier noise dominated, for electrodes with large capacitances the noise from the resistance of the electrochemical cell was dominant, while in the intermediate region the current noise scaled with electrode capacitance. The experimental results and the model presented here can be used for choosing an electrode material and dimensions, and when designing chip-based devices for low-noise current measurements.

Keywords: current noise, electrode, capacitance, pedot, amperometry

Introduction

Electrochemical detection using constant-potential amperometry is a widely used technique in biosensor applications. Many biologically interesting molecules are electroactive and can thus be oxidized at an electrode held at a sufficient positive potential. Amperometric detection is used in applications such as capillary electrophoresis[1][2], high performance liquid chromatography[3], and measurements of neurotransmitter release from living cells[4]. Electrical background noise is one of the major limitations of amperometric detection defining the limit for smallest possible detectable signals. The signal-to-noise ratio is often used to quantify the precision of amperometric data.

Microelectrodes coupled with low-noise amplifiers have been used to measure currents with noise levels down to the femto-ampere region[5]. Traditionally carbon-fiber microelectrodes have received the most attention due to their excellent low-noise properties, but in the last decade much research has focused on developing thin-film microelectrodes from different electrode materials for amperometric detection using chip-based devices. These materials include gold[6, 7], platinum[8], indium tin oxide[9], pyrolyzed photoresist[10], diamond-like carbon[11] and conductive polymers like Pedot:Pss[12] and Pedot:tosylate[13].

Current noise is generally measured in terms of the root mean square of the current. General theories on current noise in electrochemical detectors covering also faradaic currents have been presented [14, 15]. Amperometric background noise is often thought of as being proportional to electrode capacitance and hence electrode area[16, 17, 18]. For carbon fiber-microelectrodes this was shown to be the case except for very small electrodes where the amplifier noise became predominant[19]. The proportionality between the root mean square noise and the electrode area was also demonstrated for thin-film electrodes made of gold[20] and indium tin oxide[21, 22]. For Pedot:Pss conductive polymer microelectrodes larger electrodes were shown to be more noisy[21, 22], while for micrometer-sized platinum electrodes the current noise was indistinguishable from amplifier noise in the open loop configuration[12].

In this paper we present extensive amperometric noise data for thin-film microelectrodes held at a constant potential in a physiological buffer. Electrodes were made of gold and conductive polymers Pedot:Pss and Pedot:tosylate. These materials differ widely in capacitive properties, allowing for the analysis of noise behavior for a wide range of electrode capacitances. In addition, we present a simple and adequate noise expression, depending only on the electrode capacitance, the resistance of the cell, the filter frequency, and the open loop amplifier noise. Experimental data strongly supports the analytical solution. We find that the noise scales with the electrode capacitance except for very small capacitances where the potentiostat noise dominates and for sufficiently large capacitances where the noise is equal to the Johnson-Nyquist noise of the circuit resistance. The dependence of the noise on circuit resistance is also modeled. Limits for the different noise regimes are reported and some practical suggestions are provided for designing thin-film microelectrodes for low-noise amperometry applications.

Materials and Methods

Pedot:tosylate band microelectrodes were fabricated on polymer (TOPAS) substrates as described earlier[8]. Pedot:Pss band electrodes were prepared by spin-coating Pedot:Pss aqueous solution (483095, Sigma-Aldrich) at 1000 rpm for 30 s onto polymer (TOPAS) substrates. Pedot:Pss samples were subsequently covered with 70% DMSO(>99% purity, Merck, Germany) in water, heated at 70°C for 5 minutes and washed in deionized water. Patterning of the Pedot:Pss layer was done as described earlier for Pedot:tosylate microelectrodes[13].

Gold microelectrodes were fabricated on 4'' Boron glass wafers. The glass wafers were placed over night in a 250 °C oven and then vapor-primed with hexamethyldisilazane (HMDS). A 1.5 µm layer of AZ5214E photoresist was spin-coated on the glass wafers. The samples were baked at 90 °C for 60 seconds before being exposed in a Karl Suss MA6/BA6 Mask Aligner for 6 seconds (intensity 7.0 mW/cm²) and developed with AZ351B Developer. The photomask was ordered at Delta Mask B.V. Residual resist was removed with a Plasma Asher (TePla). A Wordentec QCL800 Metal evaporator was used to first evaporate a 5 nm adhesion layer of chrome (1 n/s, 5 s) and then 150 nm of gold (1 n/s, 150s). Finally, resist was lifted off in acetone, and the electrode substrates were rinsed with isopropanol and water and dried. For all electrode materials, electrodes between 3 µm and 50 µm wide and 6 mm long were fabricated.

Electrochemical noise measurements were made using an Axopatch 200B (Molecular Devices) amplifier. The with resistive feedback was used. In order not to limit the measurement bandwidth we worked in the $\beta = 0.1$ configuration with feedback resistance $R_f = 50$ MΩ, while low-pass filtering at 1 kHz using the 4 pole Bessel filter of the amplifier. The gain used was 20 mV/pA for noise measurements, but in general the noise did not depend on the gain unless a very low gain was used. A PDMS well was fabricated and bonded to an electrode surface. The band electrode protruded into the bonded PDMS well which was filled with PBS buffer (phosphate-buffered saline, Sigma Aldrich). The electrode length depended on the penetration depth into the well and it was measured using a microscope. A Ag/AgCl reference electrode (RE-5B, BASi) was placed with the tip in the PDMS well and connected to the amplifier headstage. Connections to the working electrode were made using conductive epoxy glue (Conductive Epoxy, Chemtronics).

Current data was collected using an amperometry program written in LabVIEW (National Instruments, Austin, Texas). The voltage was applied at the Axopatch 200b amplifier. For each noise measurement, five short noise traces were measured and the average of the offset corrected root mean square of the current was used to describe the magnitude of the noise. Conductivity was measured with a four-point probe (Jandel Engineering Ltd) connected to a Keithley 2400 SourceMeter (Keithley Instruments Inc).

The uncertainty of experimental noise data was estimated by using the uncertainties of capacitance, resistance and open loop current noise values and calculating the propagated error of the theoretical value for the same parameters. For discrete resistors and capacitors, the uncertainty was provided by the manufacturer to be 5 % for resistors and 20 % for capacitors. For electrodes, the capacitance uncertainty was dominated by the uncertainty in area estimation using optical microscopy.

Results and Discussion

All noise measurements were carried out using an Axopatch 200B amplifier connected to an electrochemical cell corresponding to the one depicted in Figure 1a. Thin-film band electrodes were fabricated on either glass or polymer substrates and active areas were defined by bonding

the substrates to PDMS wells. After bonding, the exact electrode area could be determined by microscopic observation. Noise traces were recorded after applying a constant voltage (100 mV) to the electrochemical cell and waiting until the current had decayed to approximately zero (Figure 1b). Interference noise from 50 Hz noise sources was avoided by shielding with two separate faraday cages, an outer cage held at earth ground and an inner cage connected to signal ground from the amplifier.

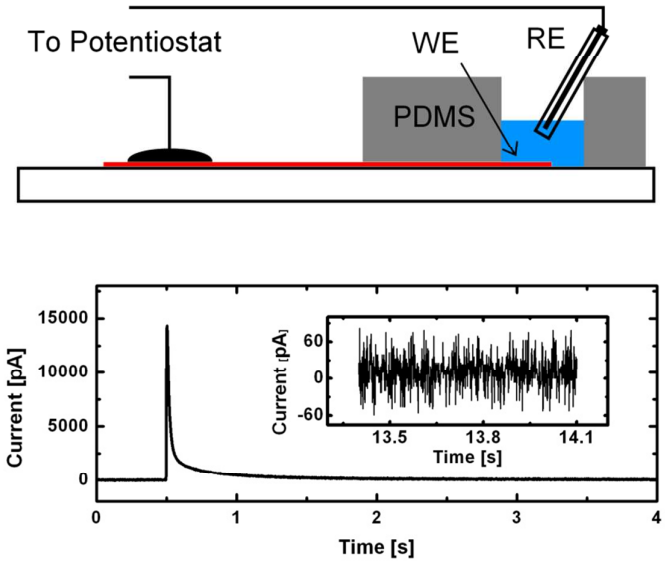

Figure 1. a) Electrochemical set-up. The active working electrode (WE) is defined by the area of a thin film band electrode (red) protruding into a well made of PDMS. The reference electrode (RE) is placed in the buffer solution (PBS). b) Current response following a voltage step (0 mV to 100 mV) at a Pedot:tosylate microelectrode. The inserted graph is showing the noisy current trace at a later time where the current has reached a constant value.

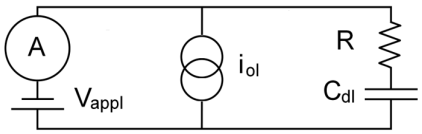

Figure 2: Simple equivalent circuit for electrochemical cell. V_{appl} is the applied potential, C_{dl} the double-layer capacitance of the electrode, R the sum of resistances in series with the electrode and i_{ol} the open-loop current noise represented as a current source in parallel with the cell.

The noise model used in this work is based on the simplified equivalent circuit shown in Figure 2. Here the electrode is represented as a perfect capacitor while the solution resistance of the buffer and the resistance of wires and isolated electrode connections is represented by a resistor with resistance R. The current noise measured at an open loop configuration is represented as a current source in parallel with the cell. We describe the total current power spectral density S_i as the sum of power spectral densities from uncorrelated random noise sources. Shot noise has been disregarded as a noise source since the background current in our experiment is close to zero. This leaves the open loop current noise $I_{RMS,ol}$ with power spectral density $S_{i,ol}$ as well as current noise from ohmic behavior of voltage noise sources. Since, in this work we are interested in microfabricated thin film electrodes where isolated electrode segments and the buffer solution typically give rise to series resistances above 10^4 Ω, the Johnson-Nyquist noise from R is the main contribution of voltage noise. Since the current noise is given by the voltage noise divided by the impedance, we write the total power spectral density of the current noise as

$$S_i(f) = \frac{4kTR}{R^2 + \frac{1}{(2\pi fC)^2}} + S_{i,ol}(f) \qquad 1$$

where k is Boltzmann's constant (1.38 x 10^{-23} J/K), T the absolute temperature and f the frequency in Hz. The interesting experimental noise parameter is the root mean square of the current trace. The current trace is typically filtered with a low-pass active analog filter with cut-off frequency f_c. Assuming the low-pass filter is ideal, i.e. all signals below f_c pass and all signals above f_c are stopped, the root mean square current noise can be found by integrating the power spectral density from f=0 to f=f_c.

$$I_{RMS}{}^2 = \int_0^{f_c} S_i(f)df \qquad 2$$

Integrating equation 1, we obtain:

$$I_{RMS}{}^2 = \frac{4kT}{R}\left(f_c - \frac{1}{2\pi RC} Arctan(2\pi RC f_c)\right) + I_{RMS,ol}{}^2 \qquad 3$$

Here, $I_{RMS,ol}$ is the root mean square current noise of the headstage in an open loop configuration.

For real low-pass filters, the cut-off is not sharp but extends over a range of frequencies. Therefore a more accurate estimate for the root mean square current noise is found by multiplying the power spectral density of the unfiltered input by the square of the filter transfer function's magnitude response $|H(j\omega)|$ before integration.

$$I_{RMS}{}^2 = \int_0^{\infty} |H(j\omega)|^2 S_i(f)df \qquad 4$$

where j is the imaginary unit and ω=2πf the angular frequency. Transfer functions are typically comprehensive mathematical functions, which makes equation 4 better suited for numerical integration than analytical evaluation.

In this paper, we used the analog 4 pole Bessel filter of the Axopatch 200B amplifier for noise measurements. The filter cut-off frequency was held at 1 kHz for all measurements. The open loop root mean square current noise was measured before each experiment. It was typically around 0.7 pA in the measurement bandwidth[1]. This leaves only two unknown quantities in equations 1 and 3, the electrode capacitance and the resistance in series.

First we test our model by replacing the electrochemical cell by discrete resistors and capacitors. The blue line in Figure 3 shows the measured power spectral density of the current noise, when using a 1 nF capacitor and a 100 kΩ resistor in series. The dashed black line shows the calculated power spectral density using equation 1. The noise power is plotted as pA^2/Hz and the open loop noise is neglected in this example since it is much lower than the Johnson-Nyquist noise from the resistor. Assuming an ideal filter with cut-off at 1 kHz, the filtered power spectral density would correspond to the solid black line and the root mean square noise would be equal to the integral of this. Taking into account the 4 pole Bessel filter and multiplying the power spectral density with the square of the filter transfer function's magnitude response $|H(j\omega)|$ [13], a better estimate of the power spectral density can be found (red line, Figure 3). It should be noted that the choice of resistor and capacitor in this example was made to illustrate the difference between using equation 2 and 4. In most cases, the difference in root mean square currents calculated by taking the Bessel filter transfer function into account or using the simpler analytical solution for an ideal filter is less pronounced than in Figure 3.

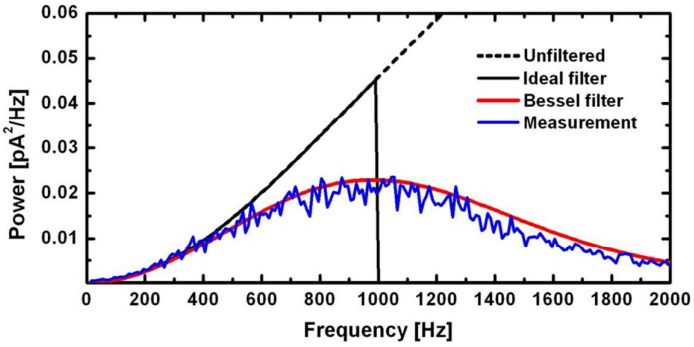

Figure 3: Measured power spectral density of the current noise for a 1 nF capacitor and a 100 kΩ resistor in series held at 100 mV and low-pass filtered at 1 kHz through an analog 4 pole Bessel filter at an Axopatch 200B amplifier (blue) plotted along with theoretical plots for ideally filtered and 4 pole Bessel filtered power spectral densities.

[1] The relatively high open loop noise is due to choice of feedback element on the Axopatch amplifier. The lower (and noisier) feedback resistor (50 MΩ) was chosen in order to get a larger output bandwidth of the probe.

In Figure 4, we show measured root mean square current noise values for a wide range of different resistors and capacitors. Five short noise traces were measured for each configuration and the average of the offset corrected root mean square current noise was plotted. Along with experimental values, theoretical curves are plotted corresponding to root mean square current noise values calculated using equations 3 and 4. Clearly, the theoretically calculated values fit the measured values nicely. This indicates that equation 3 and 4 can describe current noise at electrodes if the equivalent circuit of the electrochemical cell can be described as a resistor and capacitor in series. As expected, taking the Bessel filter behavior into account, the best match with experiments is obtained, but also the simpler analytical solution of equation 3 describes the noise very well.

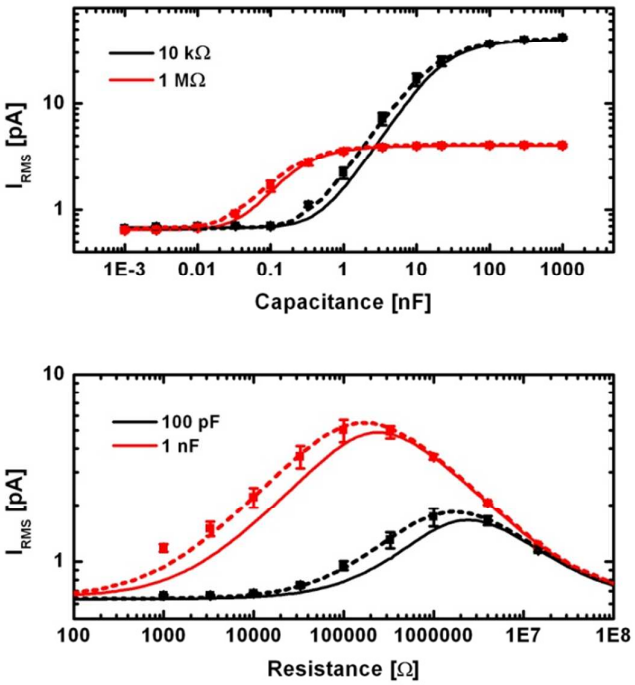

Figure 4: The root mean square current noise values for sets of discrete resistors and capacitors in series. Capacitance is varied in the upper graph while resistance is varied in the lower graph. Solid lines show calculated noise values corresponding to equation 3. Dashed lines show noise values calculated by numerical integration of equation 4. (Filter frequency: 1 kHz, $I_{RMS,ol}$=0.65 pA.)

Observing the noise behavior in Figure 4, we notice three domains; the noise is constant for 1. very low or 2. very large capacitances. At lower capacitances, the open loop current noise dominates completely, while at the large capacitances, the noise is equal to the Johnson-Nyquist noise from the resistor meaning the capacitance has no effect on the noise. 3. In the intermediate

region, the root mean square scales with capacitance. Indeed, for small capacitances, using the two first terms of the Arctan Taylor expansion, equation 3 becomes

$$I_{RMS}{}^2 = \frac{4}{3} kTR(2\pi C)^2 f_c{}^3 + I_{RMS,ol}{}^2 \qquad 5$$

Equation 5 fits the measured noise values shown in Figure 4 corresponding to low and intermediate capacitances. As long as the open loop noise has no effect, the root mean square current noise is directly proportional to the capacitance. Since the capacitance of an electrode is generally proportional to the electrode area, the root mean square noise is proportional to area. This result is in agreement with literature on the subject of microelectrode noise (*vide supra*). The criterion for being in the large capacitance region is that resistance dominates the total cell impedance, i.e. $R^2 \gg 1/(2\pi f C)^2$. Oppositely, if capacitance dominates the impedance, noise scales with capacitance until amplifier noise becomes dominant.

Varying the resistance results in peak-shaped noise curves (Figure 4). For very large resistances, the current noise decreases, but for these values the time constant of the electrochemical cell $\tau = RC$ also increases. This is an unwanted side effect for fast sampling experiments. Reducing the resistance is often the best approach although this can be difficult in chip-based devices, where solution resistance in microfluidic channels is often significant.

In the experimental work presented here we limit our noise investigation to variations in cell resistance and capacitance. This is due to the fact that the two other variables in equation 3, the open loop amplifier noise and the low pass cut-off filter frequency, have a much simpler effect on the noise. As mentioned above, the open loop amplifier noise just determines the noise level for very low capacitances. For the filter cut-off frequency, noise increases with increasing frequency except for very low capacitances.

Next, we turn our attention to real electrodes. If the electrochemical cell can be described by a capacitor and resistor in series, the model presented here should apply to the current noise. As mentioned above, the capacitance of an electrode is generally proportional to the electrode area. It can be described by the expression

$$C = \left(\frac{C}{A}\right)_i A\,, \qquad 6$$

where the capacitance per area $(C/A)_i$ is a constant depending on the electrode material. In this work, we find $(C/A)_i$ for each electrode material by measuring the capacitance of a large electrode and dividing it by the area. The apparent capacitance is found by dividing the charging current measured at a cyclic voltammogram by the scan rate. Although this method is based on a simplification since capacitance can also be a function of voltage and scan rate, it is an appropriate estimate of the electrode capacitance for many electrodes. Substituting C in equation 3 by the

above expression (eq. 6) gives us a noise theory depending on electrode area and series resistance of the electrode.

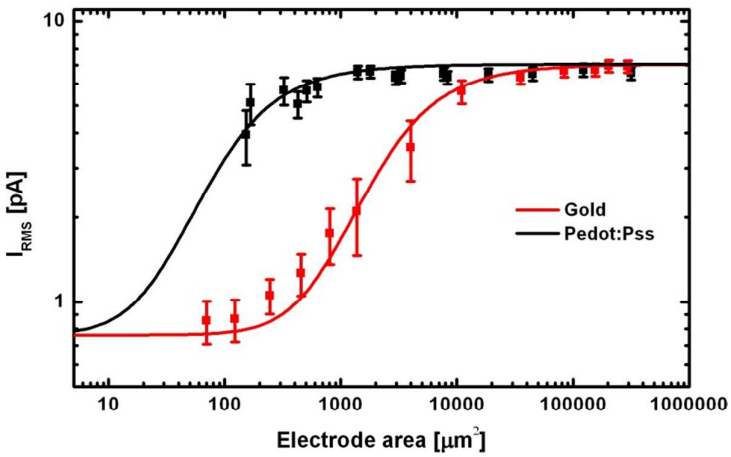

Figure 5: Measured current noise values as a function of electrode area at gold and Pedot:Pss electrodes. A large external resistor (330 kΩ) was connected in series with the electrodes to give a dominate resistance. Solid lines show expected theoretical noise values given by equation 3.

Estimating the series resistance of an electrode system is more difficult, since it depends on both electrode connections and the resistance of the solution. In chip-based devices, the working electrode is typically connected to the potentiostat by an electrode segment isolated by the substrate and the bonded counterpart as shown in Figure 1a. For a band electrode of length l and width w, the resistance of this wire is given by

$$R = R_s \frac{l}{w}, \qquad 7$$

where R_s is the sheet resistance of the film. For metal electrodes the resistance of isolated electrode connections is typically negligible compared to other resistance sources, but for electrodes made of materials with higher resistivity like conductive polymers or pyrolyzed photoresist, this resistance can be significant.

The solution resistance which makes up another significant part of the total resistance is generally thought to be inversely proportional to electrode radius for disk microelectrodes[23]. Assuming spherical symmetry around the microelectrode, this resistance could be described by the equation

$$R_u = \frac{1}{4\pi\kappa r_0} \quad 8$$

Here κ is the conductivity of the solution and r_0 the radius of the disk microelectrode. For the band electrodes used in this work equation 6 does not apply directly since we have neither spherical symmetry nor disk shaped electrodes. It is reasonable though to assume the solution resistance to be inversely proportional to a critical electrode dimension. If we assume this dimension to be the length of the band electrode, the total resistance of the electrochemical cell can be expressed as

$$R = R_{el} + \frac{k_s}{l} \quad 9$$

Here the first tem R_{el} is the resistance of isolated parts of the electrode (and wires), k_s is a constant depending on the buffer solution and placement of the reference electrode and l is the electrode length.

In order to test the applicability of our theory on real electrodes, we first connected a large discrete resistor (330 kΩ) in series with different band electrodes, while keeping electrode connections short and the reference electrode close to the band electrodes. The discrete resistor dominates the total resistance making the measurements easier to compare to theory. Figure 5 shows noise results for Pedot:Pss and gold electrodes varying in area between 100 μm^2 and 10000 μm^2. The noise at gold electrodes is clearly smaller than the noise at Pedot:Pss electrodes. Using cyclic voltammetry, we measured the apparent capacitance per area of the electrodes (table 1). Using these values and equations 3 and 6, we now plot the theoretical electrode noise as a function of area (solid lines, Figure 5). Clearly, the theory fits the experimental data well. The large difference in capacitance properties between Pedot:Pss and gold is reflected in the displacement of the two graphs along the x-axis. Much smaller capacitance Pedot:Pss electrodes are needed to achieve the same low noise as at gold electrodes.

Table 1 Capacitance per area and sheet resistance for electrodes used for noise measurements.

Gold	18.6 +/- 2.0 μF/cm^2	0.185 Ω +- 0.005 Ω
Pedot:Pss	460 +/- 60 μF/cm^2	3200 Ω +- 200 Ω
Pedot:tosylate	1700 +/- 100 μF/cm^2	580 Ω +- 70 Ω

Finally, we present noise measurements from electrodes with no external resistor connected. The set-up is as shown in Figure 1a. The electrode capacitance is still given by equation 6, while the resistance is now coming only from the isolated electrode segments and the solution. In Figure 6, we show noise results for Pedot:tosylate and gold electrodes. The area of the electrode is varied

by shortening the length of the electrode protruding into the PDMS well. Equation 3 is used to fit the experimental noise data. The expressions for resistance and capacitance given by equations 6 and 9 are used and least squares fitting is done using R_{el} and k_s as fitting parameters. Resulting fits are in good agreement with experimental values and are shown as solid lines in Figure 6. The least squares fitting resulted in the following parameters: R_{el} = 439 Ω,k_s = 41.8 Ω x m for Gold and R_{el} = 152000 Ω,k_s = 35.6 Ω x m for Pedot:tosylate. Since the same reference electrode and buffer solution is used for both electrodes, it is expected that the fitted k_s-values do not differ much. Further, the R_{el} values are also realistic, and reflect the large difference in sheet resistance for thin films of gold and Pedot:tosylate (table 1). Indeed, if the dimensions of the electrode connections used in this experiment (3.75 µm x 2900 µm for Gold and 4.6 µm x 900 µm for Pedot:tosylate) are used together with equation 7 and the sheet resistance values of table 1, calculated electrode connection resistances are 143 Ω for Gold and 114000 Ω for Pedot:tosylate. These values are in the same order of magnitude as the fit R_{el}-values.

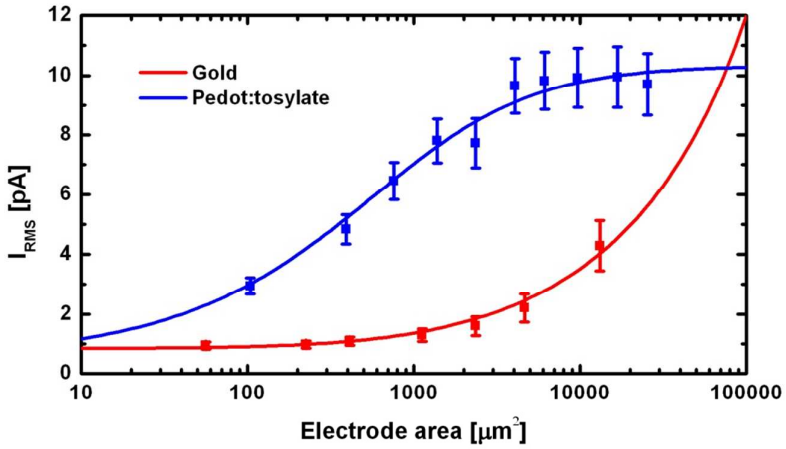

Figure 6: Current noise measurements at gold and Pedot:tosylate band electrodes. Solid lines show theoretical noise obtained by least squares fitting of equation 3.

A few practical points can be made in relation to the electrode noise measurements presented here. First, for low noise current amperometry, the choice of electrode material is important. As seen in Figure 6, Pedot:tosylate electrodes had to be made almost two orders of magnitude smaller than gold electrodes to reach the same noise level. Second, the resistance of electrode wires and the solution resistance in microfluidic channels also affect the noise. If this resistance dominates the impedance of the electrochemical cell, the noise is equal to the Johnson-Nyquist noise of the resistance as seen for the large Pedot:tosylate electrodes in Figure 6. In this regime, the noise decreases for increasing resistance but simultaneously the time constant increases, making the system more sluggish.

Acknowledgments

This work is supported by the Danish Council for Strategic Research through the Strategic Research Center PolyNano (grant no. 10-092322/DSF)

Conclusion

In this work we presented an analytical solution for the current noise at microelectrodes during constant potential amperometry experiments. Thin-film band microelectrodes were fabricated in three different electrode materials with different capacitive properties, and current noise was measured for a wide range of different electrode areas. The results agreed very well with the analytical noise expression. Our results emphasize the importance of choosing low capacitive electrode materials and small electrodes if low current noise is crucial. We observed three different noise regimes. 1. For very low capacitances, the noise was equal to the open loop noise of the potentiostat 2. For very large capacitances, the noise was equal to the Johnson-Nyquist noise of the resistance of the electrochemical cell. 3. In the intermediate region, noise scaled with capacitance. The noise expression presented here could be used for designing chip-based devices with integrated microelectrodes for low-noise amperometric sensing.

REFERENCES

1 Ge, S.; Koseoglu, S.; Haynes, C. L. *Anal.Bioanal.Chem.* **2010**, *397*, 3281-3304.

2 Vandaveer, W.; Pasas-Farmer, S.; Fischer, D.; Frankenfeld, C.; Lunte, S. *Electrophoresis.* **2004**, *25*, 3528-3549.

3 Lavrik, N. V.; Taylor, L. T.; Sepaniak, M. J. *Anal.Chim.Acta.* **2011**, *694*, 6-20.

4 Omiatek, D. M.; Cans, A.; Heien, M. L.; Ewing, A. G. *Anal.Bioanal.Chem.* **2010**, *397*, 3269-3279.

5 Wightman, R.; Jankowski, J.; Kennedy, R.; Kawaoge, K.; Schroeder, T.; Leszczyszyn, D.; Near, J.; Diliberto, E.; Viveros, O. *Proc.Natl.Acad.Sci.U.S.A.* **1991**, *88*, 10754-10758.

6 Spegel, C.; Heiskanen, A.; Pedersen, S.; Emneus, J.; Ruzgas, T.; Taboryski, R. *Lab Chip.* **2008**, *8*, 323-329.

7 Dittami, G. M.; Rabbitt, R. D. *Lab Chip.* **2010**, *10*, 30-35.

8 Berberian, K.; Kisler, K.; Fang, Q.; Lindau, M. *Anal.Chem.* **2009**, *81*, 8734-8740.

9 Amatore, C.; Arbault, S.; Chen, Y.; Crozatier, C.; Lemaitre, F.; Verchier, Y. *Angew.Chem.-Int.Edit.* **2006**, *45*, 4000-4003.

10 Hebert, N.; Snyder, B.; McCreery, R.; Kuhr, W.; Brazill, S. *Anal.Chem.* **2003**, *75*, 4265-4271.

11 Gao, Y.; Chen, X.; Gupta, S.; Gillis, K. D.; Gangopadhyay, S. *Biomed.Microdevices.* **2008**, *10*, 623-629.

12 Yang, S. Y.; Kim, B. N.; Zakhidov, A. A.; Taylor, P. G.; Lee, J.; Ober, C. K.; Lindau, M.; Malliaras, G. G. *Adv Mater.* **2011**, *23*, H184-H188.

13 Larsen, S. T.; Vreeland, R. F.; Heien, M. L.; Taboryski, R. *Analyst.* **2012**, *137*, 1831-1836.

14 Morgan, D.; Weber, S. *Anal.Chem.* **1984**, *56*, 2560-2567.

15 Hassibi, A.; Navid, R.; Dutton, R.; Lee, T. *J.Appl.Phys.* **2005**, *98*, 069903.

16 Hochstetler, S.; Puopolo, M.; Gustincich, S.; Raviola, E.; Wightman, R. *Anal.Chem.* **2000**, *72*, 489-496.

17 Long, J.; Weber, S. *Anal.Chem.* **1988**, *60*, 2309-2311.

18 Li, Z.; Zhou, W.; Wu, Z.; Zhang, R.; Xu, T. *Biosens.Bioelectron.* **2009**, *24*, 1358-1364.

19 Schulte, A.; Chow, R. *Anal.Chem.* **1998**, *70*, 985-990.

20 Chen, P.; Xu, B.; Tokranova, N.; Feng, X.; Castracane, J.; Gillis, K. *Anal.Chem.* **2003**, *75*, 518-524.

21 Sun, X.; Gillis, K. *Anal.Chem.* **2006**, *78*, 2521-2525.

22 Meunier, A.; Fulcrand, R.; Darchen, F.; Collignon, M. G.; Lemaitre, F.; Amatore, C. *Biophys.Chem.* **2012**, *162*, 14-21.

23 Winder, S. *Analog and Digital Filter Design,* 2nd ed.; Newnes:2002.

24 Bard, A. J. and Faulkner, L. R. *Electrochemical Methods,* ed.; John Wiley & Sons, Inc.:2001.

25 Zoski, C. G. *Handbook of Electrochemistry,* ed.; Elsevier:2007.

RSC Publishing Analyst

All polymer chip for amperometric studies of transmitter release from large groups of neuronal cells

Journal:	*Analyst*
Manuscript ID:	Draft
Article Type:	Paper
Date Submitted by the Author:	n/a
Complete List of Authors:	Larsen, Simon; Technical University of Denmark, Technical University of Denmark Taboryski, Rafael; Technical University of Denmark, Department of Micro- and Nanotechnology

All polymer chip for amperometric studies of transmitter release from large groups of neuronal cells

Simon T. Larsen and Rafael Taboryski*

* to whom correspondence should be addressed, rata@nanotech.dtu.dk

Department of Micro- and Nanotechnology, Technical University of Denmark, DTU Nanotech, Building 345E, DK-2800 Kongens Lyngby, Denmark

Abstract

We present an all polymer electrochemical chip for simple detection of transmitter release from large groups of cultured PC 12 cells. Conductive polymer Pedot:tosylate microelectrodes were used together with constant potential amperometry to obtain easy-to-analyze oxidation signals from potassium-induced release of transmitter molecules. The nature of the resulting current peaks is discussed, and the time for restoring transmitter reservoirs is studied. The relationship between released transmitters and potassium concentration was found to fit to a sigmoidal dose-response curve. Finally, we demonstrate how the device can be used for simple drug screening purposes, by measuring the increase of transmitter release due to short-term treatment of L-DOPA.

Keywords

Neurotransmitter, conductive polymer, pedot, pc 12 cells, amperometry, drug screening

Introduction

Neurotransmitters play an important role in signaling mechanisms of the central nervous system[1]. In response to stimulation, neurons release neurotransmitters stored in membrane-bound vesicles to the extracellular space by a process termed exocytosis. During exocytosis vesicles fuse with the plasma membrane of the cell. The released molecules are recognized by specific receptors at the target cell membrane. A range of transmitter molecules are electroactive and oxidize easily at microelectrodes held at a sufficiently high potential. In the last two decades, constant potential amperometry has therefore been used heavily to measure the activity of neuronal cells and the dynamics of exocytosis[2, 3]. Traditionally, carbon fiber microelectrodes have been the golden standard for these studies, but in the last decade much research has focused on developing thin-film microelectrodes of materials like gold[4], platinum[5], indium tin oxide[6] and diamond-like carbon[7] for amperometric detection of exocytosis in chip-based devices[8].

Amperometric studies of exocytosis have been used to investigate the effect of different drugs on the activity of neuronal cells. Rat pheochromocytoma (PC 12) cells are widely used neuronal model cells for in vitro amperometric exocytosis studies, due to their versatility for pharmacological manipulation, ease of culture and the large amount of background knowledge on their proliferation and differentiation[9, 10]. At PC 12 cells, the dopamine precursor L-DOPA has been shown to up-regulate transmitter release[11], while other drugs like reserpine[11, 12], amphetamine[13, 14] and quinpirole[15] seem to reduce transmitter release. Most of these studies were done by measuring vesicle content and release frequency on a large number of single vesicle events. Using carbon fiber microelectrodes, the mean vesicle content was shown to increase with increasing time of exposure of PC 12 cells to L-DOPA[10]. Only a few studies measure the release of transmitters from large groups of PC 12 cells. The increase in overall transmitter release due to L-Dopa and the decrease in release due to reserpine was measured using a silicon based chip with PC 12 cells attached to collagen coated gold electrodes[16, 17].

In recent years conductive polymers have emerged as an alternative to traditional metal electrodes in a wide range of biological and bioanalytical applications[18-20]. Recent work on conductive polymers include glucose sensors[21, 22], bioelectronic applications[23, 24], virus detection[25] and enzyme electrodes[26, 27]. Conductive polymer electrodes combine the electrical properties of metals and semiconductors with the light weight, biocompatibility and processing properties of common polymers. Among conductive polymers Poly(3,4-ethylenedioxythiophene) (Pedot) has been shown to be a promising material for electrochemical detection of neurotransmitters[28-30]. Transmitter release from single chromaffin cells was detected at Pedot:PSS microelectrodes[31]. The authors of this paper recently showed, that a wide range of transmitter molecules oxidize readily on Pedot:tosylate microelectrodes[30].

In this work, we present a simple, cost-efficient and disposable polymer biochip for measuring transmitter release from large groups of PC 12 cells. Pedot:tosylate microelectrodes were fabricated on polymer substrates and bonded with PDMS to create a flow cell across the microelectrode for buffer exchange. PC 12 cells were trapped on the electrodes using Poly-L-Lysine coating and easily analyzable current responses due to transmitter release were measured. The polymer chips were used to measure the time needed to restore the releasable pool of transmitters in PC 12 cells. The dose response relationship for potassium stimulation was studied and L-DOPA was used to show the potential of the device for drug screening applications.

Materials and Methods

Pedot:tosylate microelectrodes were fabricated on flat, Ø 50 mm injection molded Cyclic Olefin Copolymer (Topas Advanced Polymers GmbH) wafers using UV lithography as described earlier[30]. The electrode width was between 10 and 20 µm and the length 6 mm. A 2-3 mm wide and 3 cm long rectangular well was constructed in PDMS and bonded to the TOPAS substrate perpendicular to the microelectrode. The active area of the electrode was defined by the width of the electrode and the width of the PDMS channel. The Pedot:tosylate microelectrode was connected to a copper wire in one end using conductive epoxy glue (Conductive Epoxy, Chemtronics). Before cell experiments the bottom surface of the wells were incubated in Poly-L-Lysine solution (40 µL per chip, 0.01% solution, P4707, Sigma Aldrich) for one hour, washed with deionized water and dried.

Passage 12 rat pheochromocytoma (PC 12) cells were cultured on Collagen (type 1, SigmaAldrich) coated Nuncleon T25 flasks (Nunc A/S). When close to 100% confluency was reached, the cells were harvested, triturated thoroughly and resuspended in fresh growth medium. The cell solution was then distributed on the chips and the chips were placed in an incubator (37°C, 5% CO2 in air) for 3 – 5 hours. After incubation, the chips were mounted on an optical microscope. Buffer was introduced through a needle at one end of the channel at a uniform flow rate (80 µL/s). Electrochemical measurements were made using an Axopatch 200B (Molecular Devices) amplifier held at 400 mV constant potential. Data was collected using custom programs written in LabVIEW (National Instruments, Austin, Texas). A Ag/AgCl reference electrode (RE-5B, BASi) was placed with the tip in the PDMS well and connected to the back of the amplifier headstage. Two different buffers were used during experiments. A low potassium buffer (150 mM NaCl, 5 mM KCl, 1.2 mM $MgCl_2$, 5 mM glucose, 10 mM HEPES and 2 mM $Cacl_2$, from SigmaAldrich) and a K^+-rich buffer (KCl increased to 100 mM, NaCl decreased to 55 mM). For experiments were potassium concentration is varied, the NaCl concentration was regulated to maintain a constant total concentration of KCl and NaCl. For drug experiments, L-DOPA (L-3,4-dihydroxyphenylalanine) was acquired at Sigma Aldrich and dissolved to 100 µM in low potassium buffer.

Results and Discussion

Chips were constructed by bonding a piece of PDMS containing a long, rectangular channel to a flat polymer substrate with a Pedot:tosylate conductive polymer band microelectrode placed perpendicular to the PDMS channel (figure 1a). Buffer exchange was provided by a flow cell with uniform flow rate (80 µL/s). The chips were mounted on an optical microscope and the cells could be observed during experiments(figure 1b).

The protocol for a cell experiment is shown in figure 2. PC 12 cells were cultured in culture flasks, harvested, plated in the PDMS wells and left in an incubator for 3 – 5 hours. The cell culture medium was then exchanged with a physiological buffer. After flushing the cells a 3 – 4 times, only cells with strong attachment to the surface were left. A potentiostat was connected to the Pedot electrode and to a Ag/AgCl electrode immersed in the buffer and a constant potential at 400 mV was applied. Once the charging current had decreased to a reasonable level, the cells were exposed to a buffer containing a high concentration of potassium (100 mM). After potassium stimulation a rise in current is immediately observed. After 20 – 40 seconds, the current begins to decrease. Two representative current peaks can be seen in figure 2. After the first potassium stimulation, the cells are again flushed with low potassium buffer and left for a fixed time period before another stimulation is triggered by introduction of high potassium buffer. The peak height was estimated as shown in figure 2.

The peak shape of the current response can be interpreted as a combination of several effects. Potassium triggers exocytotic release of transmitter molecules from PC 12 cells. The rapidly increased concentration of transmitters at the cell covered surface is sensed by the Pedot:tosylate electrodes. After some time, the release of new transmitters is balanced by the diffusion of the molecules away from the surface. Also, the depletion of oxidizing molecules in close vicinity to the electrode could contribute to the decrease in current. Indeed, band microelectrodes do not provide true steady-state currents over time for constant concentration of oxidizing species[32].

The height of the second peak compared to the height of the first peak was relatively constant over a range of chip experiments and was found to be independent on the absolute height of the peaks. For a 15 minute rest period between stimulations, the ratio was measured on four different chips to be 63 ± 9 %. This quantity was therefore chosen as a measure of transmitter release. By keeping the protocol unchanged through the first stimulation, the effect of varying experiment parameters or exposing the cells to different drugs can be investigated by comparing the ratio of peaks.

First, we investigate the effect of the "rest" time between potassium stimulations. Figure 3 shows the ratio of current peaks as a function of the time period between stimulations. Clearly, the response of the second peak increases with increasing rest time with a 5 minute rest time giving approximately half the current response. This could be interpreted as the cells needing to refuel their transmitter reservoirs or to transport transmitter vesicles to release sites at the cell membrane[1].

Next, we vary the concentration of potassium used to stimulate the cells. The first potassium stimulation was carried out with a 100 mM potassium buffer, while the concentration was varied during the second stimulation. The time between the peaks was 5 minutes. As can be seen in figure 4, we observe a clear relationship between response and potassium concentration. At 20 mM, no response was measured, while the full response was observed for concentrations higher than 80 – 100 mM. In figure 4, the data is treated as a sigmoidal dose-response relationship and fitted to the Hill equation[33]. Setting the bottom level to 0, a least squares regression results in the following parameters: Maximum response: 50.0 %, half maximal effective concentration (EC50): 56.6 mM, Hill coefficient: 6.11.

Finally, we demonstrate the potential of using the device as a simple tool for drug screening. We demonstrate this by using the compound L-DOPA (L-3,4-dihydroxyphenylalanine), which is known to increase the size of transmitter vesicles in PC 12 cells[9]. L-Dopa is a precursor of the neurotransmitter dopamine and can be converted into dopamine inside neuronal cells. The experiment protocol is shown in figure 5 together with two representative current peaks. The time between potassium stimulations was set to 15 minutes. During this period the cells were exposed to a buffer containing 100 µM L-Dopa for 5 minutes. The ratio of peak currents was measured to be 97 ± 12 % for L-Dopa treated cells. In figure 6, the response of L-Dopa-treated cells is compared to that of untreated cells. The increase in peak current is statistically significant. This result supports earlier carbon fiber microelectrode experiments where treatment with L-Dopa even for very short time periods increased the mean vesicle content at PC 12 cells[10]. The results plotted in figure 6 show that the method presented in this paper can be used as a simple screening method for drugs affecting transmitter release in neuronal cells.

Conclusion

In this paper, we presented a simple chip for studying the overall release of transmitter from a large group of PC 12 cells. The chip was constructed of only polymer materials with electrodes made of micropatterned Pedot:tosylate conductive polymer. Potassium-induced stimulation of surface-trapped PC 12 cells gave rise easy-to-analyze current peaks due to oxidation of the released transmitters on the Pedot:tosylate electrodes. Subsequent stimulations of the same group of cells resulted in signals that increased in size with increasing time between stimulations. This result indicates that PC 12 cells need a certain time to refuel their transmitter reservoirs or to transport transmitter vesicles to release sites at the cell membrane. The release of transmitters depended heavily on the concentration of potassium. Experimental data of release

versus potassium concentration was fitted to a sigmoidal dose-response curve with half maximal effective concentration (EC50) at 56.6 mM potassium. The presented chip could be used for simple pharmacological screening of neurochemical drugs. This was demonstrated by measuring the increase in released transmitter of PC 12 cells being exposed to 100 µM L-DOPA for 5 minutes. The method used in this paper has both advantages and disadvantages compared to conventional single cell amperometric analysis. Information on single vesicle size is lost, but on the other hand time-consuming statistical analysis of single vesicle release events can be avoided in applications targeting overall release activity of neuronal cells. Using only polymer materials makes the presented chip an easy-to-fabricate, cost efficient and disposable device.

Acknowledgments

This work is supported by the Danish Council for Strategic Research through the Strategic Research Center PolyNano (grant no. 10-092322/DSF)

References

1 L. Squire, D. Berg, F. Bloom, S. du Lac, A. Ghosh and N. Spitzer, *Fundamental Neuroscience*, Elsevier Inc., 2008.

2 R. Wightman, J. Jankowski, R. Kennedy, K. Kawaoge, T. Schroeder, D. Leszczyszyn, J. Near, E. Diliberto and O. Viveros, *Proc. Natl. Acad. Sci. U. S. A.,* 1991, **88**, 10754-10758 (DOI:10.1073/pnas.88.23.10754).

3 D. M. Omiatek, A. Cans, M. L. Heien and A. G. Ewing, *Anal. Bioanal. Chem.,* 2010, **397**, 3269-3279 (DOI:10.1007/s00216-010-3698-4).

4 G. M. Dittami, H. E. Ayliffe, C. S. King and R. D. Rabbitt, *J Microelectromech Syst,* 2008, **17**, 850-862 (DOI:10.1109/JMEMS.2008,921726).

5 K. Berberian, K. Kisler, Q. Fang and M. Lindau, *Anal. Chem.,* 2009, **81**, 8734-8740 (DOI:10.1021/ac900674g).

6 C. Amatore, S. Arbault, Y. Chen, C. Crozatier, F. Lemaitre and Y. Verchier, *Angew. Chem. -Int. Edit.,* 2006, **45**, 4000-4003 (DOI:10.1002/anie.200600510).

7 Y. Gao, X. Chen, S. Gupta, K. D. Gillis and S. Gangopadhyay, *Biomed. Microdevices,* 2008, **10**, 623-629 (DOI:10.1007/s10544-008-9173-8).

8 Y. Huang, D. Cai and P. Chen, *Anal. Chem.,* 2011, **83**, 4393-4406 (DOI:10.1021/ac200358b).

9 R. H. S. Westerink and A. G. Ewing, *Acta Physiologica,* 2008, **192**, 273-285 (DOI:10.1111/j.1748-1716.2007.01805.x).

10 R. Westerink, A. de Groot and H. Vijverberg, *Biochem. Biophys. Res. Commun.,* 2000, **270**, 625-630 (DOI:10.1006/bbrc.2000.2470).

11 K. D. Kozminski, D. A. Gutman, V. Davila, D. Sulzer and A. G. Ewing, *Anal. Chem.,* 1998, **70**, 3123-3130 (DOI:10.1021/ac980129f).

12 E. Pothos, M. Desmond and D. Sulzer, *J. Neurochem.,* 1996, **66**, 629-636.

13 D. Sulzer, T. K. Chen, Y. Y. Lau, H. Kristensen, S. Rayport and A. Ewing, *Journal of Neuroscience,* 1995, **15**, 4102-4108.

14 L. Hondebrink, J. Meulenbelt, J. G. Timmerman, M. van den Berg and R. H. S. Westerink, *J. Neurochem.,* 2009, **111**, 624-633 (DOI:10.1111/j.1471-4159.2009.06357.x).

15 E. N. Pothos, S. Przedborski, V. Davila, Y. Schmitz and D. Sulzer, *Journal of Neuroscience,* 1998, **18**, 5575-5585.

16 H. Cui, J. Ye, Y. Chen, S. Chong and F. Sheu, *Anal. Chem.,* 2006, **78**, 6347-6355 (DOI:10.1021/ac060018d).

17 Y. Chen, C. Guo, L. Lim, S. Cheong, Q. Zhang, K. Tang and J. Reboud, *Anal. Chem.,* 2008, **80**, 1133-1140 (DOI:10.1021/ac071182j).

18 N. Rozlosnik, *Anal. Bioanal. Chem.,* 2009, **395**, 637-645 (DOI:10.1007/s00216-009-2981-8).

19 S. Nambiar and J. T. W. Yeow, *Biosens. Bioelectron.,* 2011, **26**, 1825-1832 (DOI:10.1016/j.bios.2010.09.046).

20 E. S. Forzani, X. Li and N. Tao, *Anal. Chem.,* 2007, **79**, 5217-5224 (DOI:10.1021/ac0703202).

21 D. J. Macaya, M. Nikolou, S. Takamatsu, J. T. Mabeck, R. M. Owens and G. G. Malliaras, *Sensors and Actuators B-Chemical,* 2007, **123**, 374-378 (DOI:10.1016/j.snb.2006.08.038).

22 J. Liu, M. Agarwal and K. Varahramyan, *Sensors and Actuators B-Chemical,* 2008, **135**, 195-199 (DOI:10.1016/j.snb.2008.08.009).

23 M. Berggren and A. Richter-Dahlfors, *Adv Mater,* 2007, **19**, 3201-3213 (DOI:10.1002/adma.200700419).

24 M. Asplund, T. Nyberg and O. Inganas, *Polymer Chemistry,* 2010, **1**, 1374-1391 (DOI:10.1039/c0py00077a).

25 K. Kiilerich-Pedersen, C. R. Poulsen, T. Jain and N. Rozlosnik, *Biosens. Bioelectron.,* 2011, **28**, 386-392 (DOI:10.1016/j.bios.2011.07.053).

26 A. K. Sarma, P. Vatsyayan, P. Goswami and S. D. Minteer, *Biosens. Bioelectron.,* 2009, **24**, 2313-2322 (DOI:10.1016/j.bios.2008.09.026).

27 L. Setti, A. Fraleoni-Morgera, I. Mencarelli, A. Filippini, B. Ballarin and M. Di Biase, *Sensors and Actuators B-Chemical,* 2007, **126**, 252-257 (DOI:10.1016/j.snb.2006.12.015).

28 N. F. Atta, A. Galal and R. A. Ahmed, *J. Electrochem. Soc.,* 2011, **158**, F52-F60 (DOI:10.1149/1.3551579).

29 S. S. Kumar, J. Mathiyarasu, K. L. N. Phani and V. Yegnaraman, *J. Solid State Electrochem.,* 2006, **10**, 905-913 (DOI:10.1007/s10008-005-0041-7).

30 S. T. Larsen, R. F. Vreeland, M. L. Heien and R. Taboryski, *Analyst,* 2012, **137**, 1831-1836 (DOI:10.1039/c2an16288a).

31 S. Y. Yang, B. N. Kim, A. A. Zakhidov, P. G. Taylor, J. Lee, C. K. Ober, M. Lindau and G. G. Malliaras, *Adv Mater,* 2011, **23**, H184-H188 (DOI:10.1002/adma.201100035).

32 A. J. Bard and L. R. Faulkner, *Electrochemical Methods*, John Wiley & Sons, Inc., 2001.

33 H. Motulsky and A. Christopoulos, *Fitting Models to Biological Data using Linear and Nonlinear Regression*, GraphPad Software, Inc., 2003.

Figures

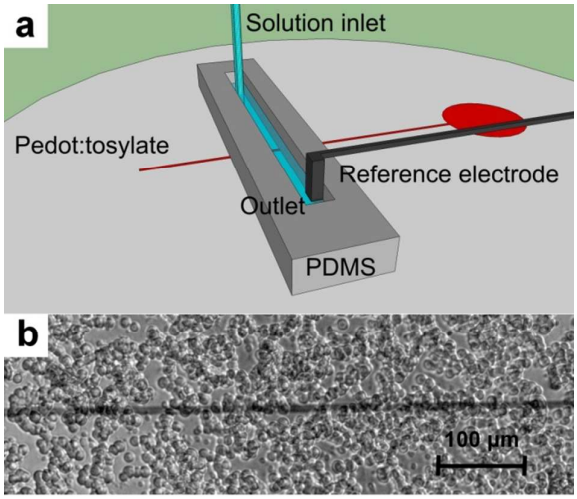

Figure 1: a) Model of chip design. A 10 – 20 µm wide pedot:tosylate band microelectrode (red) is fabricated on a polymer substrate. A 2-3 mm wide and 3 cm long rectangular well is constructed in PDMS and placed perpendicular to the microelectrode. B) Microscope image of PC 12 cells sedimented on a Poly-L-Lysine covered Pedot:tosylate microelectrode.

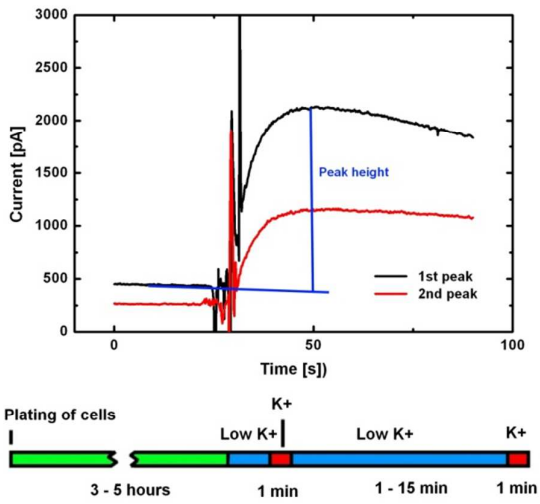

Figure 2: Two current responses measured at the same chip. The responses were triggered by stimulating PC 12 cells with a buffer containing 100 mM potassium concentration. The protocol of the experiment is shown under the graph. The time between stimulations was varied in this experiment. During this period the cells were exposed to a low concentration of potassium (5 mM).

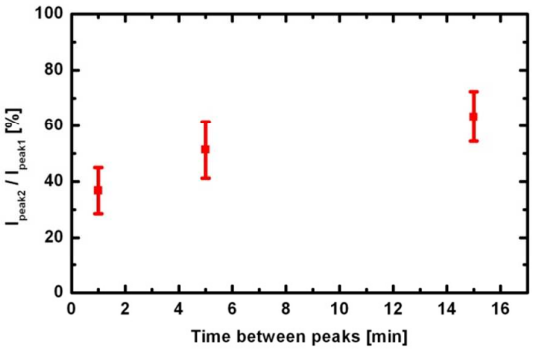

Figure 3: The ratio of the second peak compared to the first peak as a function of the time between stimulations. The protocol for this experiment is shown in figure 2.

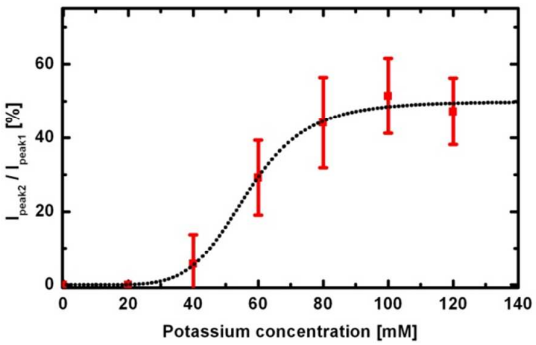

Figure 4: The ratio of current peaks as a function of potassium concentration during second stimulation. The time period between stimulations was 5 minutes. The concentration during the first stimulation was 100 mM. The experimental data was least squares fitted to the Hill Equation with fitting parameters: Maximum response: 50.0 %, EC50: 56.6 mM, Hill coefficient: 6.11. The baseline response was set to 0.

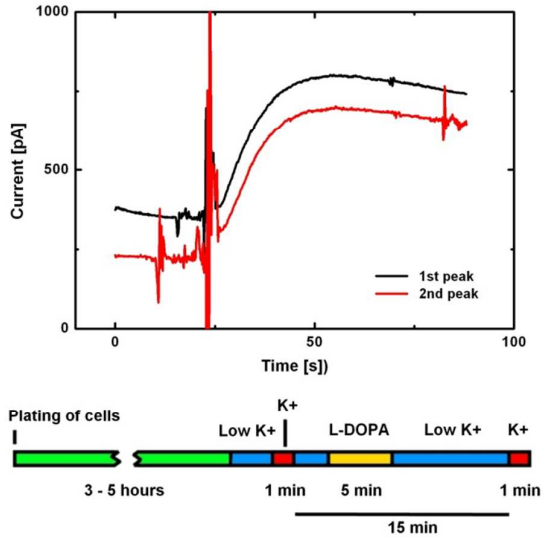

Figure 5: Two representative current responses and protocol for drug exposure experiment. During the 15 minute rest period between stimulations, a buffer containing 100 µM L-Dopa was introduced to the chip for 5 minutes.

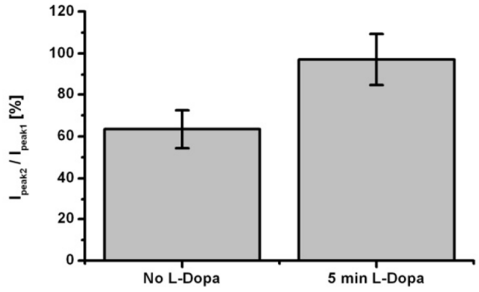

Figure 6: Ratio of current peaks for cells exposed to L-Dopa and for cells only exposed to low potassium buffer. The time between stimulations was 15 minutes for both experiments.

Conductive Polymer Microelectrodes for on-chip measurement of transmitter release from living cells

S. T. Larsen*, M. Matteucci* and R. Taboryski

*Department of Micro- and Nanotechnology,
Technical University of Denmark, DTU Nanotech, Building 345E,
DK-2800 Kongens Lyngby, Denmark

ABSTRACT

In this paper, we present techniques to trap a group of neuronal cells (PC 12) close to band microelectrodes and quantitatively measure cellular transmitter release. Different trapping approaches were investigated including coating of electrodes by layers enhancing cell attachment and by pressure driven cell trapping inside closed chip devices. Conductive polymer microelectrodes were used to measure transmitter release using electrochemical methods such as cyclic voltammetry and constant potential amperometry. By measuring the oxidation current at a cyclic voltammogram, the concentration of released transmitter molecules could be estimated.

Keywords: pedot, conductive polymer, exocytosis, neurotransmitter, amperometry

1 INTRODUCTION

Exocytosis is the principal means of communication between neuronal cells and connected to several central nervous system disorders. In this process, neurotransmitters stored in intracellular vesicles are released to the surroundings by fusion of the vesicle membrane with the cell membrane. Exocytosis can be evoked in cultured neuronal model cell lines (we use PC 12) by exposing the cells to a high concentration of potassium. A range of neurotransmitters oxidize at a certain potential and can be detected as a current signal, by holding an electrode at a constant potential higher than the oxidation potential.

The idea of using conductive polymer electrodes for electrochemical measurement of transmitters is new [1] and is here utilized by using photolithographically patterned Poly(3,4-ethylenedioxythiophene):tosylate (Pedot:tosylate) microelectrodes. A wide range of transmitters were shown to oxidize readily on these electrodes in a recent study by the authors of this work [2].

Much research has been focused on measuring single exocytotic events on carbon fiber microelectrodes or thin film metallic microelectrodes [3], [4]. On the other hand, little work has been done on measuring transmitter release from large cell groups, although this method is experimentally easier and has a high potential in drug screening applications [5]

In this paper, we investigate some novel approaches of trapping a population of cells close to a microelectrode and keeping them fixed during buffer exchange. This is done in all-polymer chip devices. Further, we make use of conductive polymer electrodes with excellent electrochemical properties. We demonstrate how cellular release of transmitters can be measured using constant potential amperometry at these electrodes.

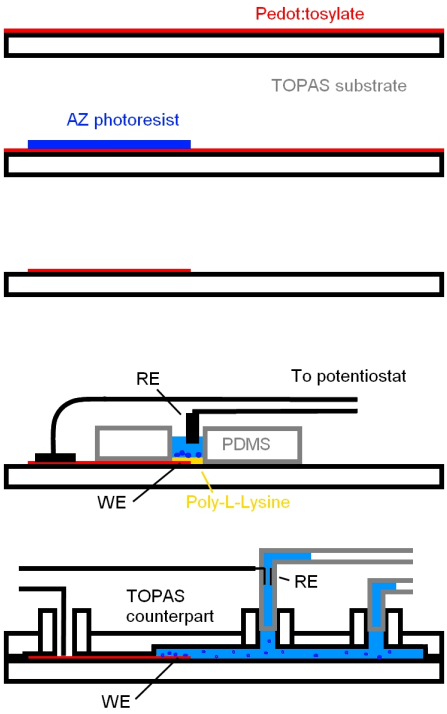

Figure 1: Fabrication of Pedot:tosylate microelectrodes and chip integration. After application of the Pedot:tosylate, patterning is done with UV lithography using AZ resists and reactive ion etching. Two different chip designs have been used in this work, by bonding to either a well structure in PDMS or an injection molded TOPAS counterpart with microchannels. Abbreviations: WE – Working Electrode, RE – Reference Electrode.

2 FABRICATION

Micropatterned conductive polymer electrodes were fabricated on flat injection molded TOPAS 5013 (TOPAS Advanced Polymers GmbH) substrates as described in detail earlier [2] and shown in figure 1. Two different methods of integration of electrodes into chip devices have been used in this work.

In the first approach, the electrode substrate was bonded to a well shaped PDMS part. The electroactive area of the electrode was defined by the area protruding into the well. Attachment of cells to the electrode could be achieved by incubating the electrodes with a 0,01 mg/ml Poly-L-Lysine or Collagen solution for 1 hour prior to cell experiments. A 2-electrode configuration was used with a Ag/AgCl reference electrode placed in the cell buffer.

The second approach which is shown in the bottom drawing in figure 1, involved thermal bonding of the TOPAS substrate to an injection molded TOPAS counterpart. In order to fabricate samples by means of injection molding, Nickel shims with channel design are fabricated with standard UV-LIGA techniques. Parts are then injection molded from TOPAS using an Engel Victory 80/45 Tech hydraulic injection molding machine. Before bonding, the two TOPAS parts need to be aligned by eye with an optical microscope. Thermal bonding is done at 120° C and 10 kN for 5 minutes. Microchannels can be accessed through luer holes in the injection molded top part. A VEMA 8 channel pressure regulator (Festo) was used to control and move fluids inside the chip. A Ag/AgCl electrode was constructed to fit inside a luer connector and was used as reference electrode.

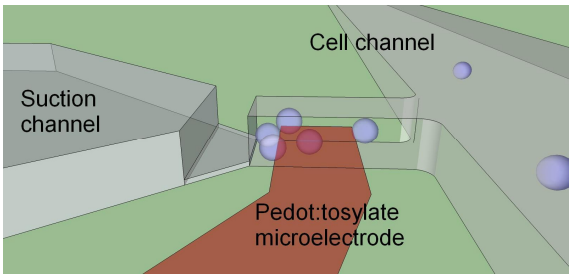

Figure 2: Illustration of cell trapping approach where cells are trapped inside a 20 µm x 30 µm x 100 µm chamber due to suction from a separate suction channel. A 2 µm high slit section ensures cells being left in the chamber.

3 CELL TRAPPING

3.1 Cell chamber approach

One of the approaches used in this study to trap cells is shown in figure 2. By applying suction through a 3 µm high slit, cells are pulled into a 30 µm x 20 µm x 100 µm box from the adjacent cell channel. A Pedot:tosylate microelectrode can be fabricated and aligned to protrude into the cell chamber from one side. A microscope image of a final chip is shown in figure 3 (right). The electrode shown here is 50 µm wide which makes the electroactive area 50 µm x 30 µm.

Passage 12 rat pheochromocytoma (PC 12) cells were used to test the cell trapping technique. After applying a small vacuum pressure (around 50 mbar), cells started to flow in and fill the chamber. After filling approximately ¼ of the chamber the pressure had to be increased to attract more cells. A final pressure of 500 mbar was used to fill up the chamber as seen in figure 4.

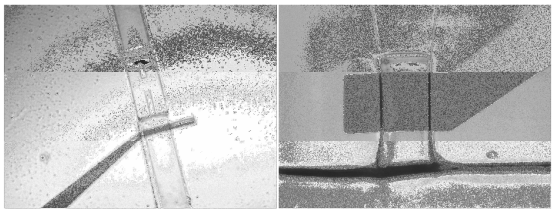

Figure 3: Microscope images of injection molded and thermally bonded polymer chip devices. Left: 1-dimensional trapping technique with Pedot:tosylate electrode placed right before shallow channel region. Right: Cell chamber trapping technique as shown in figure 2.

3.2 One-dimensional channel with slit

Another cell trapping approach consisted of only one large cell channel with a 100 µm slit region approximately half way between the inlet and outlet openings. A Pedot:tosylate electrode was fabricated to cross the large channel on the inlet side of the slit (fig 3, left side). Although this approach seems to be simpler, it did not perform as well as the cell chamber approach in terms of channel filling and cell capture.

3.3 Cell trapping by “sticking” surfaces

The method of trapping cells at an electrode by coating the electrode with a “cellophilic” biomolecule was successfully applied by Liu et al [6] and used to measure transmitter release from single cells at a DLC:N/ITO electrode. In this work, we coated Pedot:tosylate electrodes with Poly-L-Lysine and Collagen (both acquired at Sigma Aldrich). These compounds are frequently used to coat cell culture substrates. Both surfaces exhibited superior cell attachment compared to bare polymer substrates even though the time allowed for attachment is limited to less than 20 minutes due to cell viability. Poly-L-Lysine seemed to be slightly better than Collagen. Further, the additional layer did not compromise the good electrochemical

characteristics of Pedot:tosylate electrodes. Once cells are trapped on and around a band electrode, transmitter release can be triggered simply by exchanging the buffer solution with a buffer containing a high potassium concentration. Figure 5 shows a microscope image of a large group of PC 12 cells sedimented on a Pedot:tosylate band microelectrode.

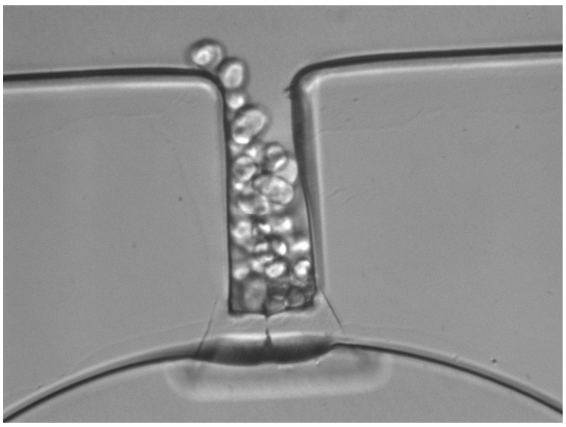

Figure 4: Microscope image showing the filling of a micro-chamber by PC 12 cells

.

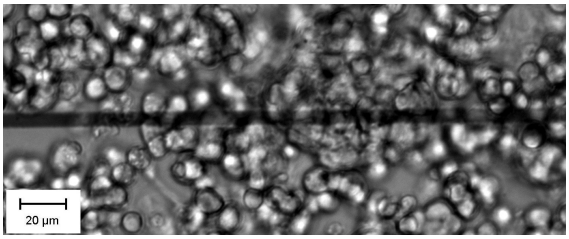

Figure 5: Sedimentation of PC 12 cells on a 7 µm wide Poly-L-Lysine coated Pedot:tosylate electrode.

4 ELECTROCHEMICAL MEASUREMENTS

Before cell experiments, we tested the Pedot:tosylate electrodes by performing slow scan cyclic voltammograms with electrodes immersed in varying dilutions of dopamine in PBS buffer. The result is shown in figure 6. As expected, cyclic voltammogram step height is proportional to dopamine concentration. For small concentrations of dopamine a voltage independent oxidation current is reached.

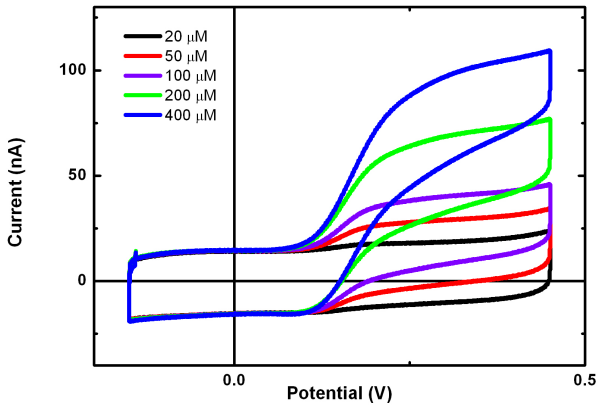

Figure 6: Cyclic voltammograms showing the oxidation of Dopamine on a Pedot:tosylate microelectrode. Dopamine was diluted at different concentrations in PBS. Scan rate: 10 mV/s, Potential referenced to Ag/AgCl

Next, we coated a Pedot:tosylate band electrode with Poly-L-Lysine and let a population of PC 12 cells sediment on the surface. After sedimentation, the buffer used to transport the cells could be exchanged with fresh physiological buffer without moving the attached cells. A cyclic voltammogram performed with the cell-covered electrode immersed in fresh PBS showed no sign of oxidizing compounds (black line, figure 7). By exchanging the buffer with a similar buffer containing higher potassium concentration (105 mM), transmitter release from the PC 12 cells could be detected as a step on the cyclic voltammogram (blue line, figure 7). The step occurs at the same potential (~150 mV) as seen for dopamine dilutions (fig 6), which strongly indicates that dopamine or other catecholamine release is observed.

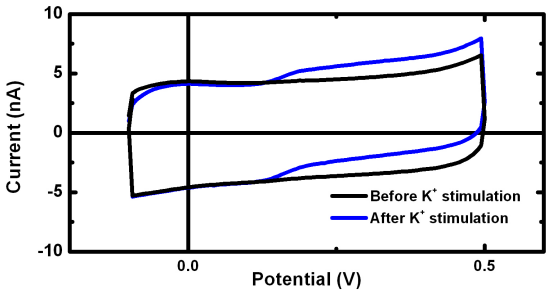

Figure 7: Cyclic voltammograms performed at a Pedot:tosylate electrode covered with Poly-L-Lysine and PC 12 cells. The black voltammogram was measured before K^+ stimulation and the blue voltammogram right after K^+ stimulation.

Since the oxidation current, measured as the step height in figure 7, is directly proportional to the concentration of oxidizing molecules, we can calculate the concentration of

released transmitter molecules. The quasi-steady state oxidation current at a band electrode is given by the following equation:

$$i_{qss} = \frac{2\pi nFlDC}{\ln(64Dt / w^2)} \quad (1)$$

where C is the bulk concentration, n the number of electrons in the reaction, F Faraday's constant, t the time after oxidation onset, D the diffusion coefficient, and the dimensions of the band electrode are given by the width w and length l. In figure 7, the measured oxidation currents of the dopamine dilution voltammograms from figure 6 are plotted together with values calculated using eq. 1. This result shows, that eq. 1 is valid for oxidation of dopamine at Pedot:tosylate and we can now use it to estimate the concentration of transmitter molecules released from PC 12 cells and electrochemically detected in figure 7. Using the electrode dimensions 12 µm x 1560 µm, time 15 s and the measured oxidation current 1,2 nA, we obtain a calculated transmitter concentration of 10 µM around the electrode.

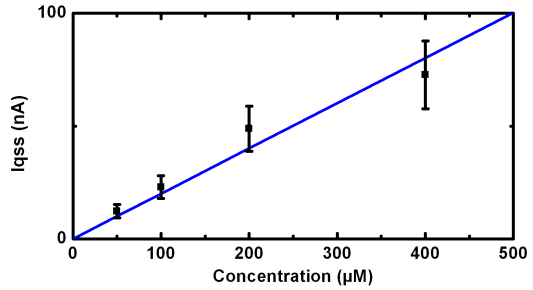

Figure 7: Measured quasi-steady state oxidation currents corresponding to voltammograms in figure 6, and theoretical values (eq. 1, blue line)

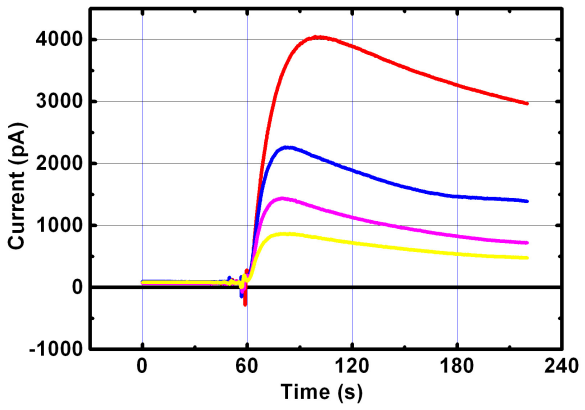

Figure 8: Amperometric current traces at a Pedot:tosylate electrode covered with Poly-L-Lysine and PC 12 cells. The cells were alternately exposed to a potassium rich and low potassium buffer. The largest response corresponds to the first K^+ stimulation, while subsequent responses decrease.

Finally, we measure the increase of released transmitter molecules from a group of PC 12 cells, by applying a constant potential to the Pedot:tosylate microelectrodes and measuring the current before and after potassium stimulation. In figure 8, the current traces corresponding to 4 subsequent potassium stimulations at the same group of PC 12 cells are shown. Between stimulations, the cells are given rest periods in low potassium buffer for 4 minutes. The decreasing current responses could be interpreted as the cells depleting their transmitter reservoirs due to heavy release.

5 CONCLUSION

In this paper, we measured transmitter release from large groups of neuronal cells by using electrochemical detection at Pedot:tosylate conductive polymer microelectrodes. We investigated three different cell trapping approaches. Trapping cells inside a cell chamber or on top of a sticking coating layer gave good results. Finally, we measured transmitter release from PC 12 cells at Pedot:tosylate electrodes using cyclic voltammetry and constant potential amperometry. Oxidation currents could be related to dopamine concentrations by a simple formula, and concentration of released transmitter could be estimated.

6 ACKNOWLEDGMENTS

This work is supported by the Danish Council for Strategic Research through the Strategic Research Center PolyNano (grant no. 10-092322/DSF)

REFERENCES

[1] S. Y. Yang, B. N. Kim, A. A. Zhakidov, P. G. Taylor, J.-K. Lee, C. K. Ober, M. Lindau and G. G. Malliaras, Adv. Mater., 23, H184-H188, 2011

[2] S. T. Larsen, R. F. Vreeland, M. L. Heien, and R. Taboryski, Analyst, 137 (8), 1831 - 1836, 2012

[3] R. M. Wightman, J. A. Jankowski, R. T. Kennedy, K. T. Kawagoe, T. J. Schroeder, D. J. Leszczyszyn, J. A. Near, E. J. Diliberto and O. H. Viveros, Proc. Natl. Acad. Sci., 88, 10754-10758, 1991

[4] C. Spegel, A. Heiskanen, L. H. D. Skjolding, J. Emneus, Electroanalysis, 20, 680-702, 2008

[5] H.-F. Cui, J.-S. Ye, Y. Chen, S.-C. Chong, and F.-S. Sheu. Anal. Chem**,** 78, 6347-6355. 2006

[6] X. Liu, S. Barizuddin, W. Shin, C. J. Mathai, S. Gangopadhyay, and K. D. Gillis. Anal. Chem., 83, 2445–2451, 2011

[7] A. J. Bard and L. R. Faulkner, John Wiley & Sons Inc, 2001